NTNU

Norwegian University of
Science and Technology

Medium-term Hydropower Scheduling with Provision of Capacity Reserves and Inertia

Jacob Koren Brekke

Master of Energy and Environmental Engineering
Submission date: June 2016
Supervisor: Magnus Korpås, ELKRAFT
Co-supervisor: Martin Nødland Hjelmeland, ELKRAFT

Norwegian University of Science and Technology
Department of Electric Power Engineering

Title:	Medium-term Hydropower Scheduling with Provision of Capacity Reserves and Inertia
Student:	Jacob Koren Brekke

Problem description:

Study the effects of participation in a hypothetical rotational energy market alongside the day-ahead and primary frequency reserve markets on medium-term hydropower scheduling. A case study of a hydropower system with synchronous condenser mode of operation of one or several hydropower plants should be performed and modelled in a prototype SDDP/Simulator model, programmed in C++, based on SDDP.

Sub-tasks are as follows:

- Extend the SDDP/Simulator model to include provision of rotational energy.
- Study rotational energy market designs.
- Establish data series for inflow and prices.
- Analyze the effects of rotational energy market participation on the hydropower scheduling strategy.
- Evaluate the required remuneration for investment incentives.

Responsible professor:	Magnus Korpås, ELKRAFT
Supervisor:	Martin Nødland Hjelmeland, ELKRAFT

Abstract

The European power system has seen an increased penetration of renewable energy sources in the recent years, especially wind and solar power, causing a greater demand for balancing services. Renewable power generation varies a lot depending on weather conditions and does not easily provide the grid with inertia, compromising the stability of the grid. It is therefore crucial to ensure sufficient capacity and energy reserves, and system inertia to secure stability in the power grid. Especially during summer months, it is expected that low dispatchable generation and a significant import of cheap renewable energy will reduce the system inertia in the Nordic region. This provides an incentive for the TSO to either invest in equipment, or remunerate power producers, for the provision of inertia to the power system. This provision of inertia would, however, impose a cost on the hydropower producer.

The main objective of this thesis is to study the effects of participation in a hypothetical rotational energy market alongside the day-ahead and primary frequency reserve markets on medium-term hydropower scheduling. Participants in the rotational energy market are remunerated for provision of rotational energy that does not alter production. A case study on a Norwegian hydropower system will be conducted with focus on evaluating the cost of providing ancillary services.

Stochastic medium-term hydropower scheduling models are usually based on optimization techniques which require Linear Programming (LP) problems to ensure computational tractability. This imposes simplifications on the problem formulation, such as operating states which typically have a binary nature. Utilizing a strategy obtained by Stochastic Dual Dynamic Programming (SDDP) in a simulator model based on Mixed Integer Programming (MIP) yields a detailed system description and practical computation time.

For the given case study, it was found that rotational energy provision has a small effect on medium-term hydropower scheduling, due to the short time period of critically low inertia. It was also found that the necessary price to cover the investment cost, associated with rotational energy provision, was at a level that caused interference with the optimal production strategy. However, increasing the price in certain time steps and decreasing it in others was shown to mitigate this problem.

Sammendrag

Det europeiske kraftsystemet har opplevd en økende andel fornybare energikilder de siste årene, spesielt sol- og vindkraft, noe som skaper en sterkere etterspørsel etter balansetjenester. Fornybare energikilder er svært væravhengige og lite regulerbare, samtidig som de ikke forsyner systemet med rotasjonsenergi. Dette virker stabilitetsforringende på kraftsystemet og øker behovet for å sikre nok kapasitets- og energireserver, samt rotasjonsenergi. Det er forventet at lite regulerbar kraftproduksjon og en betydelig import av billig fornybar kraft om sommeren, vil føre til en lav mengde rotasjonsenergi i det nordiske kraftsystemet. Dette gir systemoperatøren insentiver til å enten investere i utstyr, eller godtgjøre kraftprodusenter for forsyningen av rotasjonsenergi til kraftsystemet. Det sistnevnte vil medføre en kostnad for kraftprodusentene.

Formålet med denne oppgaven er å studere påvirkningen av deltagelse i et hypotetisk rotasjonsenergimarked, ved siden av spotmarkedet og primærreservemarkedet, på mellomlangsiktig vannkraftplanlegging. Deltagere i rotasjonsenergimarkedet blir godtgjort for tilførsel av rotasjonsenergi som ikke endrer deres kraftproduksjon. Et case studie av et norsk vannkraftsystem vil fokusere på å evaluere kostnaden ved forsyning av rotasjonsenergi.

Stokastiske mellomlangsiktige vannkraftplanleggingsmodeller baseres vanligvis på optimeringsmetoder som krever lineære programmeringsproblemer, for å sikre en håndterbar kjøretid. Dette medfører imidlertid flere forenklinger av problemformuleringen, som formuleringen av driftstilstander som ofte har en binær oppførsel. Ved å benytte strategien fra stokastisk dual-dynamisk programmering (SDDP) i en simulatormodell basert på blandet heltallsprogrammering (MIP), kan en detaljert systembeskrivelse oppnås med en fornuftig kjøretid.

Resultatene fra case studiet viste at forsyning av rotasjonsenergi hadde liten effekt på mellomlangsiktig vannkraftplanlegging, grunnet den korte tiden med kritisk lite rotasjonsenergi i kraftsystemet. Det ble også funnet at den nødvendige prisen for å dekke investeringskostnaden knyttet til forsyningen av rotasjonsenergi var på et nivå som påvirket den optimale produksjonsstrategien. Det ble imidlertid observert at ved å redusere prisen i enkelte tidssteg og øke den i andre unngås dette problemet, samtidig som investeringskostnaden dekkes.

Preface

This master was written at the Department of Electric Power Engineering at the Norwegian University of Science and Technology (NTNU). The thesis was carried out during the autumn semester of 2015, in cooperation with SINTEF Energy Research AS.

I would like to thank my supervisor Magnus Korpås for his guidance and encouragement throughout the semester. I also wish to thank my co-supervisor Martin Nødland Hjelmeland for his help with understanding the model, which has been of paramount importance for the work achieved. Further, I am grateful for the help of Erik Alexander Jansson at Statnett, for providing me with data of the rotational energy in the Nordic power system. I am also grateful for all the help and hydropower system data provided by Magnus Landstad and his colleagues at Lyse Produksjon AS.

Finally, I am thankful for the many fruitful discussions with my fellow students, providing valuable help with problems concerning my own thesis, as well as giving me insight into the interesting topics of theirs.

Trondheim, June 10, 2016
Jacob Koren Brekke

Contents

List of Figures

List of Tables

List of Algorithms

Nomenclature

Indices

c	Time block for capacity allocation.
d	Backward opening.
i	PQ curve segment.
j	Cut.
k	Upstream hydropower module.
m	Hydropower module.
n	Scenario.
r	Price point.
t	Time stage.
w	Time block.
y	Historical inflow scenario.

Sets

$\mathcal{B}_m$	Set of reservoirs connected to the same power station.
$\mathcal{C}$	Set of time blocks for capacity allocation.
$\mathcal{D}$	Set of backward openings.
$\mathcal{H}$	Set of cuts.
$\mathcal{M}$	Set of hydropower modules.
$\mathcal{N}$	Set of scenarios.
$\mathcal{R}$	Set of price points.

$\mathcal{S}_m$ Set of PQ curve segments for hydropower module m.

$\mathcal{T}$ Set of time stages.

$\mathcal{W}$ Set of time blocks.

$\mathcal{Y}$ Set of historical inflow scenarios.

Ω_m Set of upstream hydropower modules for module m.

Parameters

Δf Deviation from system frequency, in [Hz].

ϵ_t Inflow white noise error.

$\eta_{w,m,i}$ Energy equivalent for time block w, module m and PQ segment i, in [MWh/Mm^3].

$\gamma_{w,m,i}$ Power equivalent for time block w, module m and PQ segment i, in [MW/Mm^3].

$\kappa^S_{t,w}$ Energy price profile for time stage t and time block w.

$\lambda^B_{t,c}$ Price for capacity allocation in time stage t and capacity time block c, in [NOK/MW/h].

λ^F Cost of spillage, in [NOK/Mm^3].

λ^G State transition cost, in [NOK].

$\lambda^R_{t,w}$ Price for provision of rotational energy in time stage t and time block w, in [NOK/MWs/h].

λ^S_t Energy price for time stage t, in [NOK/MWh].

λ^T Cost of tank water, in [NOK/Mm^3].

λ^U Start-up cost, in [NOK].

$\mu^j_{t+1,m}$ Dual value of normalized inflow, in [NOK/Mm^3].

$\overline{I_t}$ Mean of historical inflows in time stage t, in [Mm^3].

$\phi^j_{t+1,m}$ Dual value of start-up, in [NOK].

$\pi^j_{t+1,m}$ Dual value of reservoir volume, in [NOK/Mm^3].

ψ Sequential autocorrelation of historical inflows.

$\rho_{r'r}(t)$ Price point transition probability.

σ_t Standard deviation of historical inflows in time stage t.

τ Model parameter representing the transaction fee of purchasing energy.

ζ_t^r Price point in time stage t.

B_m^{max} Maximum bypass from module m, in [Mm^3].

C_c Length of time block c, in [h].

E_m^R Rotational kinetic energy of power station in module m, in [MWs].

f_0 System frequency, in [Hz].

h_0 Nominal head, in [m].

I_t^y Historical inflow for time stage t and inflow scenario y, in [Mm^3].

$P_m^{B,max}$ Maximum power available for capacity reservation for module m, in [MW].

P_m^{max} Maximum power output from module m, in [MW].

P_m^{min} Minimum power output from module m, in [MW].

Q_m^{max} Maximum discharge for module m, in [m^3/s].

$Q_{m,i}^{max}$ Maximum discharge of PQ segment i for module m, in [m^3/s].

Q_m^{min} Minimum discharge for module m, in [m^3/s].

$Q_{m,i}$ Discharge of PQ segment i for module m, in [m^3/s]. Used in the Simulator Model.

S_m Droop setting in the turbine governor for module m, in %.

V_m^{max} Maximum reservoir volume for module m, in [Mm^3].

W_w Length of time block w, in [h].

Variables

α_t Future income function, in [NOK].

$\delta_{t,w,m}^{sim}$ Binary start-up variable, used in the Simulator Model.

$\delta_{t,w,m}$ Start-up variable, in [p.u.].

$\theta_{t,w,m}^{sim}$ Binary state transition variable, used in the Simulator Model.

$\varpi_{t,w,m}$ Tank water, in [Mm^3].

$b_{t,w,m}$ Bypass, in [Mm^3].

$e^{P}_{t,w}$ Energy purchased, in [MWh].

$e^{R}_{t,w}$ Rotational kinetic energy provided, in [MWs(h/h)].

$e^{S}_{t,w}$ Energy sold, in [MWh].

h Head, in [m].

$I_{t,w,m}$ Inflow function, in [Mm^3].

$o^{sim}_{t,w,m}$ Binary state of synchronous condenser mode of operation, used in the Simulator Model.

$o_{t,w,m}$ Relaxed binary state of synchronous condenser mode of operation, in [p.u.].

$p^{B}_{t,w,m,}$ Spinning capacity, in [MW(h/h)].

$p^{B_{tot}}_{t,c}$ Total spinning capacity, in [MW(h/h)].

$p_{t,w,m,i}$ Production in time block w, for module m and PQ segment i, in [MWh].

$p_{t,w,m}$ Production in time block w, for module m, in [MWh].

$q_{t,w,m,i}$ Discharge in time block w, for module m and PQ segment i, in [Mm^3].

$s_{t,w,m}$ Spillage, in [Mm^3].

$u^{H}_{t,w,m}$ Discharge above minimum, in [p.u.].

$u^{L}_{t,w,m}$ Discharge below minimum, in [p.u.].

$u^{sim}_{t,w,m}$ Binary state of power station, used in the Simulator Model.

$v_{t,w,m}$ Reservoir volume, in [Mm^3].

$x^{sim}_{t,w,mi}$ Binary state of PQ segment i, used in the Simulator Model.

$z_{t,m}$ Normalized inflow.

Abbreviations

AC Alternating Current.

CfD Contract for Differences.

DC Direct Current.

DDP Dual Dynamic Programming.

DOR Degree of Regulation.

DP Dynamic Programming.

EMPS EFI's Multi-area Power market Simulator.

FCR Frequency Containment Reserves.

FCR-D Frequency Containment Reserves - Disturbance.

FCR-N Frequency Containment Reserves - Normal.

FRR-A Frequency Restoration Reserves - Automatic.

FRR-M Frequency Restoration Reserves - Manual.

HVDC High Voltage Direct Current.

iid independent and identically distributed.

LP Linear Programming.

MIP Mixed Integer Programming.

NPV Net Present Value.

PCR Price Coupling of Regions.

PQ Power Discharge.

PX Power Exchange.

RPM Regulating Power Market.

RPO Regulating Power Options.

RPOM Regulating Power Options Market.

SC Synchronous Condenser.

SDDP Stochastic Dual Dynamic Programming.

SDP Stochastic Dynamic Programming.

SIR Synchronous Inertial Response.

TSO Transmission System Operator.

1 Introduction

In this thesis the effects of participation in a hypothetical rotational energy market alongside the day-ahead and primary frequency reserve markets on medium-term hydropower scheduling are studied.

1.1 Thesis Motivation

In the EU there are ambitious targets for increasing the renewable electricity generation, especially wind and solar power. In order to facilitate this large scale integration of renewable energies, a set of mechanisms has to be established. By improving the transmission capacity in the power system, by coupling of regions through HVDC cables, synergies can be exploited, reducing the need for dispatchable thermal generation in the regions, and subsequently the CO_2-emissions. A challenge is however that the renewable power generation varies a lot depending on weather conditions and do not easily provide the grid with inertia [5], compromising the stability of the grid. It is therefore crucial to ensure sufficient capacity and energy reserves, and system inertia to secure stability in the power grid.

Especially during summer months, it is expected that low dispatchable generation and a significant import of cheap renewable energy from the continent will reduce the system inertia in the Nordic region. This provides an incentive for the Transmission System Operator (TSO) to either invest in equipment, such as flywheels, or remunerate power producers, for the provision of inertia to the power system. This provision of inertia would, however, impose a cost on the hydropower producer.

The main objective of this work is to study the effects of participation in several markets, including a rotational energy market, on hydropower scheduling using a combined Stochastic Dual Dynamic Programming (SDDP) and simulator approach. A case study on a Norwegian hydropower system will be conducted with focus on evaluating the cost of providing ancillary services. The novel contribution of the work will henceforth be to present a method for evaluating the cost of providing inertia, which could provide decision support, especially in a future market with

large amounts of variable renewable generation and HVDC interconnectors.

1.2 Hydropower Scheduling Model

The hydropower scheduling model used in this thesis is based on the same principles as SINTEF Energy's ProdRisk model, which performs long- and midterm hydropower optimization and simulation using SDDP. Price is taken as an exogenous stochastic variable calculated using Stochastic Dynamic Programming (SDP) [6]. The model used in this thesis is a prototype C++ model developed by Arild Helseth at SINTEF Energy Research and Martin Nødland Hjelmeland at the Department of Electric Power Engineering, NTNU which has been extended by the author to include provision of rotational energy from synchronous condenser mode of operation of hydropower plants. The model combines the SDDP algorithm in a strategy model with a detailed system description in a Mixed Integer Programming (MIP) based simulator model. The Strategy Model will incorporate provision of inertia and balancing reserves to the system and generate a strategy, represented by the expected future profit function, which is used in the detailed Simulator Model.

1.3 Thesis Structure

The thesis is divided into four main parts. Chapter 2 will first present a theoretical background relevant for the understanding of the model, including the Nordic power markets and optimization techniques. This is followed chapters 3 and 4, which provide a detailed description of the model and a case study of the modelled hydropower system, respectively. Finally, result based on a submitted conference paper will be presented and discussed in Chapter 5 before the thesis conclusion and a presentation of further work is given in 6. The submitted paper is included in Appendix A

2 Theory

This chapter will present a theoretical background relevant for understanding the model used in the thesis as well as the thesis objective. The power markets of the Nordic system will be explained first, followed by a description of inertia and actions to ensure a sufficient amount of it in the power system. Finally, a review of relevant optimization techniques will be performed.

2.1 The Power Market

The power market is comprised of several market places for different kinds of physical and financial trade. Together, they provide stability[1] and security in the power system as well as financial risk reduction. Table 2.1 shows these market places and the trade they offer.

2.1.1 Nord Pool Spot

Nord Pool Spot is the world's first international power market [8], owned by the TSOs in the Nordic countries. 380 companies from 20 countries trade on the two markets, accommodating day-ahead and intraday trade.

Elspot

In the day-ahead market, Elspot, daily auctions for day-ahead physical delivery of power are held 365 days a year. The participants trade in certain bidding areas, decided by the location of their production or consumption. The bidding areas reflect constraints in the transmission grid and are determined by the TSO in each country[9]. The prices in the Elspot market are determined by finding the equilibrium for the aggregated supply and demand curves, with a goal of maximizing social welfare. For every hour of the following day, a system price and area prices are calculated. The

[1] The Nordic power system is said to be in balance when the frequency is 50 Hz [7]. A frequency higher than this level indicates that the production is higher than the demand and a frequency lower than this level indicates the opposite. In this thesis, system stability refers to the ability to maintain this frequency level and to meet the demand.

Market place	Physical trade	Financial trade
Nord Pool Spot	Elspot Elbas	
NASDAQ OMX Commodities		Futures Forwards Options CfDs
TSO	Balancing markets Regulating Power Options (RPO)	
Bilateral (Brokers, traders)	Full delivery Load factor contracts	Forwards Options

Table 2.1: Markets in the Nordic System [3].

system price is based on the assumption that the transmission capacity in the grid is infinite, and serves as a reference price in the financial market [3]. The area prices are calculated based on the actual condition of the grid and may differ from one another due to transmission capacity limitations between the areas. Today there are 15 bidding areas distributed across seven countries; five in Norway, four in Sweden, two in Denmark and Finland, Estonia, Lithuania and Latvia are treated as one area each.

The Elspot market is the world's largest day-ahead power market with a traded volume of 361 TWh in 2014 [10]. With a total traded volume of 501 TWh in 2014 [11], Elspot accounted for 72.1 % of the power trade in the Nordic and Baltic region.

In 2009, seven European Power Exchanges (PXs) initiated the Price Coupling of Regions (PCR) project. The project aims at coupling the prices of the day-ahead electricity markets across Europe by use of a common clearing algorithm, efficiently allocating cross-border capacity and optimizing social welfare [12]. In February 2014, PCR was implemented in North Western Europe. The coupled area, referred to as Multi-Regional Coupling, has since expanded, presently covering 19 countries and 85 % of the European power consumption [13].

Elbas

The intraday market, Elbas, covers the Nordic and Baltic region, Germany, and the United Kingdom [14]. Participants may place bids continuously until one hour before physical delivery giving them the opportunity to adjust their positions and reduce

financial risk while increasing system stability. The prices are based on a "first-come, first-serve" principle where the bids corresponding to the highest buy and lowest sell price are prioritized.

The intraday market had a volume of 4.9 TWh in 2014 [15], accounting for 0.98 % of the total power trade. With the expected growth of wind power in the Nordic region, Elbas is expected to grow in both volume and importance [14].

2.1.2 Balancing markets

The balancing markets are operated by the TSOs in each country and are used to ensure a stable system in real-time. The market equilibrium obtained through the day-ahead and intraday market is subject to the occurrence of unforeseen events that may affect the system, causing imbalances. The balancing markets consist of primary, secondary and tertiary reserves which are activated in sequence, depending on the duration of an imbalance. Figure 2.1 shows a principle activation sequence of reserves after an imbalance has occurred.

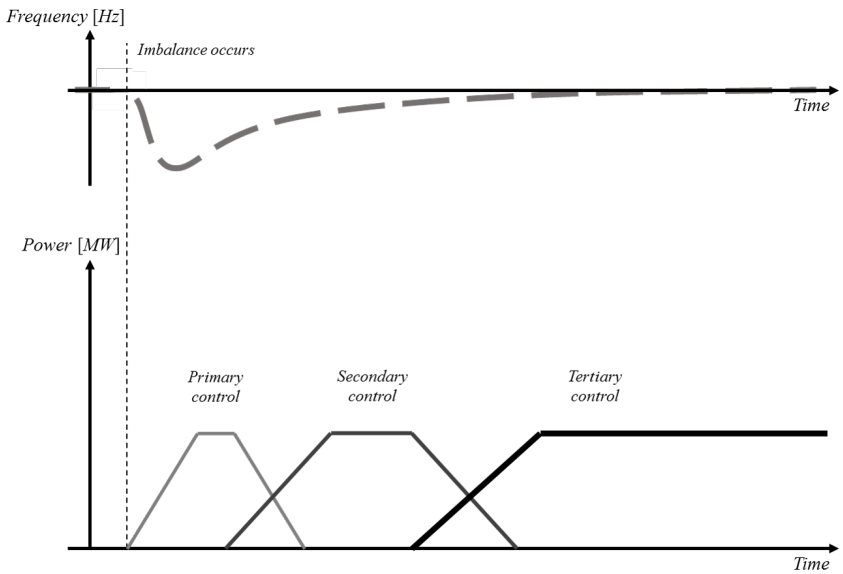

Figure 2.1: Principle activation sequence of reserves after an imbalance [1].

The increased interconnection with Europe in combination with more unregulated power will lead to a higher demand in flexible power for regulating purposes [1]. This can lead to larger traded volumes in the balancing markets. Figure 2.2 shows the trend of frequency deviations in the recent years.

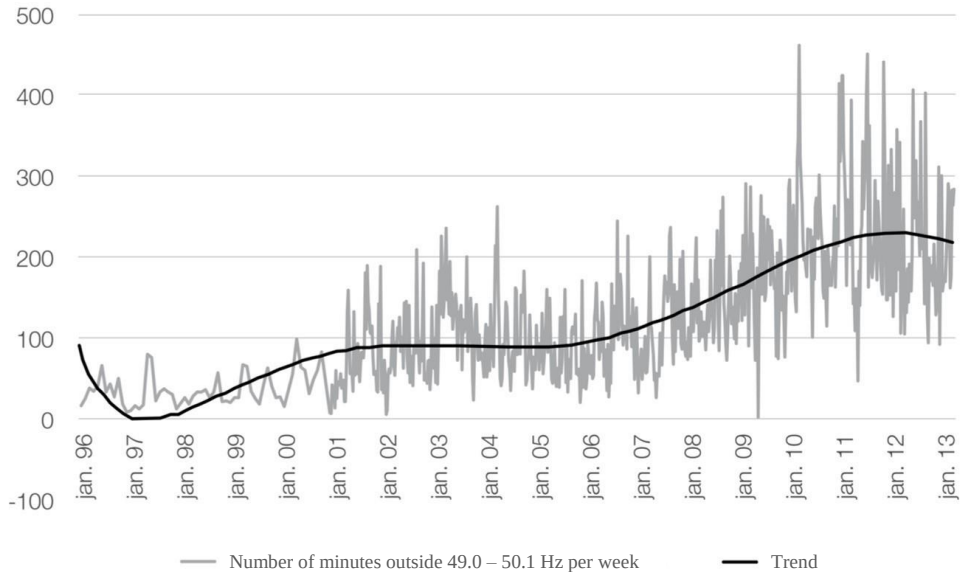

Figure 2.2: Development of frequency deviation [1].

Primary reserves

The primary reserves, also called Frequency Containment Reserves (FCR), are the first to be activated when an imbalance occurs. They respond automatically within seconds of activation and last for a few minutes [3]. For hydropower generators, the reserves are assured by the droop setting in the turbine governors. This entails that a hydropower generator must be running to provide primary reserves.

The primary reserve market ensures a sufficient amount of primary reserves in the system. Two products are traded in this market, Frequency Containment Reserves - Normal (FCR-N) for normal operation and Frequency Containment Reserves - Disturbance (FCR-D) for contingencies. FCR-N is activated for frequencies within 49.90 - 50.10 Hz and handles both upwards and downwards regulation. FCR-D is used to prevent the stationary frequency from reaching its lower limit of 49.50 Hz, being activated when the frequency drops below 49.90 Hz [16]. There is a requirement of at least 600 MW of FCR-N and 1200 MW of FCR-D in the Nordic power system. The FCR-N requirement is divided between the countries comprising the Nordic power system based on their annual consumption, while the FCR-D requirement is distributed proportionally to each country's dimensioning fault[2] [17].

[2]The faults having the largest impact on the power system, for which it is still assumed to be intact [17].

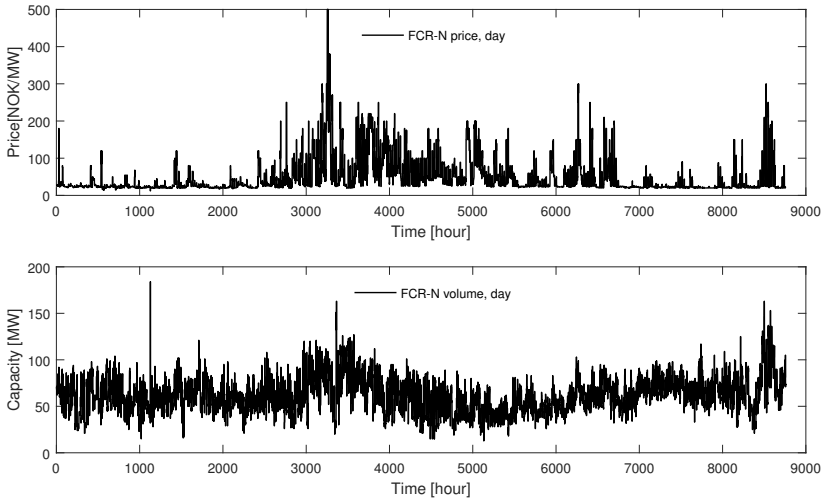

Figure 2.3: 2015 prices (top) and volumes (bottom) in the daily FCR-N market for Elspot area NO2.

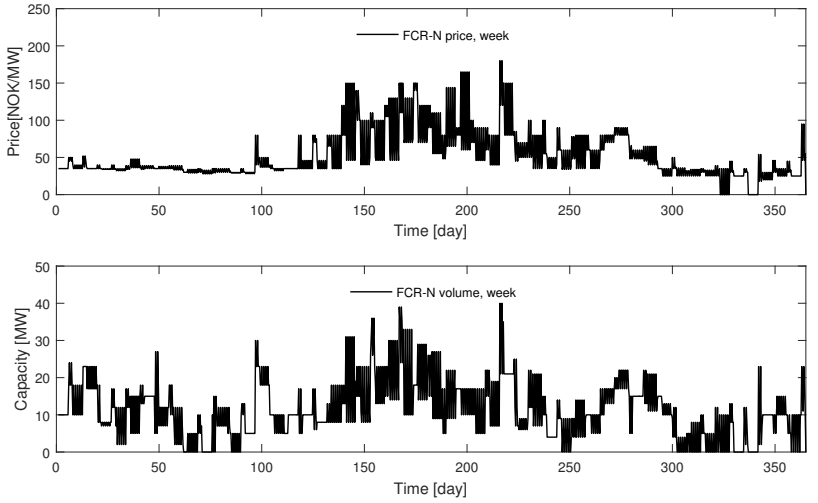

Figure 2.4: 2015 prices (top) and volumes (bottom) in the weekly FCR-N market for Elspot area NO2.

The primary reserve market is divided into a weekly and a daily market. The weekly market is divided into six time periods; night (00:00-08:00), day (08:00-20:00) and

evening (20:00-00:00) for weekdays and weekends, and only accommodates trade of FCR-N. Bids are given per price area and time period for the coming week. In the daily market both FCR-N and FCR-D is traded. Bids for the two types of reserves are given per price area and hour of the next day. Both primary reserve markets are cleared with marginal pricing[3] and market participants are expected to reserve the committed capacity solely for primary regulation. If it is required, the Norwegian TSO, Statnett, can perform a "special purchase", buying reserves at higher prices than the marginal price, to avoid violating certain constraints [18].

To ensure a distribution of reserves amongst the running generators, all generators above 10 MVA participate in the regulation regardless of their participation in the primary reserve market. To accomplish this, the TSO demands the generators be operated below a maximum droop setting and remunerates those that are not active in the market [19].

Figure 2.3 and Figure 2.3 show the prices and volumes of the daily and weekly FCR-N market in 2014. The prices and volumes are low most parts of the year with occasional peaks, the highest found during the early summer and early winter. In [18] is is found that the volume tends to increase during the summer in all the Norwegian price areas, indicating that Statnett has a strong incentive to secure reserves at an early stage in periods with low water values. Statnett expects several hours with almost no regulated production during summers with low spot prices [1]. In [4] it was shown that including the weekly FCR-N market in the hydropower scheduling process lead to an increased income.

Secondary reserves

When frequency deviations last longer than a few minutes, the secondary reserves, also known as Frequency Restoration Reserves - Automatic (FRR-A), are activated to restore the frequency and at the same time free the primary reserves so that they may handle new disturbances. To activate the FRR-A, the TSO sends a signal to a supplier's control system which automatically responds by regulating its production or demand. To participate in the secondary reserve market a direct link between the participant and TSO must be in place. The response time is usually within two to three minutes of receiving the signal [20].

The FRR-A was implemented in the Nordic power system in 2013, due to the unfavorable development of frequency deviations, seen in Figure 2.2. It is aimed at improving the operational system security and handling an increasing level of energy exchange and renewable energy [21]. Today the Nordic countries have somewhat

[3]The highest accepted bid determines the price in the market.

different secondary reserve market structures, but the goal is to create one common market in the future [20].

Tertiary reserves

Tertiary reserves, Frequency Restoration Reserves - Manual (FRR-M), are used for two purposes; frequency regulation and handling regional bottle necks between price areas. The former purpose concerns imbalances lasting longer than 15 minutes. With a response time of 15 minutes and duration of more than one hour [18], the FRR-M can provide a sustained correction while freeing primary and secondary reserves. The secondary purpose secures power exchange between price areas within the available grid capacity [22]. The activation method varies from country to country, in Norway the FRR-M are manually activated by phone [1].

The tertiary reserves are traded on the Regulating Power Market (RPM). Bids for altering production or consumption are placed in a list with bids from all Nordic countries sorted so that the bid with the lowest price is activated first. Stated in the Nordic system operation agreement [17], all Nordic countries are required to have available capacity in the RPM equal to the dimensioning faults in their part of the system. Each TSO ensures this capacity in a different way. In Norway the dimensioning faults amount to 1200 MW. In addition to this Statnett has deemed it necessary to secure 800 MW to handle regional bottlenecks in the grid [1]. This is acquired by utilization of the Regulating Power Options Market (RPOM), where participants are paid to guarantee their participation in the RPM.

Market	**Traded product**	**Bid deadline**
Elspot	Physical delivery	12:00 the day before
Elbas	Physical delivery	One hour before
Primary reserves, week	FCR-N	Thursday 12:00 for the weekend, Friday 12:00 for weekdays
Primary reserves, day	FCR-N, FCR-D	18:00 the day before
Secondary reserves	FRR-A	Thursday 13:00 the week before
RPM	FRR-M	45 minutes before
RPOM, season	RPM commitment	1. October
RPOM, week	RPM commitment	Friday 12:00 the week before

Table 2.2: Market bidding deadlines.

2.1.3 Market bidding deadlines

In Table 2.2 deadlines for placing bids in the different markets are given, as well as a summary of the products traded. Several of the balancing markets have deadlines before the Elspot market, which imposes an uncertainty on the participation

In Figure 2.5 the set point limitation induced by balancing market commitment for a power producer is given.

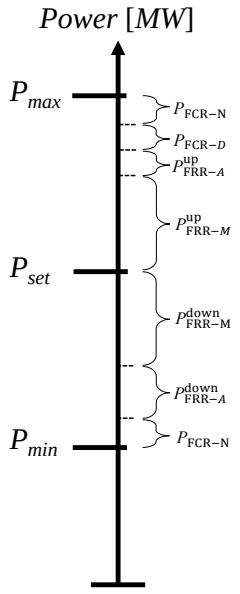

Figure 2.5: Set point limitation of a power producer with balancing market commitments.

2.2 Inertia in the Power System

2.2.1 Inertial dependency of stability

Most power stations use rotating machines to generate electric power. These may be connected either directly or indirectly to the grid. The electrical frequency of the rotating machines which are directly connected to the grid, also referred to as synchronous machines, is equal to the system frequency f [Hz]. The mechanical angular velocity ω [radians/s] of a synchronous machine is coupled to its electrical frequency, and therefore to the system frequency, by the following equation

$$\omega = \frac{2\pi f}{P} \tag{2.1}$$

where P is the number of poles per phase of the machine. Each rotating machine has a moment of inertia J [kgm^2], which determines its resistance to change in its state of motion [23]. Based on a machine's moment of inertia and mechanical angular velocity, the kinetic energy due to rotation E^R [Ws] can be expressed as

$$E^R = \frac{1}{2} J\omega^2 \tag{2.2}$$

The inertia constant H [s] is the ratio between a machine's rotational kinetic energy in [MWs] at synchronous speed and its rated power in [MVA]. It is given by the equation

$$H = \frac{E_n^R}{S_n} = \frac{\frac{1}{2} J\omega_n^2}{S_n} \tag{2.3}$$

where S_n, E_n^R, and ω_n are the machine's rated values. The inertia constant gives the time, in seconds, it would take for a rotating machine to generate an amount of electrical energy equal to its rotational kinetic energy, when operating at synchronous speed.

The system inertia is defined as the ability of a power system to oppose changes in the system frequency due to resistance provided by rotating masses [2]. It can be found by dividing the sum of the rotational kinetic energy stored in each synchronous machine by the rated power of the system, as shown in the following equation

$$H_{sys} = \frac{\Sigma_{m \in \mathcal{M}} S_{n,m} H_m}{S_{n,sys}} \tag{2.4}$$

where $S_{n,m}$ and H_m is the rated power and inertia constant of each rotating machine, respectively. In Table 2.3 the inertia constants of various energy sources are shown.

Production type	H [s]
Nuclear	6.3
Thermal	4.0
Hydropower	3.0
Hydropower (small-scale)	1.0
Wind	0.0
Solar	0.0
HVDC import	0.0

Table 2.3: Average Inertia Constants [2].

A difference in the total power production and consumption will lead to a change in the system frequency. The initial rate of change is determined by the system

inertia. This can be seen in a simplified version of the swing equation[4], in which the relationship between the power imbalance and frequency of a synchronous machine is given [24].

$$\frac{df_i}{dt} = f_n(\frac{P_m - P_e}{2H_i}) \tag{2.5}$$

The equation shows how a difference in a machine's mechanical and electrical power, $(P_m - P_e)$ causes a change in its frequency, f_i. The rate of change is inversely proportional to the inertia constant, H_i. f_n is the nominal system frequency. In Figure 2.6, the frequency response following an imbalance is illustrated for different amounts of rotational energy in the system.

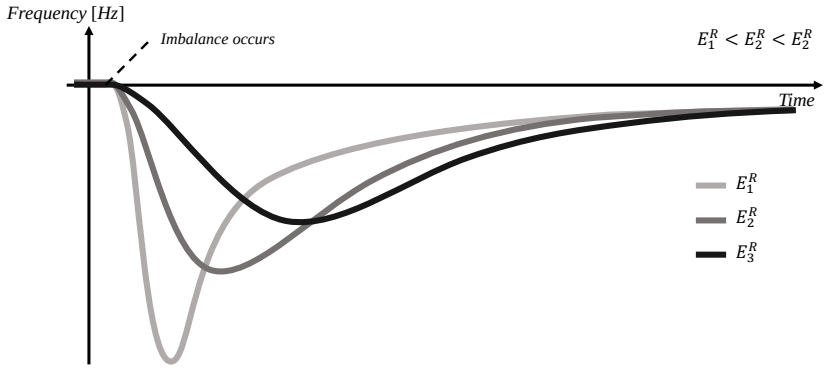

Figure 2.6: Illustration of frequency response for different amounts of rotational energy in the power system.

2.2.2 Inertia in the present and future Nordic power system

From the previous section it is clear that the system inertia is important to the stability of the grid. Traditionally, a large share of the demand in the Nordic power system has been covered by large rotating machines supplying a base load. Wind power and imported power through HVDC cables do not contribute to the system inertia with current technology. As the share of unpredictable renewable power sources and use of HVDC cables increases, there is a rising concern that the system inertia will become inadequate [1].

The TSOs in the Nordic power system initiated the project Nordic Analysis Group (NAG) - Future system inertia [2] in 2013. The project aim was to develop methods to estimate the past, present and future rotational kinetic energy in the Nordic power system. By using power system data in a retroactive calculation, an estimation of

[4]Damping effects are assumed to be negligible.

the rotational energy in Sweden, Finland and Norway from 2009 to 2015 is achieved, shown in Figure 2.7. Eastern Denmark is left out due to the lack of data. The figure shows high levels of rotational energy during the winter and lower levels during the summer. The highest estimated rotational energy is 275 GWs, occurring in the winter of 2012, and the lowest is 115 GWs, occurring in the summer of 2009 [2].

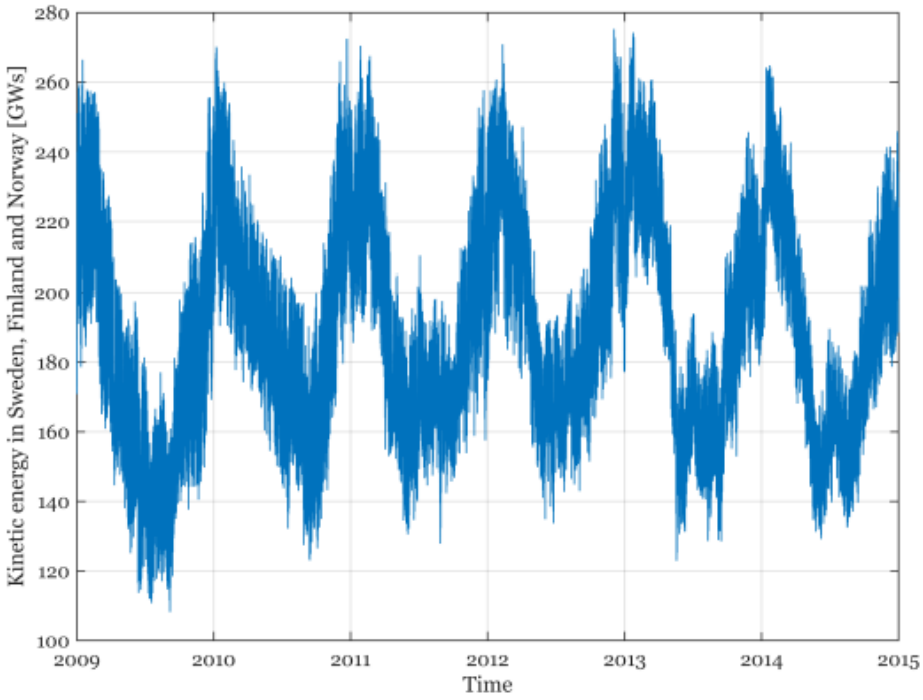

Figure 2.7: Estimated rotational kinetic energy in Sweden, Finland and Norway [2].

Figure 2.8 shows an estimation of the weekly generation mix in the Nordic power system for the year 2020, based on data provided by Statnett. The data origins from ongoing work and is not yet publicly available. The estimate shows expected values, taking planned cross-border HVDC connections and reduced production from nuclear power stations into account. Unregulated hydro is hydropower from water that cannot be stored, caused by low available storage capacity, high inflow, or a combination of the two. It should be noted that weeks with zero import can be assumed to have some export, which is not included in the figure. By using Table 2.3, the rotational energy in the system can be estimated, shown in Figure 2.9.

The rotational energy is correlated with the total production and the share syn-

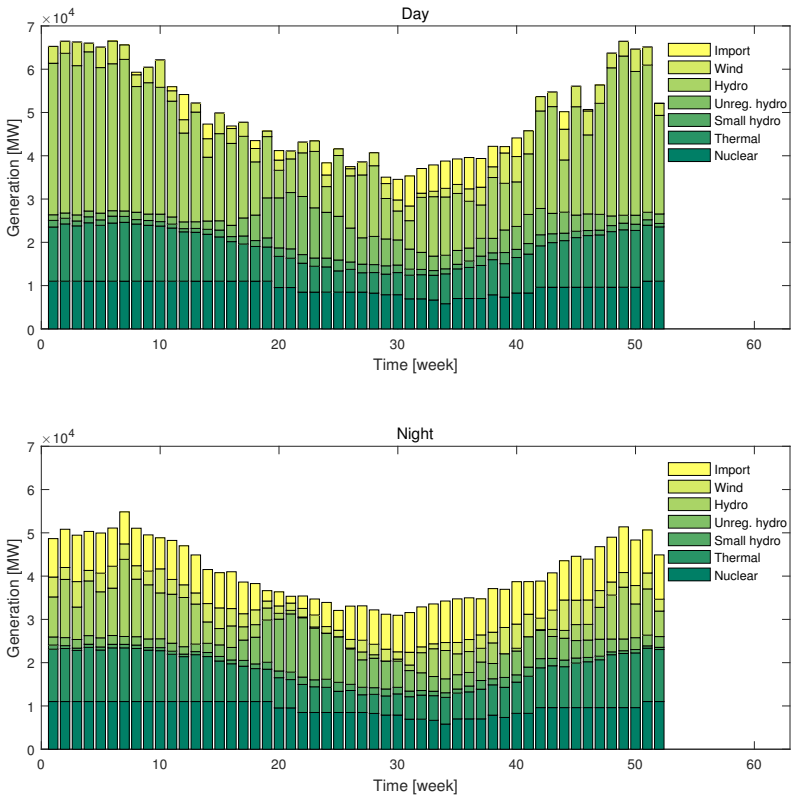

Figure 2.8: 2020 generation mix estimate in the Nordic power system during the day (top) and night (bottom).

chronous generation in the production mix. The sum of the total production and import/export is equal to the demand, which is lowest during summer nights. A low demand also results in low energy prices. This causes a high import from areas with a high penetration of wind and/or other unstorable energy sources, reducing the share of synchronous generation. During the late summer most of the snow reserves will have melted, causing less unregulated hydropower and reducing the share of synchronous generation further. In Figure 2.9 the lowest rotational energy estimate level is 98.2 GWs and occurs during the night of week 31.

Table 2.4 shows how the rotational energy changes with the production mix during week 31. In each scenario, the difference in generation and demand caused by the altered generation mix is covered by a change in import. The table shows that a

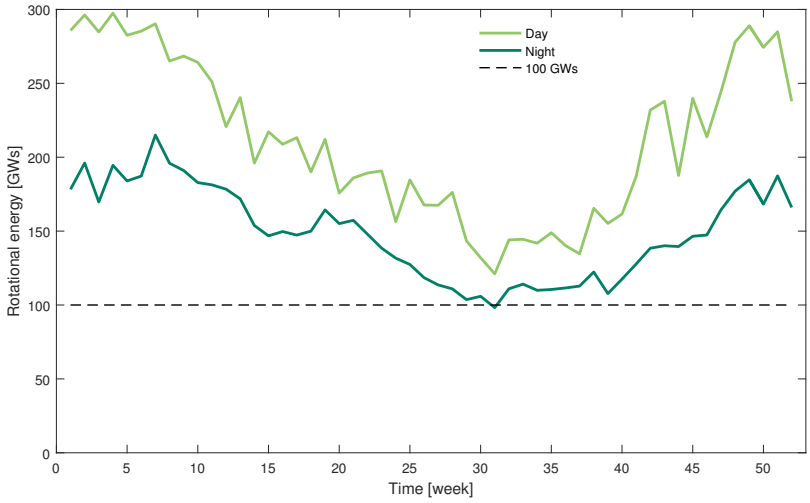

Figure 2.9: 2020 rotational energy estimate in the Nordic power system.

decrease in nuclear or thermal will lower the rotational energy, as it is replaced by imported power. An increase in wind leaves the rotational energy unchanged as both wind power and imported power have an inertia constant of zero.

Scenario	Nuclear	Thermal	Wind	Import	GWs
Base case	6994	5193	2945	9170	98
Scenario 1	6000 ↓	-	-	10114	92
Scenario 2	6000 ↓	-	6000 ↑	7059	92
Scenario 3	6000 ↓	1500 ↓	6000 ↑	10752	75

Table 2.4: Sensitivity analysis, provided by Statnett. The arrows denote a change in production from the base case.

There is currently no system requirement for the amount of rotational energy in the Nordic power system. However, [25] states that as of today only rotating machines participate in the primary reserve market. Hence, the primary reserves system requirement will ensure a certain amount of rotational energy in the system. A system requirement for rotational energy may be derived from keeping the frequency within its transient limit should a dimensioning fault occur. In [25] a limit of 90 GWs was suggested while the current limit recommended by Statnett is 100 GWs. In [26], the effects of using a dynamic rotational energy requirement was studied. Using the fault with the largest frequency impact that may occur, given the current

state of the system, to set the rotational energy requirement was found to reduce the operational costs.

2.3 Strategies to Ensure Sufficient System Inertia

In consideration to the future stability of a grid, it is of interest to ensure ways to procure a sufficient amount of rotational energy [25]. This section will discuss strategies that ensure the rotational energy to be above a system requirement.

2.3.1 Reducing the dimensioning fault

As discussed in the previous section, the rotational energy requirement may be derived from the dimensioning fault of the system. In [2] it is found that the maximum frequency deviation has a linear relation to the power imbalance and rotational energy of the system, shown in Figure 2.10. By reducing the potential power imbalance, i.e. the dimensioning fault, at times with low system inertia, the required rotational energy of the system would be reduced.

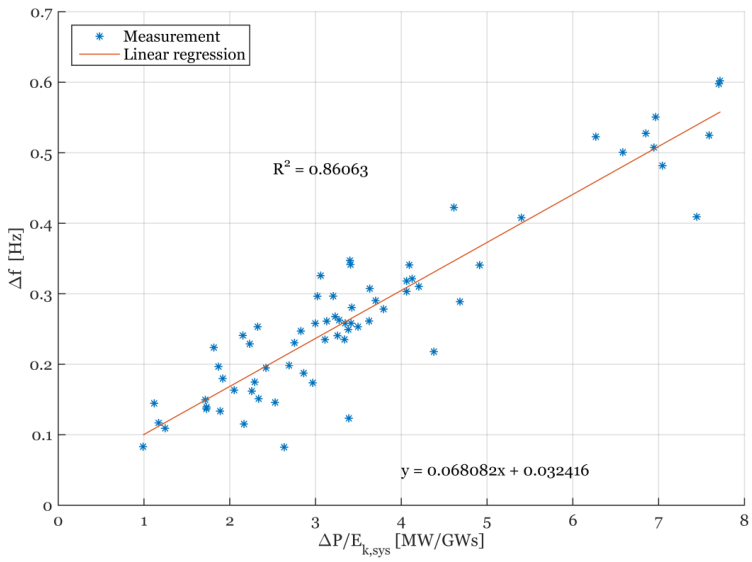

Figure 2.10: Maximum frequency deviation relative to power imbalance and estimated rotational energy [2].

2.3.2 Existing market solutions

The rotational energy requirement can be met by employing existing market solutions to increase the amount of synchronous generators in the system. This can be done

in a number of ways, some of which will be discussed in this thesis. In [25] a more detailed explanation is offered.

As previously mentioned, the primary reserve requirement ensures a certain amount of system inertia. Hence, increasing the primary reserve requirement will increase the number of rotating synchronous generators and the amount of rotational energy. The system inertia can also be increased by introducing a criteria for the number of activated bids, when clearing the primary reserves market. This allows the TSO to ensure that a certain amount of synchronous generators will be connected to the grid. There is however no regulation stating that only rotating machines may participate in the primary reserve market, and it is a viable possibility that primary reserves may be offered by participants that do not provide inertia in the future.

The amount of running synchronous generators can be increased by using the RPM. Power stations which contribute with little or no rotational energy may be regulated down and the production can be replaced by upward regulation of power stations with a more substantial contribution of rotational energy.

In [25], it is concluded that considering costs and difficulty of implementation, the RPM is the best way of ensuring sufficient amounts of rotational energy using existing market solutions.

2.3.3 New market designs

If the future power system is characterized by frequent periods of critically low system inertia requiring large volumes of rotational energy to meet the system requirement, designing a rotational energy market might be necessary. A market design will provide producers with incentives to provide rotational energy in a cost efficient manner through investments and technological improvements. A challenge is however that such a market may affect the existing power markets and provide a competitive advantage based on the production type and technology of certain power producers.

In [25] several different rotational market designs are discussed. This thesis will focus on a market design cleared after the day-ahead market, which is only active at times with critically low system inertia. The clearing of Elspot can be used by the TSO to estimate the rotational energy in the system. Should the estimate fall below the system requirement, the TSO can activate the rotational energy market. The costs of the market are proposed to be divided between the Nordic countries based on either their consumption or dimensioning faults, in the same way as FCR-N or FCR-D respectively. It is stressed that, as the TSO will have an almost perfectly inelastic demand, participants will have strong incentives to exploit potential market power. To avoid this, a sufficient number of market participants or close monitoring of the market will be necessary.

A key discussion is whether all providers of rotational energy should be remunerated. This depends on the volume of rotational energy needed and the number of power producers able to provide inertia without altering their production. Remunerating all parties supplying the grid with inertia reduces the risk of rotating power plants shutting down, should low prices in Elbas, due to unexpected renewable power, occur. However, hydropower producers not cleared in Elspot may decide to operate in order to supply rotational energy through trading in Elbas, replacing less predictable power sources. This will however result in an energy ineffective production mix, using storable water instead of instantaneous wind or solar power. Additionally, the total cost for the TSO will be high as synchronous generators already cleared in the day-ahead market are unnecessarily remunerated.

An alternative is to only remunerate the providers of the rotational energy needed to meet the system requirement, excluding rotational energy provision from synchronous generation. This market design requires participants to be able to provide rotational power without changing their production. The design is considerably more cost efficient as it remunerates fewer participants. However, a high remuneration provides incentives for power producers to speculate in refraining from day-ahead market participation at times they believe that the rotational energy market will be activated. Should a producer follow this strategy with several hydropower plants, the system inertia may drop below the system requirement as a direct result of the speculation. This shows one of the potential flaws of this market design, with exploitation of market power. Hydropower producers may also downward regulate power stations in Elbas, should the necessary up regulation be available. It is however assumed that the income from Elspot will be dominating, marginalizing this problem.

It is concluded that if both the volume of rotational energy needed and the number of power producers with technology to provide inertia without altering their production is low, all parties providing rotational energy should be remunerated. If the volume and producers with the necessary technology is high, only the parties providing the needed rotational energy after Elspot is cleared should be remunerated.

A market for inertia is already under development in Ireland, where Synchronous Inertial Response (SIR) has been approved as a new service [27]. The service is only approved in principle and not yet implemented, but it still emphasizes the importance of a sufficient amount of inertia in a power system. The SIR volume for which suppliers of the service will be remunerated is based on the provided rotational kinetic energy multiplied by the SIR factor (SIRF). SIRF is given as the rotational energy of a synchronous machine operating at nominal frequency divided by the minimum power output at which the unit can operate while providing reactive power. The service may only be offered by synchronous machines, excluding synthetic inertia.

2.3.4 Technologies for inertia provision without altering power production

Rotating synchronous condensers

A rotating synchronous condenser (SC) is a synchronous machine that operates without any load or prime mover. SCs can inject or absorb reactive power, a service remunerated by the TSO, and have traditionally been used to improve voltage conditions. From the 1980s, power electronics were preferred due to lower investment and maintenance costs [28]. In recent years, attention has been brought to two other attributes of rotating SCs; they provide inertia and counteract faults related to the commutating of rectifiers when placed near HVDC cable connections [29]. This substantially increases their utility in the power system. In 2008 a rotating SC was installed in Feda, a substation located in southern Norway. In relation to system inertia, the investment costs are estimated to 40 100 kNOK/MWs/year [30].

Hydropower generators operating as SCs

By equipping a hydropower station with a compressor, water may be pumped out of the turbine chamber. This would allow the turbine to idle, acting as a SC. Several costs are associated with SC mode of operation. These include, but are not limited to, higher maintenance costs due to an increased number of operational hours and technical components, operation of compressors and cooling system and power consumption due to friction. If the cooling system uses water that could potentially be used for production, there is a cost associated with the resulting lost income as well. In [30] the investment cost was estimated to 10-20 kNOK/MWs.

Synthetic inertia

By employing power electronics, wind power and HVDC cables may couple their power output to the system frequency, allowing them to imitate the effects of natural inertia. By temporarily reducing its angular velocity, wind turbines can increase their power output, borrowing energy from the rotor. Such a procedure is followed by a recovery period of decreased power output as the rotor increases its speed back to its rated value. During the recovery period, other energy sources are needed to maintain the power balance. HVDC cables may also contribute with synthetic inertia, as long as active power is available in the connected power system. In [23] a more detailed description of these two possibilities is given.

Hydropower station operation

If a hydropower producer owning several power stations has planned to operate only some of them at, or close to, maximum production, it would be possible to reduce

the power output enough to include more hydropower stations producing at a low set point. Thus, by distributing planned production over a larger number of power stations, the producer may provide more inertia without altering production at times when this might be needed.

2.3.5 Comparison of strategies

In [30], three strategies to ensure sufficient inertia for different scenarios are evaluated. These are investment in SC mode of operation of hydropower stations, reducing the dimensioning fault and increasing the amount of hydropower stations by reducing wind power. The strategies are evaluated from a socioeconomic view and the system requirement is assumed to be 90 GWs. It is found that reducing the dimensioning fault has the lowest socioeconomic cost.

Considering investment in SC mode of operation of hydropower stations the hydropower producer would require a remuneration for supplying the service. In this thesis, the impacts of SC mode of operation on hydropower scheduling will be studied and the required remuneration evaluated.

2.4 Stochastic Dual Dynamic Programming

This section will explain the SDDP algorithm the model is based on. The optimization technique is first explained for a deterministic case, using a simple income maximization problem as an example to provide a more intuitive understanding. SDDP and Dual Dynamic Programming (DDP) have previously been described in [31] and [32], which are both used as references.

2.4.1 Dual dynamic programming

In [32] and [31] DDP is explained in a step-wise manner for a two-stage deterministic optimization problem. This explanation follows that of [32] and [31] closely both in notation and procedure, with some exceptions to better suit the model used in this thesis. In [32], the following cost minimization problem is used as a starting point:

$$z = \min\ C_1 x_1 + C_2 x_2 \tag{2.6a}$$

s.t.

$$A_1 x_1 \geq b_1 \tag{2.6b}$$

$$E_1 x_1 + A_2 x_2 \geq b_2 \tag{2.6c}$$

Vectors x_1 and x_2 are the state and decision variables for stage 1 and 2. C_1 and C_2 are the associated costs. A and E are system specific matrices. Equation (2.6b) shows the first stage constraints on the system and equation (2.6c) connects the first

and second stage of the problem. To visualize a multistage problem, stage 1 can be regarded as a representation of the present and stage 2 a representation of the future. The model used in this thesis has an objective of maximizing income, so the starting point is altered to an income maximization problem:

$$\max\ I_1x_1 + I_2x_2 \tag{2.7a}$$

s.t.

$$A_1x_1 \leq b_1 \tag{2.7b}$$

$$E_1x_1 + A_2x_2 \leq b_2 \tag{2.7c}$$

Where I_1 and I_2 is the income for stage 1 and 2 respectively. By setting some feasible solution to the first stage x_1^* problem, i.e. a solution that satisfies constraint (2.7b), the second stage problem becomes

$$\max\ I_2x_2 \tag{2.8a}$$

s.t.

$$A_2x_2 \leq b_2 - E_1x_1^* \tag{2.8b}$$

As x_1^* is known, it has been moved it to the right hand side of constraint (2.8b). Let (2.8a) be denoted as the second stage income function, α_2. By solving the second stage problem for different values of x_1^*, an approximation of α_2 can be obtained. By utilizing DDP, the approximation of α_2 can be obtained from the dual information of the second stage problem as will be shown. Following the decision of setting x_1^* first, the problem can be formulated recursively.
Stage 2:

$$\alpha_2(x_1) = \max\ I_2x_2 \tag{2.9a}$$

s.t.

$$A_2x_2 \leq b_2 - E_1x_1 \tag{2.9b}$$

Stage 1:

$$\alpha_1(b_1) = \max\ I_1x_1 + \alpha_2(x_1) \tag{2.10a}$$

s.t.

$$A_1x_1 \leq b_1 \tag{2.10b}$$

The value of b_1 in equation (2.10b) can be seen as an initial state for the first stage recursive equation. It is possible to substitute $b_1 = b_1' + E_0x_0$ so that the first stage problem becomes a function of x_0. The alternate formulation of the first stage recourse equation would then be

$$\alpha_1(x_0) = \max\ I_1x_1 + \alpha_2(x_1) \tag{2.11a}$$

s.t.

$$A_1x_1 \leq b_1' + E_0x_0 \tag{2.11b}$$

This formulation is more consistent in notation with the second stage problem and gives a better understanding of the future income function $\alpha_{t+1}(x_t)$ for a problem with more than two stages. However, for simplicity the formulation in (2.10) will be used in the following derivations.

The dual of the second-stage recourse problem is given by

$$\alpha_2(x_1) = \min \ \pi(b_2 - E_1 x_1) \tag{2.12a}$$

$$\text{s.t.}$$

$$\pi A_2 \geq I_2 \tag{2.12b}$$

where π is the dual value of equation (2.9b). By the strong duality theorem[5] equation (2.12a) represents α_2. Note that in the dual formulation x_1 is found in the objective function (2.12a) and that there are no state and decision variables in constraint (2.12b). The consequence of this is that the feasible region defined by (2.12b) can be characterized independently of the objective function (2.12a). From Linear Programming (LP) it is known that the basic solutions of (2.12a) are the vertices of the aforementioned feasible region. By defining these vertices as a set $\Pi = \{\pi^1, \pi^2, ...\pi^{\mathcal{P}}\}$, problem (2.12) can be written as

$$\alpha_2(x_1) = \min \ \pi^j(b_2 - E_1 x_1) \tag{2.13a}$$

$$\text{s.t.}$$

$$\pi^j \in \Pi \tag{2.13b}$$

Consider now the following maximization problem.

$$\alpha_2(x_1) = \max \ \alpha_2 \tag{2.14a}$$

$$\begin{aligned} &\text{s.t.} \\ &\alpha_2 \leq \pi^1(b_2 - E_1 x_1) \\ &\alpha_2 \leq \pi^2(b_2 - E_1 x_1) \\ &\quad \vdots \\ &\alpha_2 \leq \pi^{\mathcal{P}}(b_2 - E_1 x_1) \end{aligned} \tag{2.14b}$$

where α_2 is a scalar variable. Problem (2.14) states that α_2 is less than or equal to every $\pi^j(b_2 - E_1 x_1)$. Because (2.14) is a maximization problem, α_2 will meet the smallest $\pi^j(b_2 - E_1 x_1)$, i.e. $\min\{\pi^j(b_2 - E_1 x_1)\}$, with equality. This entails that problem (2.14) is an equivalent of (2.13). Every $\pi^j(b_2 - E_1 x_1)$ defines a hyperplane, or cut. In this thesis, these will be referred to as cuts. Following the formulation of

[5] If a linear programming problem has an optimal solution producing a finite optimal value, the dual of that problem has an optimal solution producing a finite optimal value that coincides with that of the original problem.

problem (2.14), α_2 will have the geometric properties of a piecewise linear function, where each linear segment is a cut.

The calculation of all vertices π^j in Π can be problematic. Instead a subset $\mathcal{H} \subset \Pi$ is calculated for different feasible solutions, $x^*_{1,j}$, $j \in \mathcal{H}$, of the first stage problem (2.10), as shown below:

$$\alpha_2(x^*_{1,j}) = \max\ I_2 x_2 \tag{2.15a}$$

$$\text{s.t.}$$

$$A_2 x_2 \leq b_2 - E_1 x^*_{1,j} \qquad \forall j \in \mathcal{H} \tag{2.15b}$$

Using the vertices calculated by solving (2.15) and looking at a small deviation from the feasible solution $x_1 - x^*_{1,j}$, as in [33], provides the sought approximation of the second stage income function:

$$\alpha_2(x_1) = \max\ \alpha_2 \tag{2.16a}$$

$$\text{s.t.}$$

$$\alpha_2 \leq \pi^j(b_2 - E_1(x_1 - x^*_{1,j})) \qquad \forall j \in \mathcal{H} \tag{2.16b}$$

A geometric representation of how the cuts make up a piecewise linear function is shown in Figure 2.11. As $\mathcal{H}$ is a subset of Π, the approximation will be an upper bound to the actual second stage income function. The combination of this

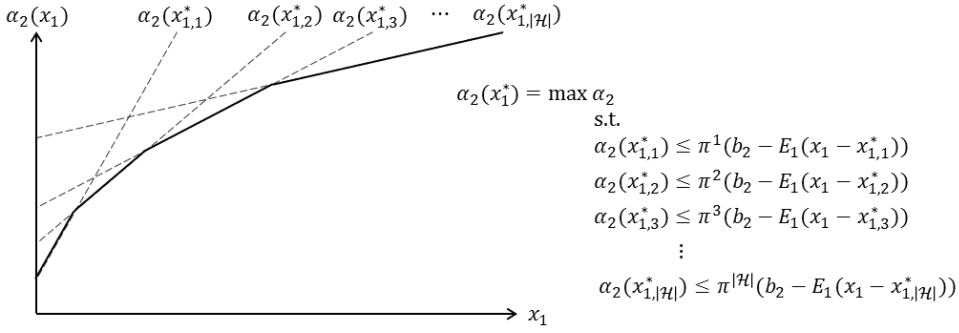

Figure 2.11: Approximation of the second stage income function.

approximation and the first stage problem (2.10) results in the final formulation for the two-stage problem. Because the approximation of α_2 is an upper bound, the optimal solution value to the final formulation will be an upper bound to the actual

optimal income.

$$\overline{z} = \max\ I_1 x_1 + \alpha_2 \tag{2.17a}$$
$$\text{s.t.}$$
$$A_1 x_1 \leq b_1 \tag{2.17b}$$
$$\alpha_2 - \pi^j(b_2 - E_1(x_1 - x^*_{1,j})) \leq 0 \qquad \forall j \in \mathcal{H} \tag{2.17c}$$

A lower bound to the actual optimal income is found by solving the two stage recursive problem (2.10) and (2.9) for the initial optimal solution x^*_1.

$$\underline{z} = I_1 x^*_1 + \alpha_2(x^*_1) \tag{2.18}$$

The difference between the upper and lower bound $\overline{z} - \underline{z}$ can be used as a measure to determine whether the solution is accurate enough. By iteratively adding new sets of cuts derived from samples of feasible solutions, the bounds will converge. When the difference reaches a set tolerance, the problem is solved.

2.4.2 Stochastic extension

To handle the uncertainties of the real world, the deterministic DDP method above can be extended to include a stochastic dimension. As in [32], two possible scenarios of the second stage will be considered. These are represented by realizations of the random right hand side vectors b_{21} and b_{22} with probabilities p_1 and p_2, respectively. The two scenarios also have corresponding state and decision variable vectors x_{21} and x_{22}.

$$z = \max\ I_1 x_1 + p_1 I_2 x_{21} + p_2 I_2 x_{22} \tag{2.19a}$$
$$\text{s.t.}$$
$$A_1 x_1 \leq b_1 \tag{2.19b}$$
$$E_1 x_1 + A_2 x_{21} \leq b_{21} \tag{2.19c}$$
$$E_1 x_1 + A_2 x_{22} \leq b_{22} \tag{2.19d}$$

where $p_1 + p_2 = 1$. Following the same procedure as in equations (2.8) - (2.15) the second stage income function can be approximated by

$$\alpha_2(x_{1,j}) = \max\ p_1 \alpha_{21} + p_2 \alpha_{22} \tag{2.20a}$$
$$\text{s.t.}$$
$$\alpha_{21} \leq \pi^j_1(b_{21} - E_1(x_1 - x^*_{1,j})) \qquad \forall j \in \mathcal{H}_1 \tag{2.20b}$$
$$\alpha_{22} \leq \pi^j_2(b_{22} - E_1(x_1 - x^*_{1,j})) \qquad \forall j \in \mathcal{H}_2 \tag{2.20c}$$

where π^j_1 and π^j_2 are the vertices corresponding to scenario 1 and 2 respectively, calculated for the feasible solutions $x^*_{1,1}$ and $x^*_{1,1}$. The upper bound formulation can

then be written as

$$\overline{z}_t = \max\ I_1 x_1 + p_1 \alpha_{21} + p_2 \alpha_{22} \tag{2.21a}$$

s.t.

$$A_1 x_1 \leq b_1 \tag{2.21b}$$

$$\alpha_{21} - \pi_1^j (b_{21} - E_1(x_1 - x_{1,j}^*)) \leq 0 \qquad \forall j \in \mathcal{H}_1 \tag{2.21c}$$

$$\alpha_{22} - \pi_2^j (b_{22} - E_1(x_1 - x_{1,j}^*)) \leq 0 \qquad \forall j \in \mathcal{H}_2 \tag{2.21d}$$

In problems (2.20) and (2.21), $\mathcal{H}_1$ and $\mathcal{H}_2$ are subsets of $\mathcal{H}$.

An important aspect of SDDP is that with stage-wise independent and identically distributed (iid) realizations of the stochastic right hand side variable, the cuts can be shared among scenarios, and the future cost function is scenario independent. An illustration of this is shown in In Figure 2.12. Each time stage after the initial stage has the same three data realizations. If the data is stage dependent, the scenario tree quickly becomes very large, but with stage-wise independence the data points can be aggregated in each stage.

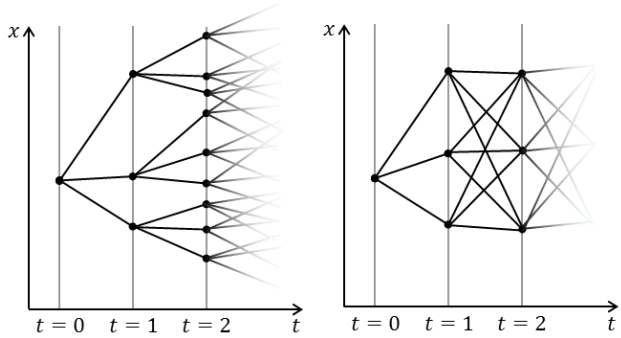

Figure 2.12: Stage-wise dependent scenario tree (left) and stage-wise independent scenario tree (right).

By extending the two-stage problem a general SDDP optimization algorithm can be obtained. The algorithm uses the definitions in Table 2.5. The variables and parameters are the same as in the two-stage example.

The algorithm solves the problem in two stages; a forward iteration and a backward iteration. The starting point of the algorithm is the initialization shown in Table 2.6.

The forward iteration begins by sampling a set of scenarios, i.e. a set of realizations of the right hand side. The corresponding LP problems are solved for each scenario

Index	Set	Description
t	$\mathcal{T}$	Time stages
n	$\mathcal{N}$	Scenarios
j	$\mathcal{H}$	Hyperplanes/cuts
d	$\mathcal{D}$	Discrete realizations of the random variable b_t

Table 2.5: SDDP algorithm definitions.

Future income function	$\hat{\alpha}_{t+1}(x_t) = 0,\ \forall t \in \mathcal{T}$
Sets of hyperplanes/cuts	$\mathcal{H} = 0$
Initial optimal solution	$x_0^* = 0$

Table 2.6: SDDP algorithm initialization.

in the first time stage, which gives a set of first stage optimal solutions, one for each scenario. This process is repeated for every time stage. Then, the upper and lower bounds are calculated. The upper bound is the given by the optimal solution for the first stage problem, as in the deterministic case. The lower bound is estimated from the solutions from the forward iteration. If the difference is larger than the convergence tolerance limit, the backward iteration is performed.

The backward iteration is performed by solving the LP problem for the optimal solutions found in the forward iteration starting in the last time stage. Dual values are calculated for all the possible realizations. When iterating backwards to the previous time stage, the dual values are used to form a cut added to the future income function.

The first forward iteration is solved without any cuts. This implies that the LP problem is optimized for the current time stage without regard to the future income. When cuts are added, the future income is taken to account in the LP problem by the future income function. As previously mentioned, cuts can be shared amongst scenarios. For computational efficiency, only violated cuts are added, tightening the solution space until the bounds converge within the tolerance limit.

The forward iteration and backward iteration algorithms are shown in Algorithm 2.1 and Algorithm 2.2, respectively.

Algorithm 2.1: Forward SDDP iteration

for $t = 1...|\mathcal{T}|$ **do**
  for $n = 1...|\mathcal{N}|$ **do**
    Sample a set of scenarios $b_{t,n}$ from the realizations of $b_{t,d}, d \in \mathcal{D}$
    Solve forward LP problem:

$$\max\ I_t x_{t,n} + \hat{\alpha}_{t+1}$$
$$\text{s.t.}$$
$$A_t x_{t,n} \leq b_{t,n} - E_{t-q} x^*_{t-1,n}$$
$$\hat{\alpha_{t+1}} - \frac{1}{|\mathcal{D}|} \Sigma_{d \in \mathcal{D}} \pi^j_{t+1,n,d} (b_{t+1,d} - E_t(x_{t,n} - x^*_{t,n,j})) \leq 0, \quad \forall j \in \mathcal{H}$$

    Store the optimal solution $x^*_{t,n}$ and I_t
  end
end
Calculate upper and lower bounds:
$\overline{z} = I_1 x^*_1 + \hat{\alpha}^*_2$
$\underline{z} = \frac{1}{|\mathcal{N}|} \Sigma_{n \in \mathcal{N}} \Sigma_{t \in \mathcal{T}}\ I_t x^*_{t,n}$
if $\overline{z} - \underline{z} \leq$ *Tolerance limit* **then**
  End
else
  Backward iteration
end

Algorithm 2.2: Backward SDDP iteration

$\mathcal{H} = \mathcal{H} + 1$
for $t = |\mathcal{T}|..2$ **do**
  for $n = 1...|\mathcal{N}|$ **do**
    for $d = 1...|\mathcal{D}|$ **do**
      Solve the backward LP problem:

$$\max\ I_t x_{t,n} + \hat{\alpha}_{t+1}$$
$$\text{s.t.}$$
$$A_t x_{t,n,d} \leq b_{t,d} - E_{t-q} x^*_{t-1,n} \qquad \pi^j_{t,n,d}$$
$$\hat{\alpha_{t+1}} - \frac{1}{|\mathcal{D}|} \Sigma_{d \in \mathcal{D}} \pi^j_{t+1,n,d} (b_{t+1,d} - E_t(x_{t,n} - x^*_{t,n,j})) \leq 0, \quad \forall j \in \mathcal{H}$$

      Store dual values $\pi^j_{t,i,d}, \forall j \in \mathcal{H}$, for the constraints, and form an additional cut for stage $t-1$
    end
  end
end
Go to forward recursion

2.4.3 Practical considerations of SDDP

The main characteristics of SDDP compared to other optimization techniques is that SDDP requires a concave future income function and is stage wise independent. The first characteristic implies that SDDP can only be used to solve convex problems[6] and cannot handle non-linearities. This will often induce simplifications and relaxations in the modelling of various problems. The second characteristic, is related to the curse of dimensionality which entails that the run time of the stage-wise dependent optimization techniques increases exponentially with the number of state and decision variables due to the increase in sequential combinations. This is a problem both for the modelling of complex systems and to keep the number of discretizations at a satisfying level. The SDDP method does not suffer from the curse of dimensionality as it is defined in this thesis.

An aspect of stochastic programming that should be noted is the importance of relatively complete recourse. A stochastic program has relatively complete recourse if every feasible solution of a stage t also has a feasible solution in the next stage, $t-1$ [35]. This property should be kept in mind when modelling a problem with this optimization method.

2.5 Relevance to Hydropower Scheduling

To better understand the relevance of sections 2.1, 2.3 and 2.4, consider the income maximization problem (2.7). For a hydro power scheduling problem, the decision part of variables x_1 and x_2 would include production, capacity allocation, provision of rotational energy, spillage and bypass. The state of the system would be given by reservoir levels and the operational states of power stations. The income vectors include income for production, provision of rotational energy and capacity allocation in one or several of the markets described in sections 2.1 and 2.3. Operational costs and penalties for spillage and bypass would also be included in the vector. The constraints would include reservoir and energy balances, limits on production and reservoir volumes, and other operational constraints. The dual values of the constraints most notably include the water value.

[6] For a maximization problem this refers to a concave objective function. A problem can either be convex or non-convex. There is no such thing as a concave problem [34].

3 Methodology

In this chapter, the combined SDDP and Simulator Model used in this thesis will be described. It has previously been described in [4] and [36], which have been used as references.

The model is solved over a set of time stages $t \in \mathcal{T}$. Each time stage consists of a number of time blocks $w \in \mathcal{W}$. The model's objective is to maximize income by selling power in the day-ahead market, capacity in the weekly FCR-N market and rotational energy to a hypothetical inertia market. The first section of this chapter will describe the strategy part of the model and the application of SDDP to a hydropower scheduling problem. The second section will describe the Simulator Model and the hydropower scheduling problem modelled with MIP.

3.1 Strategy Model

The Strategy Model is based on an extended version of the combined SDP/SDDP algorithm presented in [37] which incorporates sales of capacity and provision of rotational energy. This section will derive the hydropower scheduling problem, which is solved for each time stage. Additionally, the simplifications necessary to employ the SDDP algorithm will be displayed.

3.1.1 Hydropower module

The hydro system is modelled by combining hydropower modules. A hydropower module is built up of a reservoir and a power station, with associated variables and parameters. Information about the connectivity to other modules is included as well.

Reservoir

Figure 3.1 shows how a reservoir is modelled. The reservoir balance for time block w

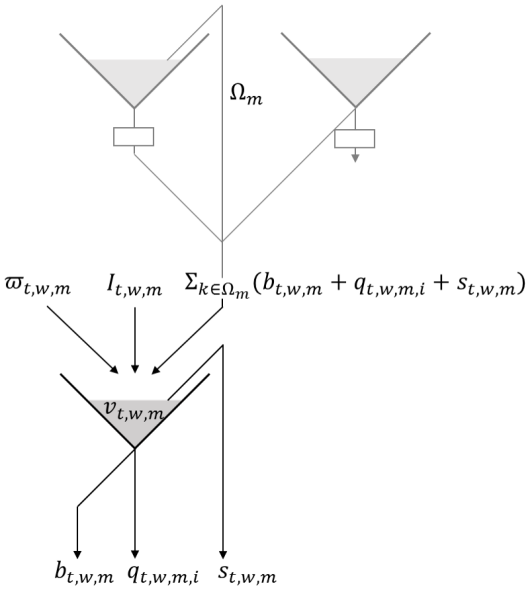

Figure 3.1: Illustration of a reservoir with associated variables.

in time stage t for a hydropower module m is given by the equation

$$\begin{aligned} & v_{t,w,m} + \Sigma_{i\in\mathcal{S}_m} q_{t,w,m,i} + s_{t,w,m} \\ & \quad - \Sigma_{k\in\Omega_m}(s_{t,w,k} + b_{t,w,k} + \Sigma_{i\in\mathcal{S}_m} q_{t,w,k,i}) \\ & \qquad + b_{t,w,m} - \varpi_{t,w,m} = v_{t,w-1,m} + I_{t,w,m}(z_{t-1,m}), \qquad \forall w \in \mathcal{W}, \forall m \in \mathcal{M} \end{aligned} \tag{3.1}$$

which states that the difference in reservoir volume from the previous to the current time block must be equal to the sum of water flowing in and out of the reservoir[1]. For the coupling of time stages, time block $w = 0$ in time stage t is a reference to time block $w = |\mathcal{W}|$ in time stage $t - 1$, i.e. the last time block of the previous time stage.

The inflow model which will be shown in Section 3.1.2 has the ability of generating negative inflows. Should the reservoir be empty at the time a negative inflow is sampled, the reservoir volume would also become negative. To avoid this and maintain relatively complete recourse, the fictitious tank water variable is included in the balance. The use of tank water is heavily penalized in the objective function and will influence the cuts which will be described in Section 3.1.8. For the following iteration, the model will have a strong incentive to avoid emptying the reservoir [38].

[1]Positive water flow is defined as water flowing out of the reservoir

Spillage is also penalized in the objective function, but with a small cost compared to the tank water. This is to avoid spillage in inappropriate states, e.g. when the reservoir is not full. The contribution of tank water and spillage from a hydropower module to the objective function is given by the following term.

$$-(\lambda^T \varpi_{t,w,m} + \lambda^F s_{t,w,m}) \tag{3.2}$$

where λ^T and λ^F is the cost of tank water and spillage respectively.

Power station

The power station is modelled by a piecewise linear curve of PQ segments, shown in Figure 3.2. As mentioned earlier, the SDDP algorithm can only be used to solve convex problems. Hence, it is a necessity of the SDDP algorithm that this curve is concave. The gradient of each segment i, scaled to time block w, is the power equivalent $\gamma_{w,i}$, which in turn is used to derive the energy equivalent $\eta_{w,i}$. Let $q_{t,w,m,i}$ be the water flow of segment $i \in \mathcal{S}_m$, for hydropower module m, time stage t and time block w. The energy and power will then be given by $\Sigma_{i \in \mathcal{S}_m} \eta_{w,m,i} q_{t,w,m,i}$ and $\Sigma_{i \in \mathcal{S}_m} \gamma_{w,m,i} q_{t,w,m,i}$ respectively.

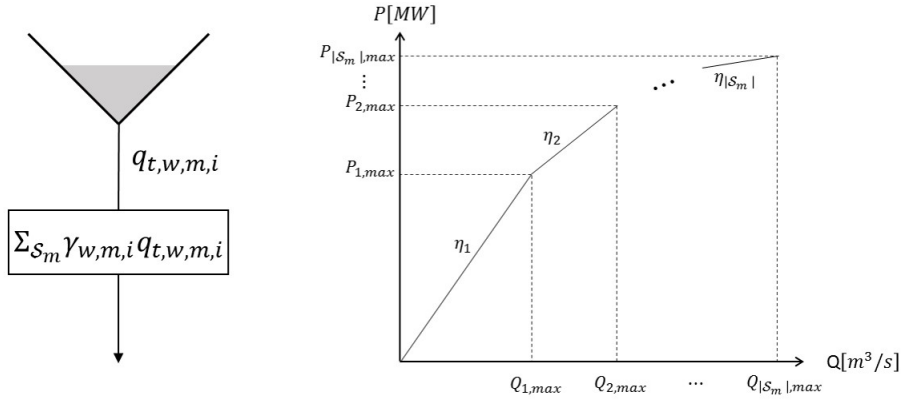

Figure 3.2: Illustration of a power station (left) and PQ segment curve (right).

In [37] it is assumed that

$$P = f(Q)\frac{h}{h_0} \tag{3.3}$$

where $f(Q)$ is the piecewise linear curve mentioned above and $\frac{h}{h_0}$ a head correction factor. Although this results in a more correct modelling of the power station, [37] further states that it may lead to non-convex problems. Consequently, the power station is modelled with a constant head. In [39] it is argued that this is a fair approximation for power stations with large head compared to the head variations.

3.1.2 Inflow

The inflow is sampled per time stage and is modelled in a similar manner to [39]. As mentioned earlier, the SDDP algorithm relies on iid right hand side variables, so that every state of the system is independent of its stage. The inflow however, often shows strong correlation from one time step to another, stated in [39]. This is solved by including information about the previous inflows in the state vector. Historical inflow data is used to create an inflow distribution. Every available year of inflow data is treated as an inflow scenario. From each year, $\mathcal{T}$ weeks are sampled (if $\mathcal{T}$ is more than 52, all weeks of every available year will be sampled, and the distribution will be repeated for the weeks of the next year). The inflow for week t and scenario y is denoted I_t^y. To eliminate seasonal variations and ensure stage-wise independence, the weekly inflows of each inflow scenario are normalized

$$z_t = \frac{I_t - \overline{I_t}}{\sigma_t}, \quad \forall t \in \mathcal{T} \tag{3.4}$$

where $\overline{I_t}$ is the mean of the inflows in week t for all inflow scenarios $y \in \mathcal{Y}$, and σ_t is the corresponding sample standard deviation. A first stage auto-regressive model is used to obtain a linear stochastic inflow model.

$$z_t = \psi z_{t-1} + \epsilon_t, \quad \forall t \in \mathcal{T} \tag{3.5}$$

In the auto-regressive model, ψ is the sequential auto correlation of the inflows I_t^y and ϵ_t is white noise given as a random variable with the distribution $\epsilon_t \backsim N(0, \sigma^2)$, making it independent of z_{t-1}. This model is not always very accurate, but it does provide computational feasibility. In practice, it has been found that it is best to model each season separately [39].

Rewriting (3.4) with respect to I_t and substituting z_t with equation (3.5) gives

$$I_t(z_{t-1}) = \sigma_t(\psi z_{t-1} + \epsilon_t) + \overline{I_t} \tag{3.6}$$

Naturally the inflow will be different for each hydropower module so the notation $I_{t,m}$ will be used. As the inflow is given for a whole week, the inflow for time block w is given by

$$I_{t,w,m}(z_{t-1,m}) = \frac{W_w}{\Sigma_{w \in \mathcal{W}} W_w} I_{t,m}(z_{t-1,m}), \quad \forall m \in \mathcal{M}, \forall w \in \mathcal{W} \tag{3.7}$$

3.1.3 Energy balance

The energy balance is given by

$$\Sigma_{m \in \mathcal{M}} \Sigma_{i \in \mathcal{S}_m} \eta_{w,m,i} q_{t,w,m,i} - e^S_{t,w} + e^P_{t,w} = 0, \quad \forall w \in \mathcal{W} \tag{3.8}$$

stating that the sum of energy produced in all modules must be equal to the difference in energy sold and bought.

Sales and purchases of energy are included in the objective function by the following term

$$\lambda_t^S \kappa_{t,w}^S (e_{t,w}^S - \tau e_{t,w}^P) \tag{3.9}$$

where λ_t^S and $\kappa_{t,w}^S$ is the spot price and energy profile respectively, further described in Section 3.1.7. τ is a model parameter greater than 1, representing a transaction fee for purchasing energy.

3.1.4 Capacity reservation

Delivery to the capacity market is in the form of spinning capacity supplying up or down regulation. This is represented by the following constraints

$$\Sigma_{i \in \mathcal{S}_m} \gamma_{w,m,i} q_{t,w,m,i} + p_{t,w,m}^B \leq P_m^{max}, \qquad \forall m \in \mathcal{M}, \forall w \in \mathcal{W} \tag{3.10}$$

$$\Sigma_{i \in \mathcal{S}_m} \gamma_{w,m,i} q_{t,w,m,i} - \frac{P_m^{min} + P_m^{B,max}}{P_m^{B,max}} p_{t,w,m}^B \geq 0, \qquad \forall m \in \mathcal{M}, \forall w \in \mathcal{W} \tag{3.11}$$

where $p_{t,w,m}^B$ is the spinning capacity. The maximum capacity allocation possible, $P_m^{B,max}$, is given by the droop setting in the turbine governor, S_m, by the relation:

$$P_m^{B,max} = \frac{100\%}{S_m} \frac{P_m^{max}}{f_0} \Delta f \tag{3.12}$$

The factor in front of $p_{t,w,m}^B$ in the down regulation constraint (3.11), decreases the solution space in regard to sales of capacity and more viable results will be achieved [38]. Capacity sold in the FCR-N weekly market must be available for every time block of the capacity delivery period. This is given by the following constraint

$$\Sigma_{m \in \mathcal{M}} \; p_{t,w,m}^B - p_{t,c}^{B_{tot}} = 0, \quad \forall c \in \mathcal{C}, \forall w \in \mathcal{W} \tag{3.13}$$

where $p_{t,c}^{B_{tot}}$ is the total spinning capacity.

Spinning capacity has the following contribution to the objective function

$$\lambda_{t,c}^B p_{t,c}^{B_{tot}} \tag{3.14}$$

where $\lambda_{t,c}^B$ is the price for capacity allocation, further described in Section 3.1.7.

3.1.5 Start-up cost

There are costs associated with both the start-up and stopping of a power station. For hydropower, the most important costs are caused by malfunctions in the control

equipment and maintenance of windings and mechanical equipment [40]. Only the start-up cost is included in the model, so the start-up and stop cost are added together as a start must follow a stop. Ideally, this would be modelled as a binary cost, but the SDDP algorithm can only be solved for LP problems. The start-up is therefore modelled by relaxed binary constraints.

$$\begin{aligned}
&\Sigma_{i\in\mathcal{S}_m} q_{t,w,m,i} - Q_m^{min} u_{t,w,m}^L \\
&\quad - (Q_m^{max} - Q_m^{min}) u_{t,w,m}^H = 0, && \forall m \in \mathcal{M}, \forall w \in \mathcal{W} && (3.15)\\
&u_{t,w,m}^L - u_{t,w,m}^H \geq 0, && \forall m \in \mathcal{M}, \forall w \in \mathcal{W} && (3.16)\\
&u_{t,w,m}^L - u_{t,w-1,m}^L - \delta_{t,w,m} \leq 0, && \forall m \in \mathcal{M}, \forall w \in \mathcal{W} && (3.17)\\
&u_{t,w,m}^L, u_{t,w,m}^H, \delta_{t,w,m} \in [0,1], && \forall m \in \mathcal{M}, \forall w \in \mathcal{W} && (3.18)
\end{aligned}$$

Equation (3.15) states that the total discharge must be equal to the sum of discharge above and below minimum. Equation (3.17) couples the change between previous and current discharge below minimum with the start-up variable $\delta_{t,w,m}$. This variable is also associated with a cost in the objective function:

$$-\lambda^U \delta_{t,w,m} \tag{3.19}$$

where λ^U is the start-up cost. From the constraints it can be seen that a power station may vary its production between minimum and maximum at no cost, as $\delta_{t,w,m}$ is coupled to stage-wise changes only in $u_{t,w,m}^L$.

3.1.6 Provision of rotational energy

Similar to the start-up of a power station, SC mode of operation is modelled by relaxed binary variables.

$$\begin{aligned}
&u_{t,w,m}^L + o_{t,w,m} \leq 1 && \forall m \in \mathcal{M}, \forall w \in \mathcal{W} && (3.20)\\
&o_{t,w,m} - u_{t,w-1,m}^L - o_{t,w-1,m} - \delta_{t,w,m} \leq 0 && \forall m \in \mathcal{M}, \forall w \in \mathcal{W} && (3.21)
\end{aligned}$$

(3.20) limits simultaneous generation and SC operation. The start-up cost of SC mode of operation is approximately equal to that of generation. Transitioning from generation to SC mode has a small cost, which is neglected in the Strategy Model. These characteristics are modelled by (3.21).

When generating power or running as a SC, the power station provides the grid with an amount of rotational energy, E_m^R, dependent on power station specific parameters.

$$\begin{aligned}
&\Sigma_{m\in\mathcal{M}} E_m^R o_{t,w,m} - e_{t,w}^R = 0 && \forall w \in \mathcal{W} && (3.22a)\\
&\Sigma_{m\in\mathcal{M}} E_m^R (u_{t,w,m}^L + o_{t,w,m}) - e_{t,w}^R = 0 && \forall w \in \mathcal{W} && (3.22b)
\end{aligned}$$

(3.22a) and (3.22b) couples the provision of rotational energy to the power stations for two different market solutions.

The provision of rotational energy is included in the objective function by the following term

$$\lambda^R_{t,w} e^R_{t,w} \tag{3.23}$$
$$\tag{3.24}$$

where $\lambda^R_{t,w}$ is the price for provision of rotational energy, further described in Section 3.1.7.

From equations (3.23) it can be seen that (3.22a) provides the model with a market solution which remunerates rotational energy provided only by SC mode of operation while (3.22b) remunerates rotational energy provided by power generation as well. In the remainder of this chapter, (3.22a) is used.

3.1.7 Price and market modelling

Day-ahead prices

Similar to the inflow, the spot price has a strong sequential correlation [41]. Information about the previous prices must therefore be included in the system state. In contrast to the inflow, the spot price is included in the objective function as seen in equation (3.9). The consequence of this is that the future cost functions, which will be described in Section 3.1.8, cannot be guaranteed to be concave [39]. This is solved by modelling the spot price λ^S_t as discrete values so that it is represented by a set of price points $\zeta^r_t, r \in \mathcal{R}$.

It is further assumed that the price and inflow are uncorrelated. This simplification is done to establish the price and inflow distributions, as it would be difficult to include a correlation between them in the model. Since the inflow varies geographically and the spot price is set for the entire market this simplification is not seen as unreasonable when the model is solved for a small hydro system.

The following Markov model is used to describe the transitions between the discrete price points from time stage $t-1$ to t.

$$P(\lambda^S_t = \zeta^r_t | \lambda^S_{t-1} = \zeta^{r'}_{t-1}) = \rho_{r'r}(t), \quad \forall r, r' \in \mathcal{R} \tag{3.25}$$

In words, $\rho_{r'r}(t)$ is the probability that the spot price in time stage t will be equal to ζ^r_t, given that the spot price in time stage $t-1$ was $\zeta^{r'}_{t-1}$. The spot price in time stage t is calculated by generating a random variable between 0 and 1, and setting the price equal to the price point that has a higher accumulated probability than the

random variable. As the system is assumed to be a price taker, the price points are simulated using the fundamental market model, EMPS [42].

An energy price profile $\kappa^S_{t,w}$ is included to incorporate inter-time stage variations. The energy price profile consists of mean values of the time block prices in a time stage, scaled so that its average is 1.

Capacity prices

The capacity prices are modelled as a deterministic time series of historical prices in the FCR-N weekly market from recent years. The prices are given for the time blocks for capacity allocation $c \in \mathcal{C}$ as well as time stage $t \in \mathcal{T}$.

Rotational energy prices

The prices for provision of rotational energy are modelled as a deterministic time series with the same time resolution as the day-ahead prices; time block $w \in \mathcal{W}$ and time stage $t \in \mathcal{T}$. As the market will be active only at times of critically low inertia, the prices will be zero except for the time stages and blocks when inertia is needed. The prices for provision of rotational energy may be chosen freely to suit the purpose of employing the model. The necessary price to cover the investment cost associated with operating a hydropower station as a SC is directly related to the number of hours rotational energy is provided. This relation may be used to determine the prices and is illustrated in Figure 3.3, under the assumption of equal rotational energy prices when the market is active. Alternatively, the rotational energy price may be governed by the supply and demand of hydropower producers and the TSO, respectively. This would likely cause a price equal to the marginal cost of rotational energy provision. The marginal cost would either be equal to the operational costs of SC operation, or equal to the lost income from not participating in the Elspot market. The latter applies when considering the speculation of when the rotational energy market is active, discussed in Section 2.3.3. It should be possible to determine such a price by the dual values of demand and supply balance constraints of an aggregated system in a similar manner to the power price in the EMPS model, described in [42]. This is however not further studied in this thesis. The rotational energy market and its prices are further described in sections 4.1.4 and 4.1.5 respectively.

Market clearing

The various market prices for a time stage is known at the beginning of that time stage, clearing all markets simultaneously. This provides the optimization of resource allocation in a given time stage with more information than what is actually available

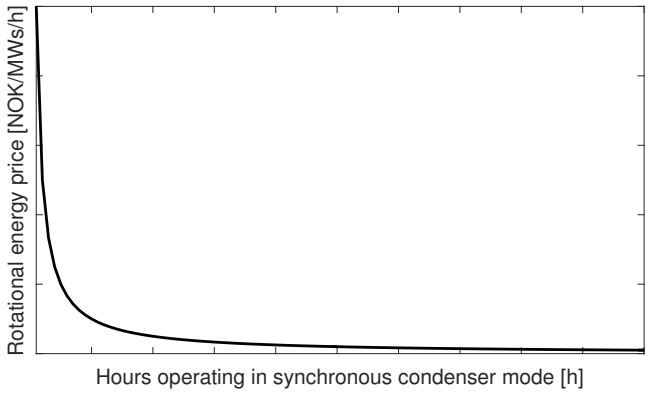

Figure 3.3: Illustration of necessary rotational energy price in relation to number of hours of SC mode of operation.

and fails to incorporate the sequential allocation process which governs short-term planning.

Altering the one-stage problem to allow simultaneous rotational energy provision and generation provides a strategy which incorporates sequential clearing of the day-ahead and rotational energy market. This done by removing Equation (3.20) and requires some modification of the results, to remove impossible operational states.

3.1.8 Cuts

As described in Section 2.4.2, the future income function is defined by cuts from the current state. Since the cuts couple the current time stage with the future, state variables that are coupled in time are included in the cuts. This includes the reservoir volume $v_{t,w,m}$, the start-up associated variable $u^L_{t,w,m}$, and the normalized inflow $z_{t,m}$. The time coupled constraints for these variables are reproduced below:

$$\begin{aligned} &v_{t,w,m} + \Sigma_{i\in\mathcal{S}_m} q_{t,w,m,i} + s_{t,w,m} \\ &\quad - \Sigma_{k\in\Omega_m}(s_{t,w,k} + b_{t,w,k} + \Sigma_{i\in\mathcal{S}_m} q_{t,w,k,i}) \\ &\qquad + b_{t,w,m} - \varpi_{t,w,m} = v_{t,w-1,m} + I_{t,w,m}(z_{t-1,m}) \end{aligned} \tag{3.1}$$

$$I_t(z_{t-1,m}) = \sigma_t(\psi z_{t-1,m} + \epsilon_t) + \overline{I}_{t,m} \tag{3.6}$$

$$u^L_{t,w,m} - u^L_{t,w-1,m} - \delta_{t,w,m} \leq 0, \tag{3.17}$$

It should be noted that (3.21) is also a time coupled constraint. Considering the added computational complexity compared to its impact on the objective function, it is assumed to have a negligible effect on the cuts.

The dual values represent the change in the objective function for a small change in the right hand side of a constraint. Restructuring the constraints in the manner showed in Section 2.4.2 results in the right hand sides being given by the previous time stage variables. The change in the objective function is given by the partial derivative with respect to that variable. For simplicity, the variables will be evaluated for time stage $t-1$ and scenario n in the following derivation. Because of stage-wise independence, the future income function is scenario independent.

Let $\pi^j_{t,n}$ be the dual value of constraint (3.1). Being the dual value of the reservoir balance, $\pi^j_{t,n}$ is the water value; the increase in the objective function for a marginal increase in reservoir volume. The right hand side of the constraint consists of both $v_{t-1,n}$ and $I_(z_{t-1,n})$.

$$\pi^j_{t,n} = \frac{\partial \alpha_t}{\partial v_{t-1,n}} = \frac{\partial \alpha_t}{\partial I_t(z_{t-1,n})} \tag{3.26}$$

It is desirable to observe the change in α_t for the previous time stage variables, i.e. z_{t-1} and not I_t. Observe that

$$\frac{\partial \alpha_t}{\partial z_{t-1,n}} = \frac{\partial \alpha_t}{\partial I(z_{t-1,n})} \frac{\partial I(z_{t-1,n})}{\partial z_{t-1,n}} \tag{3.27}$$

From equation (3.6) it can be seen that

$$\frac{\partial I(z_{t-1,n})}{\partial z_{t-1,n}} = \sigma_t \psi \tag{3.28}$$

Let $\mu^j_{t,n}$ be the dual value referring to $z_{t-1,n}$ given by

$$\mu^j_{t,n} = \frac{\partial \alpha_t}{\partial z_{t-1,n}} = \pi^j_{t,n} \sigma_t \psi \tag{3.29}$$

Solving the differential equations for α_t:

$$\int_{\alpha^*_t}^{\alpha_t} \partial \alpha_t = \int_{v^*_{t-1,n}}^{v_{t-1,n}} \pi^j_{t,n} \partial v_{t-1,n} \tag{3.30}$$

$$\alpha_t - \alpha^*_t = \pi^j_{t,n}(v_{t-1,n} - v^*_{t-1,n}) + f(z_{t-1,n}, u^L_{t-1,n}) \tag{3.31}$$

and

$$\int_{\alpha^*_t}^{\alpha_t} \partial \alpha_t = \int_{z^*_{t-1,n}}^{z_{t-1,n}} \mu^j_{t,n} \partial z_{t-1,n} \tag{3.32}$$

$$\alpha_t - \alpha^*_t = \mu^j_{t,n}(z_{t-1,n} - z^*_{t-1,n}) + f(v_{t-1,n}, u^L_{t-1,n}) \tag{3.33}$$

The integrations are from the optimal solution, marked with (*), found in the forward stage, to a small deviation from this value, which is unknown. The difference between

them represents the change in the right hand side and the corresponding change in the objective function.

The same procedure is followed for $u^L_{t-1,n}$:
Let $\phi^j_{t,n}$ be the dual value of constraint (3.17)

$$\phi^j_{t,n} = \frac{\partial \alpha_t}{\partial u^L_{t-1,n}} \tag{3.34}$$

Solving the differential equation for α_t:

$$\int_{\alpha^*_t}^{\alpha_t} \partial \alpha_t = \int_{u^{L*}_{t-1,n}}^{v_{t-1,n}} \phi^j_{t,n} \partial u^L_{t-1,n} \tag{3.35}$$

$$\alpha_t - \alpha^*_t = \phi^j_{t,n}(u^L_{t-1,n} - u^{L*}_{t-1,n}) + f(v_{t-1,n}, z_{t-1,n}) \tag{3.36}$$

Aggregating equations (3.31), (3.33), and (3.36) gives

$$\alpha_{t+1} \leq \alpha^*_{t+1} + \pi^j_{t+1,n}(v_{t,n} - v^*_{t,n}) + \mu^j_{t+1,n}(z_{t,n} - z^*_{t,n}) + \phi^j_{t+1,n}(u^L_{t,n} - u^{L*}_{t,n}) \tag{3.37}$$

Following the argumentation in Section 2.4.2, this will be an upper bound to the actual future income function. It is therefore denoted $\hat{\alpha}_{t+1}$. Before adding this constraint to the problem, it is rewritten for time stage t and modified to incorporate time blocks and modules:

$$\begin{aligned} \hat{\alpha}_{t+1} \leq\ & \alpha^*_{t+1} + \Sigma_{m \in \mathcal{M}} \pi^j_{t+1,m}(v_{t,w,m} - v^*_{t,w,m}) \\ & + \Sigma_{m \in \mathcal{M}} \mu^j_{t+1,m}(z_{t,m} - z^*_{t,m}) \\ & + \Sigma_{m \in \mathcal{M}} \phi^j_{t+1,m}(u^L_{t,w,m} - u^{L*}_{t,w,m}), \qquad \forall j \in \mathcal{H}, w = |\mathcal{W}| \end{aligned} \tag{3.38}$$

The future income function is also added to the objective function.

A problem occurs in the final time stage, as the cuts are added for the future time stage. This is solved by adding an estimated end cut in the final iteration. Ideally a set of valid cuts would be used, but one end cut simplifies the results [4]. As shown in Section 2.4.1, the future income function is a concave piecewise linear function. The end cut is modelled by a single estimated water value. As a consequence, the estimate of the end reservoir volume value becomes poorer and poorer the larger the deviation from the reservoir volume used to find the end cut water value. Especially large end reservoir volumes might be valued too high. This is illustrated in Figure 3.4, where it can be seen that the actual and modelled end future income values are equal for $v^1_{|\mathcal{T}|}$, but for $v^2_{|\mathcal{T}|}$ there is a difference equal to $\alpha^{2*}_{|\mathcal{T}|+1} - \alpha^2_{|\mathcal{T}|+1}$. Additionally, the end cut consists only of a water value, while the future income function also includes the dual value of start-up. As a result, the value of running power plants at the end of the simulation period is not captured by the end cut. However, considering the size of the start cost, it can be argued that this has a negligible effect.

The end cut is given by the dual value $\pi^1_{|\mathcal{T}|+1,m}$ and a right hand side coefficient $b_{|\mathcal{T}|}$, shown in the following equation:

$$\hat{\alpha}_{|\mathcal{T}|+1} \leq \Sigma_{m\in\mathcal{M}} \pi^1_{|\mathcal{T}|+1,m} v_{|\mathcal{T}|,w,m} + b_{|\mathcal{T}|} \tag{3.39}$$

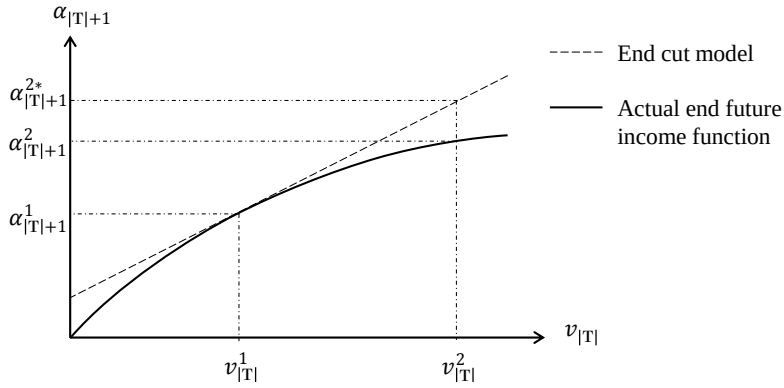

Figure 3.4: Illustration of the actual and modelled end reservoir values for two different end reservoir volumes.

3.1.9 System constraints

Certain system constraints are needed to facilitate power stations connected to multiple reservoirs. Such a power station is included in the modules of all connected reservoirs and modelled by the constraints below.

$$\Sigma_{m\in\mathcal{B}_m}(u^L_{t,w,m} + o_{t,w,m}) \leq 1 \qquad \forall w \in \mathcal{W} \tag{3.40}$$

$$\Sigma_{m\in\mathcal{B}_m} p^B_{t,w,m} \leq \max\{P^{B,max}_m \ : \ \forall m \in \mathcal{B}_m\} \qquad \forall w \in \mathcal{W} \tag{3.41}$$

(3.40) ensures that only one module is allowed to generate power or operate as a SC for modules sharing the same power station. As (3.40) is a tighter formulation than (3.20), the latter can be excluded for modules $m \in \mathcal{B}_m$ to improve computational efficiency. (3.41) limits the total possible sales of capacity for the same modules.

3.1.10 Objective

The objective function can be found by combining equations (3.2), (3.9), (3.14), (3.19), (3.23), and adding the future income function:

$$\begin{aligned}\hat{\alpha}_t = \max \Big\{ & \Sigma_{c\in\mathcal{C}} C_c \lambda^B_{t,c} p^{B_{tot}}_{t,c} \\ & + \Sigma_{w\in\mathcal{W}} W_w \Big[\lambda^R_{t,w} e^R_{t,w} + \lambda^S_t \kappa^S_{t,w} (e^S_{t,w} - \tau e^P_{t,w}) \\ & - \Sigma_{m\in\mathcal{M}} \big(\lambda^T \varpi_{t,w,m} + \lambda^F s_{t,w,m} \big) \Big] \\ & - \Sigma_{w\in\mathcal{W}} \Sigma_{m\in\mathcal{M}} \lambda^U \delta_{t,w,m} + \hat{\alpha}_{t+1} \Big\}\end{aligned} \tag{3.42}$$

3.1.11 One stage problem formulation

The above equations and constraints result in the following problem formulation for time stage t.

$$\begin{aligned}\hat{\alpha}_t = \max \Big\{ & \Sigma_{c\in\mathcal{C}} C_c \lambda^B_{t,c} p^{B_{tot}}_{t,c} \\ & + \Sigma_{w\in\mathcal{W}} W_w \Big[\lambda^R_{t,w} e^R_{t,w} + \lambda^S_t \kappa^S_{t,w} (e^S_{t,w} - \tau e^P_{t,w}) \\ & - \Sigma_{m\in\mathcal{M}} \big(\lambda^T \varpi_{t,w,m} + \lambda^F s_{t,w,m} \big) \Big] \\ & - \Sigma_{w\in\mathcal{W}} \Sigma_{m\in\mathcal{M}} \lambda^U \delta_{t,w,m} + \hat{\alpha}_{t+1} \Big\} \end{aligned} \tag{3.43}$$

s.t.

$$\begin{aligned} & v_{t,w,m} + \Sigma_{i\in\mathcal{S}_m} q_{t,w,m,i} + s_{t,w,m} \\ & \quad - \Sigma_{k\in\Omega_m} (s_{t,w,k} + b_{t,w,k} + \Sigma_{i\in\mathcal{S}_m} q_{t,w,k,i}) \\ & \quad\quad + b_{t,w,m} - \varpi_{t,w,m} = v_{t,w-1,m} + I_{t,w,m}(z_{t-1,m}), && \forall m \in \mathcal{M}, \forall w \in \mathcal{W} \quad (3.44) \\ & \Sigma_{m\in\mathcal{M}} \Sigma_{i\in\mathcal{S}_m} \eta_{w,m,i} q_{t,w,m,i} - e^S_{t,w} + e^P_{t,w} = 0, && \forall w \in \mathcal{W} \quad (3.45) \\ & \Sigma_{i\in\mathcal{S}_m} \gamma_{w,m,i} q_{t,w,m,i} + p^B_{t,w,m} \le P^{max}_m, && \forall m \in \mathcal{M}, \forall w \in \mathcal{W} \quad (3.46) \\ & \Sigma_{i\in\mathcal{S}_m} \gamma_{w,m,i} q_{t,w,m,i} - \frac{P^{min}_m + P^{B,max}_m}{P^{B,max}_m} p^B_{t,w,m} \ge 0, && \forall m \in \mathcal{M}, \forall w \in \mathcal{W} \quad (3.47) \\ & \Sigma_{m\in\mathcal{M}}\ p^B_{t,w,m} - p^{B_{tot}}_{t,c} = 0, && \forall c \in \mathcal{C}, \forall w \in \mathcal{W} \quad (3.48) \\ & \Sigma_{i\in\mathcal{S}_m} q_{t,w,m,i} - Q^{min}_m u^L_{t,w,m} \\ & \quad - (Q^{max}_m - Q^{min}_m) u^H_{t,w,m} = 0, && \forall m \in \mathcal{M}, \forall w \in \mathcal{W} \quad (3.49) \\ & u^L_{t,w,m} - u^H_{t,w,m} \ge 0, && \forall m \in \mathcal{M}, \forall w \in \mathcal{W} \quad (3.50) \\ & u^L_{t,w,m} - u^L_{t,w-1,m} - \delta_{t,w,m} \le 0, && \forall m \in \mathcal{M}, \forall w \in \mathcal{W} \quad (3.51) \\ & o_{t,w,m} - u^L_{t,w-1,m} - o_{t,w-1,m} - \delta_{t,w,m} \le 0 && \forall m \in \mathcal{M}, \forall w \in \mathcal{W} \quad (3.52) \\ & u^L_{t,w,m} + o_{t,w,m} \le 1 && \forall m \in \mathcal{M}, \forall w \in \mathcal{W} \quad (3.53) \\ & \Sigma_{m\in\mathcal{M}} E^R_m o_{t,w,m} - e^R_{t,w} = 0 && \forall w \in \mathcal{W} \quad (3.54) \\ & \Sigma_{m\in\mathcal{B}_m} (u^L_{t,w,m} + o_{t,w,m}) \le 1 && \forall w \in \mathcal{W} \quad (3.55) \\ & \Sigma_{m\in\mathcal{B}_m} p^B_{t,w,m} \le \max\{P^{B,max}_m \ :\ \forall m \in \mathcal{B}_m\} && \forall w \in \mathcal{W} \quad (3.56) \\ & v_{t,w,m} \le V^{max}_m, && \forall m \in \mathcal{M}, \forall w \in \mathcal{W} \quad (3.57) \\ & q_{t,w,m,i} \le Q^{max}_{m,i}, && \forall m \in \mathcal{M}, \forall w \in \mathcal{W} \quad (3.58) \\ & b_{t,w,m} \le B^{max}_m, && \forall m \in \mathcal{M}, \forall w \in \mathcal{W} \quad (3.59) \\ & p^B_{t,w,m} \le P^{B_{max}}_m, && \forall m \in \mathcal{M}, \forall w \in \mathcal{W} \quad (3.60) \\ & v_{t,w,m}, q_{t,w,m,i}, b_{t,w,m}, p^B_{t,w,m} \ge 0, && \forall m \in \mathcal{M}, \forall w \in \mathcal{W} \quad (3.61) \\ & u^L_{t,w,m}, u^H_{t,w,m}, \delta_{t,w,m}, o_{t,w,m} \in [0,1], && \forall m \in \mathcal{M}, \forall w \in \mathcal{W} \quad (3.62) \\ & \hat{\alpha}_{t+1} \le \alpha^*_{t+1} + \Sigma_{m\in\mathcal{M}} \pi^j_{t+1,m} (v_{t,w,m} - v^*_{t,w,m}) \\ & \quad + \Sigma_{m\in\mathcal{M}} \mu^j_{t+1,m} (z_{t,m} - z^*_{t,m}) \\ & \quad\quad + \Sigma_{m\in\mathcal{M}} \phi^j_{t+1,m} (u^L_{t,w,m} - u^{L*}_{t,w,m}), && \forall j \in \mathcal{H}, w = |\mathcal{W}| \quad (3.63) \end{aligned}$$

Limits for the various variables have also been added to the problem. The solution algorithm of the Strategy Model can be found in Appendix B

3.1.12 Additional features

Thermal units can also be included in the model, allowing modelling of hydro-thermal systems. This feature will not be used in this thesis and is not discussed in greater detail.

3.2 Simulator Model

The Simulator Model utilizes the strategy obtained from the Strategy Model and applies a more detailed description of the system when solving the problem, adding cuts describing the opportunity cost of water at the end of each time stage [38]. It is modelled as a MIP problem, accommodating integer and binary variables. The Simulator Model is solved for the same price and inflow scenarios as the last forward iteration of the Strategy Model to facilitate comparison between the two. The one-stage problem formulation of the Simulator Model is similar to that of the Strategy Model, with some changes due to the enhanced system description. This section will describe the differences in the problem formulation from the Strategy Model.

3.2.1 Binary variables

The following binary variables are introduced to achieve an enhanced problem formulation; $x^{sim}_{t,w,m,i}$ defining the state of each PQ segment i, $u^{sim}_{t,w,m}$ determining the state of a power station, $\delta^{sim}_{t,w,m}$ determining start-up, $o^{sim}_{t,w,m}$ determining the mode of operation of a power station, and $\theta^{sim}_{t,w,m}$ determining state transitioning. A detailed description is given below.

$$x^{sim}_{t,w,m,i} = \begin{cases} 1, & \text{if PQ segment } i \text{ of module } m \text{ is used,} \\ 0, & \text{otherwise.} \end{cases}$$

$$u^{sim}_{t,w,m} = \begin{cases} 1, & \text{if the power station in module } m \text{ is generating power,} \\ 0, & \text{otherwise.} \end{cases}$$

$$\delta^{sim}_{t,w,m} = \begin{cases} 1, & \text{if the state of the power station is 1 in time block } w \\ & \text{and 0 in in time block } w-1, \\ 0, & \text{otherwise.} \end{cases}$$

$$o^{sim}_{t,w,m} = \begin{cases} 1, & \text{if the power station is operating as a SC,} \\ 0, & \text{otherwise.} \end{cases}$$

$$\theta^{sim}_{t,w,m} = \begin{cases} 1, & \text{if the state of SC operation is 1 in time block } w \text{ and the} \\ & \text{state of the power station is 1 in time block } w-1, \\ 0, & \text{otherwise.} \end{cases}$$

3.2.2 Hydropower module

The requirement of a concave PQ segment curve does not apply to the Simulator Model. In Figure 3.5 an illustration of a non-concave (and non-convex) PQ segment curve with associated parameters is shown. Let $q_{t,w,m,i}$ be the discharge of segment i, i.e. the discharge between $Q_{w,m,i-1}$ and $Q_{w,m,i}$ as in the illustration. The following

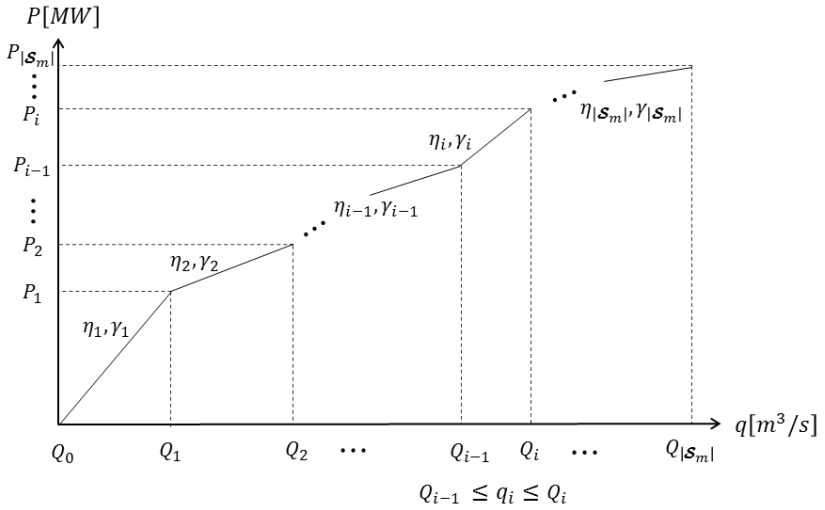

Figure 3.5: Illustration of a PQ segment curve which is neither concave nor convex.

equations may then be used to model the power station.

$$p_{t,w,m} - \Sigma_{i \in \mathcal{S}_m} p_{t,w,m,i} = 0, \qquad \forall w \in \mathcal{W}, \forall m \in \mathcal{M} \tag{3.64}$$

$$p_{t,w,m,i} - \gamma_{w,m,i} q_{t,w,m,i} = 0, \qquad \forall i \in \mathcal{S}_m, \forall m \in \mathcal{M}, \forall w \in \mathcal{W} \tag{3.65}$$

$$Q_{w,m,i-1} x^{sim}_{t,w,m,i} - q_{t,w,m,i} \leq 0, \qquad \forall i \in \mathcal{S}_m, \forall m \in \mathcal{M}, \forall w \in \mathcal{W} \tag{3.66}$$

$$Q_{w,m,i} x^{sim}_{t,w,m,i} - q_{t,w,m,i} \geq 0, \qquad \forall i \in \mathcal{S}_m, \forall m \in \mathcal{M}, \forall w \in \mathcal{W} \tag{3.67}$$

$$\Sigma_{i \in \mathcal{S}_m} x^{sim}_{t,w,m,i} = 1, \qquad \forall m \in \mathcal{M}, \forall w \in \mathcal{W} \tag{3.68}$$

Equations (3.66) and (3.67) limit the discharge, equation (3.65) couples the discharge to the generation and equation (3.64) gives the total generation from one power station. (3.68) limits the maximum number of possible segments used to one.

The production variable $p_{t,w,m}$ is also included in the energy balance, contrary to the Strategy Model where the discharge and power equivalent is used.

3.2.3 Power station

The use of binary variables allows for a better modelling of the start-up of a power station, given by the equations below, which connect the power outputs of the generators to their state.

$$p_{t,w,m} - P^{max}_m u^{sim}_{t,w,m} \leq 0, \qquad \forall m \in \mathcal{M}, \forall w \in \mathcal{W} \tag{3.69}$$

$$p_{t,w,m} - P^{min}_m u^{sim}_{t,w,m} \geq 0, \qquad \forall m \in \mathcal{M}, \forall w \in \mathcal{W} \tag{3.70}$$

3.2.4 Start-up

In the Simulator Model, a more accurate modelling of the start-up costs associated with SC mode of operation is used. Table 3.1 shows the transition costs between the various states. The cost of shutting down either generation or SC mode of operation

Transition	$u^{sim}_{t,w,m}$	$o^{sim}_{t,w,m}$	$u^{sim}_{t,w-1,m}$	$o^{sim}_{t,w-1,m}$	Cost
Standstill → Generation	1	0	0	0	λ^U
Standstill → SC	0	1	0	0	λ^U
SC → Generation	1	0	0	1	λ^U
Generation → SC	0	1	1	0	λ^G

Table 3.1: Approximate transition costs between states.

is included in the start-up costs, i.e. the transitions from standstill. The transitions are modelled by the following equations:

$$u^{sim}_{t,w,m} - u^{sim}_{t,w-1,m} - \delta^{sim}_{t,w,m} \leq 0, \qquad \forall m \in \mathcal{M}, \forall w \in \mathcal{W} \tag{3.71}$$

$$o^{sim}_{t,w,m} - u^{sim}_{t,w-1,m} - o^{sim}_{t,w-1,m} - \delta^{sim}_{t,w,m} \leq 0 \qquad \forall m \in \mathcal{M}, \forall w \in \mathcal{W} \tag{3.72}$$

$$o^{sim}_{t,w,m} - u^{sim}_{t,w,m} + u^{sim}_{t,w-1,m} - \theta^{sim}_{t,w,m} \leq 1 \qquad \forall m \in \mathcal{M}, \forall w \in \mathcal{W} \tag{3.73}$$

Equation (3.71) models the costs induced by transitioning from standstill and SC mode of operation to generation, (3.72) models transitioning from standstill to SC mode of operation and (3.73) models the transition from generation to SC mode of operation. The equations are formulated so that they induce the correct costs, should the model be run with simultaneous generation and rotational energy provision. Both $\delta^{sim}_{t,w,m}$ and $\theta^{sim}_{t,w,m}$ are included with their associated cost in the objective function.

3.2.5 Provision of rotational energy

The provision of rotational energy is modelled with the binary variables:

$$u^{sim}_{t,w,m} + o^{sim}_{t,w,m} \leq 1 \qquad \forall m \in \mathcal{M}, \forall w \in \mathcal{W} \tag{3.74}$$

to avoid simultaneous generation and SC operation and

$$\Sigma_{m \in \mathcal{M}} E^R_m o^{sim}_{t,w,m} - e^R_{t,w} = 0 \qquad \forall w \in \mathcal{W} \tag{3.75a}$$

$$\Sigma_{m \in \mathcal{M}} E^R_m (u^{sim}_{t,w,m} + o^{sim}_{t,w,m}) - e^R_{t,w} = 0 \qquad \forall w \in \mathcal{W} \tag{3.75b}$$

couples the mode of operation to the provision of rotational energy for two different market solutions. As with the Strategy Model, (3.75a) will be used in the remainder of this chapter.

3.2.6 System constraints

The following system constraints are included in the Simulator Model.

$$\Sigma_{m \in \mathcal{B}_m}(u^{sim}_{t,w,m} + o^{sim}_{t,w,m}) \leq 1 \qquad \forall w \in \mathcal{W} \qquad (3.76)$$

$$b_{t,w,m} + Q^{max}_m u^{sim}_{t,w,m} \leq Q^{max}_m \qquad \forall m \in \mathcal{M}, \forall w \in \mathcal{W} \qquad (3.77)$$

(3.76) is similar to (3.40), modelled using the binary variables described above. (3.77) refrains a hydro power module from simultaneously generating power and bypassing water to other reservoirs. This constraint is only included for modules with bypass connectivity.

3.2.7 One stage problem formulation for the Simulator Model

The above equations and constraints result in the following problem formulation for time stage t.

$$\begin{aligned}\hat{\alpha}_t = \max \Big\{ & \Sigma_{c\in\mathcal{C}} C_c \lambda^B_{t,c} p^{B_{tot}}_{t,c} \\ & + \Sigma_{w\in\mathcal{W}} W_w \Big[\lambda^R_{t,w} e^R_{t,w} + \lambda^S_t \kappa^S_{t,w} (e^S_{t,w} - \tau e^P_{t,w}) \\ & - \Sigma_{m\in\mathcal{M}} \big(\lambda^T \varpi_{t,w,m} + \lambda^F s_{t,w,m} \big) \Big] \\ & - \Sigma_{w\in\mathcal{W}} \Sigma_{m\in\mathcal{M}} (\lambda^U \delta^{sim}_{t,w,m} + \lambda^G \theta^{sim}_{t,w,m}) \\ & + \hat{\alpha}_{t+1} \Big\}\end{aligned} \tag{3.78}$$

s.t.

$$\begin{aligned} & v_{t,w,m} + \Sigma_{i\in\mathcal{S}_m} q_{t,w,m,i} + s_{t,w,m} \\ & \quad - \Sigma_{k\in\Omega_m} (s_{t,w,k} + b_{t,w,k} + \Sigma_{i\in\mathcal{S}_m} q_{t,w,k,i}) \\ & \quad + b_{t,w,m} - \varpi_{t,w,m} = v_{t,w-1,m} + I_{t,w,m}(z_{t-1,m}), \quad \forall m \in \mathcal{M}, \forall w \in \mathcal{W} \end{aligned} \tag{3.79}$$

$$\Sigma_{m\in\mathcal{M}} p_{t,w,m} - e^S_{t,w} + e^P_{t,w} = 0, \qquad \forall w \in \mathcal{W} \tag{3.80}$$

$$p_{t,w,m} + p^B_{t,w,m} \le P^{max}_m, \qquad \forall m \in \mathcal{M}, \forall w \in \mathcal{W} \tag{3.81}$$

$$p_{t,w,m} - p^B_{t,w,m} - P^{min}_m u^{sim}_{t,w,m} \ge 0, \qquad \forall m \in \mathcal{M}, \forall w \in \mathcal{W} \tag{3.82}$$

$$\Sigma_{m\in\mathcal{M}}\ p^B_{t,w,m} - p^{B_{tot}}_{t,c} = 0, \qquad \forall c \in \mathcal{C}, \forall w \in \mathcal{W} \tag{3.83}$$

$$p_{t,w,m} - P^{max}_m u^{sim}_{t,w,m} \le 0, \qquad \forall m \in \mathcal{M}, \forall w \in \mathcal{W} \tag{3.84}$$

$$p_{t,w,m} - P^{min}_m u^{sim}_{t,w,m} \ge 0, \qquad \forall m \in \mathcal{M}, \forall w \in \mathcal{W} \tag{3.85}$$

$$u^{sim}_{t,w,m} - u^{sim}_{t,w-1,m} - \delta^{sim}_{t,w,m} \le 0, \qquad \forall m \in \mathcal{M}, \forall w \in \mathcal{W} \tag{3.86}$$

$$o^{sim}_{t,w,m} - u^{sim}_{t,w-1,m} - o^{sim}_{t,w-1,m} - \delta^{sim}_{t,w,m} \le 0 \qquad \forall m \in \mathcal{M}, \forall w \in \mathcal{W} \tag{3.87}$$

$$o^{sim}_{t,w,m} - u^{sim}_{t,w,m} + u^{sim}_{t,w-1,m} - \theta^{sim}_{t,w,m} \le 1 \qquad \forall m \in \mathcal{M}, \forall w \in \mathcal{W} \tag{3.88}$$

$$u^{sim}_{t,w,m} + o^{sim}_{t,w,m} \le 1 \qquad \forall m \in \mathcal{M}, \forall w \in \mathcal{W} \tag{3.89}$$

$$\Sigma_{m\in\mathcal{M}} E^R_m o^{sim}_{t,w,m} - e^R_{t,w} = 0 \qquad \forall w \in \mathcal{W} \tag{3.90}$$

$$\Sigma_{m\in\mathcal{B}_m} (u^{sim}_{t,w,m} + o^{sim}_{t,w,m}) \le 1 \qquad \forall w \in \mathcal{W} \tag{3.91}$$

$$b_{t,w,m} + Q^{max}_m u^{sim}_{t,w,m} \le Q^{max}_m \qquad \forall m \in \mathcal{M}, \forall w \in \mathcal{W} \tag{3.92}$$

$$p_{t,w,m} - \Sigma_{i\in\mathcal{S}_m} p_{t,w,m,i} = 0, \qquad \forall w \in \mathcal{W}, \forall m \in \mathcal{M} \tag{3.93}$$

$$p_{t,w,m,i} - \gamma_{w,m,i} q_{t,w,m,i} = 0, \qquad \forall i \in \mathcal{S}_m, \forall m \in \mathcal{M}, \forall w \in \mathcal{W} \quad (3.94)$$

$$Q_{w,m,i-1} x^{sim}_{t,w,m,i} - q_{t,w,m,i} \leq 0, \qquad \forall i \in \mathcal{S}_m, \forall m \in \mathcal{M}, \forall w \in \mathcal{W} \quad (3.95)$$

$$Q_{w,m,i} x^{sim}_{t,w,m,i} - q_{t,w,m,i} \geq 0, \qquad \forall i \in \mathcal{S}_m, \forall m \in \mathcal{M}, \forall w \in \mathcal{W} \quad (3.96)$$

$$\Sigma_{i \in \mathcal{S}_m} x^{sim}_{t,w,m,i} = 1, \qquad \forall m \in \mathcal{M}, \forall w \in \mathcal{W} \quad (3.97)$$

$$v_{t,w,m} \leq V^{max}_m, \qquad \forall m \in \mathcal{M}, \forall w \in \mathcal{W} \quad (3.98)$$

$$b_{t,w,m} \leq B^{max}_m, \qquad \forall m \in \mathcal{M}, \forall w \in \mathcal{W} \quad (3.99)$$

$$p^B_{t,w,m} \leq P^{B_{max}}_m, \qquad \forall m \in \mathcal{M}, \forall w \in \mathcal{W} \quad (3.100)$$

$$v_{t,w,m}, b_{t,w,m}, p^B_{t,w,m} \geq 0, \qquad \forall m \in \mathcal{M}, \forall w \in \mathcal{W} \quad (3.101)$$

$$u^{sim}_{t,w,m}, \delta^{sim}_{t,w,m}, o^{sim}_{t,w,m} \in \{0,1\}, \qquad \forall m \in \mathcal{M}, \forall w \in \mathcal{W} \quad (3.102)$$

$$\begin{aligned} \hat{\alpha}_{t+1} \leq \alpha^*_{t+1} &+ \Sigma_{m \in \mathcal{M}} \pi^j_{t+1,m} (v_{t,w,m} - v^*_{t,w,m}) \\ &+ \Sigma_{m \in \mathcal{M}} \mu^j_{t+1,m} (z_{t,m} - z^*_{t,m}) \\ &+ \Sigma_{m \in \mathcal{M}} \phi^j_{t+1,m} (u^L_{t,w,m} - u^{L*}_{t,w,m}), \end{aligned} \qquad \begin{aligned} &(3.103) \\ &\forall j \in \mathcal{H}, w = |\mathcal{W}| \end{aligned}$$

The solution algorithm of the Simulator Model can be found in Appendix B.

4 Hydro System Modelling and Case Study

4.1 Case Study

4.1.1 Hydro system

This section aims to describe the hydro system used in the model. The system, operated by Lyse AS, is located in Forsand kommune in Rogaland fylke in Norway, belonging to Elspot area NO2. A decision to build a new power station in Lysebotn has been made, as the old power station is approaching the end of its lifetime. The new power station (Lysebotn-2) is planned to be ready to operate in the spring of 2018, running in parallel to the existing power station (Lysebotn-1). The future system will consist of four reservoirs and three power stations, resulting in four hydropower modules, $|\mathcal{M}| = 4$. A representation of the physical and modelled

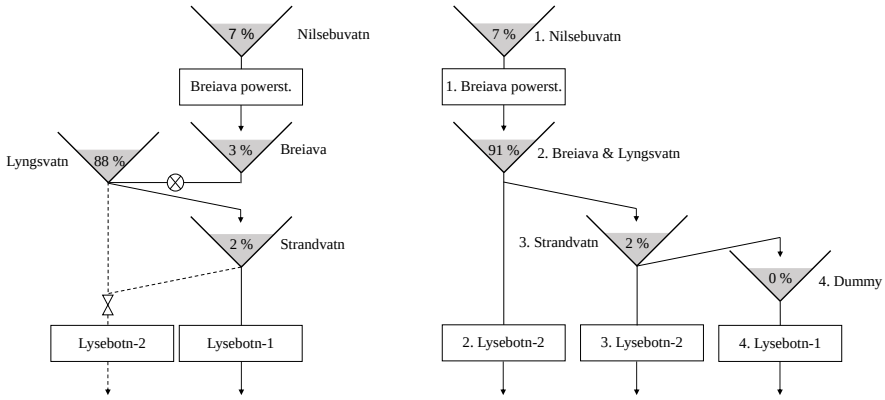

Figure 4.1: Physical (left) and modelled (right) hydro system representation.

Module	Average annual inflow	Reservoir capacity	Degree of regulation
1	51 %	7 %	0.09
2	24 %	91 %	0.80
3	25 %	2 %	0.05
4	0 %	0 %	–

Table 4.1: Reservoir parameters.

system is shown in Figure 4.1. All reservoirs are shown with their storage capacity in percent of the total system. The dashed lines in the physical model representation show the planned hydrological connections of Lysebotn-2. In the modelled system representation, each reservoir and power station is shown with its associated module number, m.

Table 4.1 shows the average annual inflows and reservoir capacities as percentages of the total values of the hydro system, as well as the degree of regulation (DOR). The latter is the ratio between the reservoir capacity and inflow indicating the amount of inflow that can be stored for regulation. The DOR level of the reservoirs in modules 1 and 3 are low compared to the DOR of the reservoir in module 2. Thus, the reservoirs of modules 1 and 3 have a shorter planning horizon and a smaller impact on the strategy of models with weekly time stages. The reservoir of module 2 may be regarded as a regulating reservoir, with a longer planning horizon and a larger impact on the overall strategy of medium- and long-term models [33]. The reservoir of module 4 is a dummy reservoir.

Lyse AS evaluated whether to install Pelton or Francis turbines in Lysebotn-2. In Figure 4.2, energy equivalents for the two turbines are shown. The Francis turbine has a higher maximum energy equivalent than the Pelton turbine. However, the Pelton turbine is characterized by a high energy equivalent for a wider area of operation. Lyse AS concluded that the Francis turbines had a better profitability due to a lower investment cost and better efficiency.

Lyse AS has yet to make a decision regarding the future operation of Lysebotn-1. Lysebotn-1 is installed with Pelton turbines and is approximately 9 % less efficient than Lysebotn-2, generating from Strandvatn. Compared to Lysebotn-2 generating from Lyngsvatn, Lysebotn-1 has a 14 % lower efficiency. However, the wider operating area of the Pelton turbines allow Lysebotn-1 to operate at a lower set point without losing efficiency. This makes the power station well suited for delivery of FCR-N. Hence, the hydro system is modelled with continued operation of Lysebotn-1 to investigate this assertion.

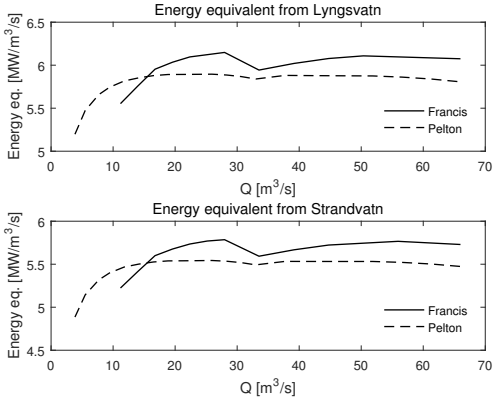

Figure 4.2: Energy equivalents for Pelton and Francis turbines in Lysebotn-2.

4.1.2 Synchronous condenser

Lyse AS has decided to invest in SC mode of operation of Lysebotn-2. Associated parameters to the operation are shown in Table 4.2.

Inertia constant	Rated power	Rotational energy
3.0 s	2×215 MVA	1290 MWs

Table 4.2: SC mode parameters for Lysebotn-2.

In Table 4.3, the investment costs associated with SC mode of operation are shown. The facilitation most notably includes the installation of a compressor, motor starters, a cooling system, and monitoring and control systems. The electrical brake is used to reduce the transition period from production to SC mode.

Investment	Cost
Facilitation of the plant	20 MNOK
Electrical brake (per generator)	2 MNOK
Total	24 MNOK

Table 4.3: Investment costs for SC operation of Lysebotn-2, provided by Lyse AS.

As these numbers are from 2014, the manufacturing producer price index is used to adjust the investment cost, collected from [43]. The numbers are shown in Table 4.4.

The resulting investment cost corresponds with the estimate of 10-20 kNOK/MWs used in [30].

Time	Manufacturing PPI	Investment cost	Cost/rotational energy
January 2014	149.3	24.00 MNOK	18.60 kNOK/MWs
January 2016	145.3	23.36 MNOK	18.11 kNOK/MWs

Table 4.4: Manufacturing producer price index adjustment.

An investment analysis can then be performed. The discount rate used in this thesis is the sum of the current risk-free real interest rate and a risk premium. The latter is set by the Norwegian Ministry of Finance to 3 % [44]. The risk-free interest rate is set equal to Norwegian 3-year government bonds, equal to 0.76 % in 2015 [45]. The investment analysis period of hydropower stations is typically set to 40 years, while their lifetime is assumed to be 60 years [46]. The yearly break-even income is found by applying the net present value (NPV) method and setting the NPV equal to zero. The result is shown in Table 4.5.

Investment cost	Discount rate	Analysis period	Yearly break-even income
23.36 MNOK	3.76 %	40 years	1 138.41 kNOK/year

Table 4.5: Investment analysis parameters and results.

The operational costs for SC mode of operation proved difficult to find and are thus neglected.

4.1.3 Time resolution

In this thesis, model results from two years will be analyzed. The model is solved with time stages in a weekly resolution, starting from week 5. Every week has seven days and every day is divided into three time blocks; night, day and evening with an hourly resolution. For the capacity market, every week has two days; one representing week days and one representing the weekend. These are divided into time blocks as previously described. See Table 4.6 for further details.

4.1.4 Rotational energy market

The rotational energy market is assumed to be open only in time periods where the rotational energy in the power system falls below a system requirement. Only provision of rotational energy from SC mode of operation is remunerated, given by equations (3.22a) and (3.75a), and the market is also assumed to be cleared after the

Time set	Length	Starting point	End point	Resolution
$t \in \mathcal{T}$	104 stages	5	$\lvert\mathcal{T}\rvert = 108$	1 week
$w \in \mathcal{W}$	21 blocks	1	$\lvert\mathcal{W}\rvert = 21$	$[8, 12, 4, 8, 12, ..., 4]$ hours
$c \in \mathcal{C}$	6 blocks	1	$\lvert\mathcal{C}\rvert = 6$	$[8, 12, 4, 8, 12, 4]$ hours

Table 4.6: Time resolution.

Elspot market. Considering the market clearing process of the model, discussed in Section 3.1.7, it is clear that a hydropower producer will be able to perfectly forecast when the rotational energy market is open, before bidding in Elspot. To counteract this effect, the model may be run without equations (3.20) and (3.74). By removing SC mode of operation from the results in time steps where simultaneous generation and SC operation occurs, an analysis of a scheduling strategy with no speculation may be achieved. The market is modelled with a fixed price in each time period it is open.

Using a system requirement for rotational energy of 100 GWs, Figure 2.9 shows that one period has a critically low amount of rotational energy; week 31 during the night. Consequently, the rotational energy market is assumed to be open in the first and last time block of each day, during week 31.

4.1.5 Prices

The price point series used are provided by SINTEF and consists of $|\mathcal{R}| = 7$ price points for each stage. To model the energy price profile, historical Elspot prices with an hourly resolution from week 5 in 2014 to week 4 in 2016 were used. These were collected from Nord Pool Spot's "Data Downloads" web page [47]. As previously mentioned, the capacity prices used in the model are historical values. Weekly FCR-N prices from week 5 in 2014 to week 4 in 2016 were collected from Statnett's download centre [48]. The Elspot prices used to model the price profile and the capacity prices can be seen in Figure 4.3.

The rotational energy price is set so that it provides the required yearly income to cover the investment cost, i.e. the yearly break-even income, adjusting for start-up costs. As mentioned, operational costs are neglected. It is calculated so that participation provides the same income in every time block and time stage it is open. The necessary rotational energy price to cover the income in Table 4.5 is shown in Table 4.7, along with other market parameters. The price is calculated under the assumption that the power station operates as a SC in every time period the rotational energy market is open. It is also assumed that the power station transitions from standstill to SC operation in every time step, so avoided start-up costs from SC

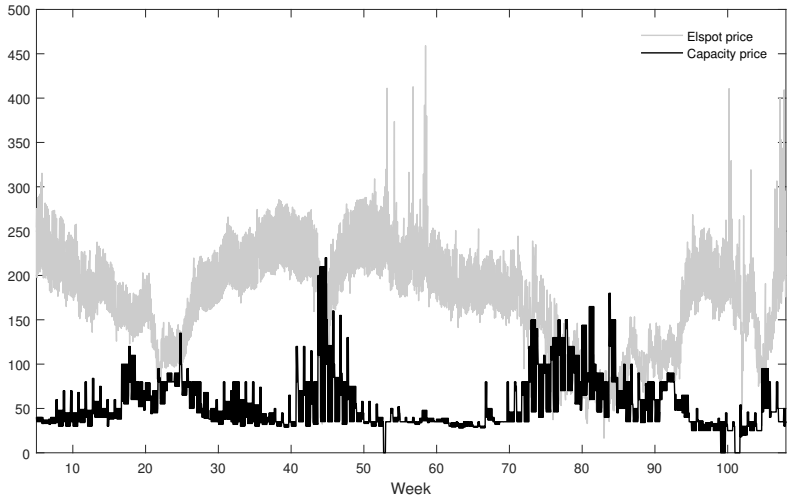

Figure 4.3: Elspot [NOK/MWh] and FCR-N [NOK/MW/h] prices, from week 5 in 2014 to week 4 in 2016.

operation in consecutive time periods are not taken into account. Figure 4.4 shows the rotational energy prices plotted against historical Elspot and FCR-N prices for each time block between week 30 and 33 in 2014. The Elspot price is the average of the hourly prices in a time block.

Time stage	Time blocks	Number of hours	Rotational energy price
31	$[1, 4, ..., 19]$	56	10.90 NOK/MWs/h
31	$[2, 5, ..., 20]$	84	0.00 NOK/MWs/h
31	$[3, 6, ..., 21]$	28	11.29 NOK/MWs/h

Table 4.7: Rotational energy price parameters.

4.1.6 Inflow

The inflow data was provided by SINTEF and consisted of 70 years of historical time series, in a daily resolution. This was used to calculate the average weekly inflow, the standard deviation and the sequential autocorrelation. The latter can be seen in Table 4.8, while the average inflows and standard deviations are shown in Figure 4.5.

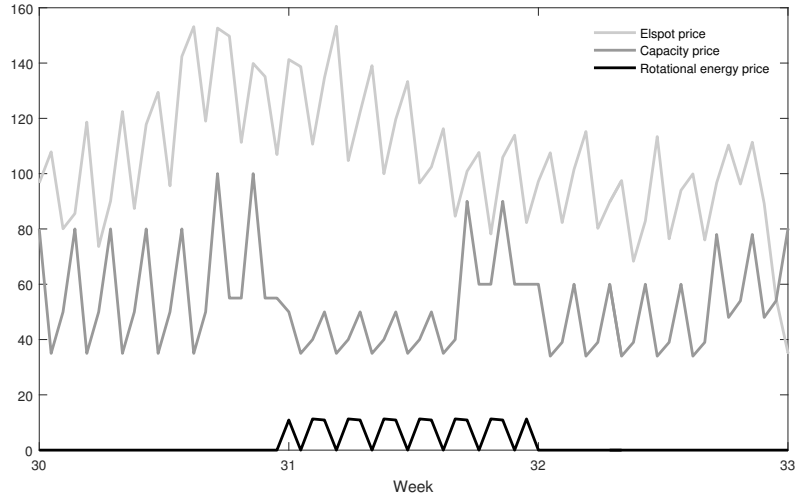

Figure 4.4: Elspot [NOK/MWh], FCR-N [NOK/MW/h], and rotational energy [NOK/MWs/h] prices from week 30 to 33.

ψ_1	ψ_2	ψ_3	ψ_4
0.4	0.4	0.4	0.4

Table 4.8: Sequential autocorrelation.

4.1.7 End cut

After running the model once, information about the reservoir level and cuts after one year is obtained. As the model is run for two years, applying this information gives an estimate of the end cut parameters given in Table 4.9. $\pi^1_{|\mathcal{T}|+1,m}$ is given in [kNOK/Mm^3] and $b_{|\mathcal{T}|}$ in [kNOK].

$\pi^1_{\|\mathcal{T}\|+1,1}$	$\pi^1_{\|\mathcal{T}\|+1,2}$	$\pi^1_{\|\mathcal{T}\|+1,3}$	$\pi^1_{\|\mathcal{T}\|+1,4}$	$b_{\|\mathcal{T}\|}$
839	765	761	758	0

Table 4.9: End cut parameters.

4.2 Modelling

In the modelling of the hydropower system, Breiava is aggregated with Lyngsvatn, due to Breiava's small size, to increase model simplicity. These two reservoirs will be

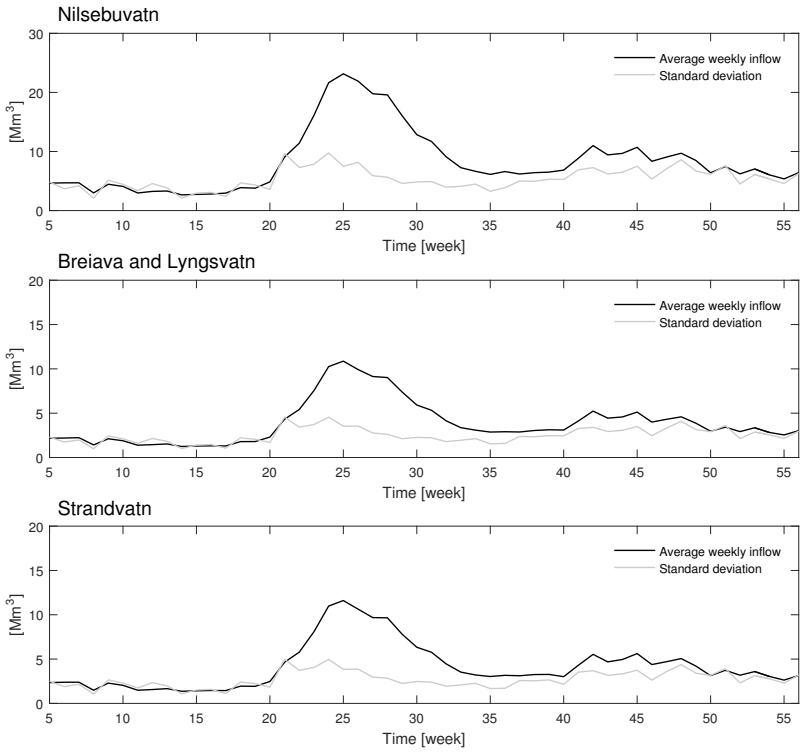

Figure 4.5: Inflow and standard deviation for weeks 5 to 56.

referred to as Lyngsvatn. Lysebotn-2 is modelled twice to facilitate its connections to both Lyngsvatn and Strandvatn. As the reservoirs have different heads in relation to Lysebotn-2, the power station can only operate from one reservoir at a time. A dummy reservoir with zero inflow and storage capability is modelled with bypass from Strandvatn, representing the inlet to Lysebotn-1.

Figure 4.6 shows plots of the PQ segment curves and associated energy equivalent curves of the power stations. The Strategy Model requires concave PQ segment curves resulting in an energy equivalent curve with a downward slope. This is obtained by removing conflicting PQ segments. The removed segments are chosen so that the total number of segments removed for a power station is kept at a minimum.

The following modelling is done with the use of Matlab scripts:

- Generate a price profile, with average values for weekday and weekend time blocks within the week. The profile is then scaled so that its mean value is 1.
- Generate a capacity price series compatible with the model.
- Generate a rotational energy price series.
- Calculate average weekly inflows, their associated standard deviation, and sequential autocorrelation.
- Calculate end cut parameters based on the average value of the cuts in week 56 and the probability of their associated price point occurring in week 108.
- Calculate average and total values of the results.

Tables 4.10 and 4.11 include some selected model parameters. A hyphen denotes that the parameter is not applicable for the given hydropower module.

The prototype model is altered to fit the aim of this thesis. The following is implemented by the author:

- SC mode of operation of power stations.
- Provision of rotational energy.
- System constraint to limit operation for modules sharing the same power station in the Strategy Model.

Parameter	Unit	Module 1	Module 2	Module 3	Module 4
P_m^{max}	[MW]	13.80	400.93	378.14	217.60
P_m^{min}	[MW]	6.90	62.14	58.45	42.00
Q_m^{max}	[m^3/s]	27.00	66.00	66.00	41.40
Q_m^{min}	[m^3/s]	13.50	11.19	11.19	8.00
V_m^{max}	[Mm^3]	40.50	511.80	12.40	0.00
B_m^{max}	[m^3/s]	-	66.00	41.40	-
λ^U	[kNOK]	2.00	4.00	4.00	2.00
λ^G	[kNOK]	-	1.50	1.50	-
S_m	[%]	2.00	2.00	2.00	2.00
$P_m^{B,max}$	[MW]	1.38	40.01	37.81	21.76
E_m^R	[MWs]	-	1290	1290	-

Table 4.10: Hydropower module parameters.

Parameter	Unit	Value
λ^T	[kNOK/Mm^3]	100000
λ^F	[kNOK/Mm^3]	1
τ	–	1.01

Table 4.11: Model specific parameters.

Every model run is executed with the model characteristics given in Table 4.12.

Model	Forward scenarios	Backward openings	Iterations
Strategy Model	50	9	15
Simulator Model	50	-	1

Table 4.12: Model run characteristics.

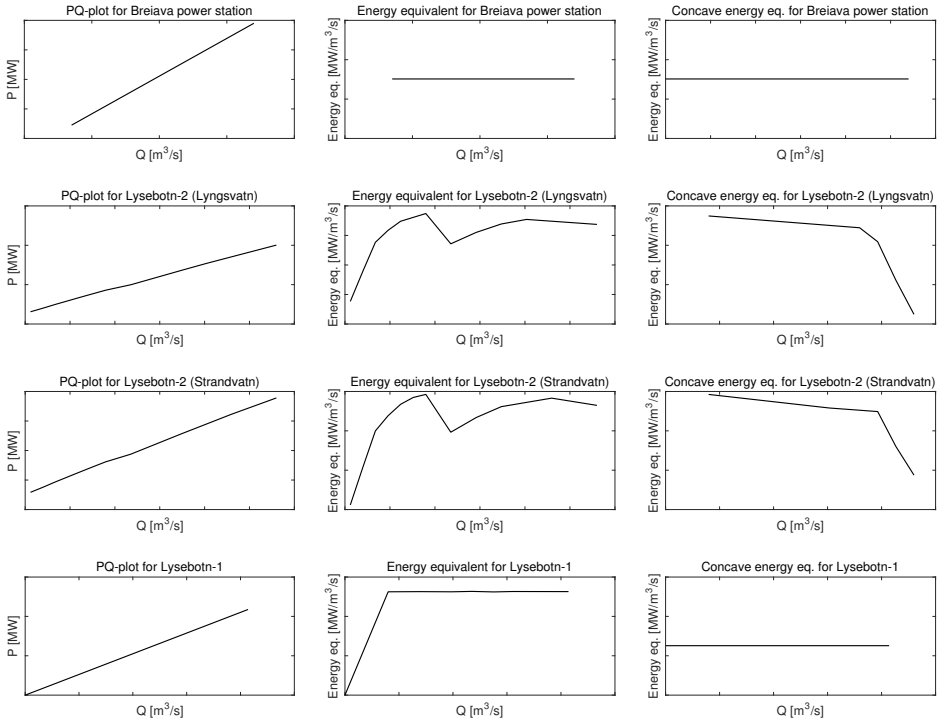

Figure 4.6: Actual and concave power station curves. The numerical values have been left out because of the sensitivity of the information.

5 Results and Discussion

This chapter will discuss the results from a conference paper submitted to the 51st International Universities' Power Engineering Conference (UPEC 2016), held in Coimbra, Portugal. Additional results and plots from the simulations that were not included from the paper due to the lack of space will also be presented. The submitted paper can be found in Appendix A. At the point of time this thesis was completed, no formal acceptance was yet received from the conference committee.

5.1 Model Runs

Two model runs were performed, one with perfect speculation of when the rotational energy market is active, and one with no speculation at all. These will be referred to as run 1 and run 2, respectively. The model runs are shown in Table 5.1.

Run	Rotational energy market speculation
1	Perfect
2	None

Table 5.1: Model run characteristics.

The scope of the submitted paper and this thesis is limited to the results of the Simulator Model, as it provides an enhanced system description. The last iteration of the Strategy Model and the Simulator Model was solved for the same pre-sampled inflow scenarios and price points in both runs, for better comparison. As the first 14 iterations of the Strategy Model, which determine the cuts, are solved for different price and inflow samples between the runs, sample variations may still affect the results.

5.2 Main Findings

This section will present the main findings of the submitted conference paper.

5.2.1 Market participation

Figure 5.1 shows the average values of Elspot, FCR-N and rotational energy market participation from modules 2 and 3 (Lysebotn-2) during weeks 30 to 32, in the first year of the simulation period. As sales of both capacity and rotational energy tends to either be at its maximum value or zero, the values provide information about the frequency of scenarios where market participation occurs. In run 1, SC mode of operation occurs in every time block the rotational energy market is open, showing that the gain from participating in the rotational energy market is higher than that of combined Elspot and FCR-N market participation. In run 2, the optimal strategy for Elspot and FCR-N market participation is followed. From Figure 4.4 it can be seen that when comparing prices within each day of week 31, the first time block of each day experiences moderate Elspot prices and high FCR-N prices. The second time block of each day experiences high Elspot and low FCR-N prices, and the last time block experiences low Elspot prices and moderate FCR-N prices. This explains the market participation in run 2. In the first time block the Elspot and FCR-N markets are participated in approximately the same number of scenarios as the rotational energy market. Due to the moderate Elspot prices and high FCR-N prices, the generation is at minimum in most scenarios to allow sales of capacity. As the Elspot prices in the last time block of each day are low, there is no Elspot or FCR-N market participation, allowing run 2 to participate in the rotational energy market.

5.2.2 Economic results

Table 5.2 shows the average income from the various markets during the whole simulation period. The end water value is calculated by multiplying the average end reservoir levels with the end cut water values given in Table 4.9. Run 1 has a slightly higher income from sales of energy, but also has less stored water in the reservoirs at the end of the simulation period. Due to perfect speculation, run 1 has a higher income from the rotational energy market. The contribution from rotational energy provision is substantial, considering the number of hours the rotational energy market is open. Run 2 has a higher income from sales of capacity, mainly caused by participation in the FCR-N market in the time blocks where run 1 participates in the rotational energy market.

Run	Elspot	FCR-N	Rotational energy	End water value
1	1 446.70	6.77	2.39	322.24
2	1 444.99	6.83	1.97	324.51

Table 5.2: Expected income from each market and the end water values in the two model runs (MNOK).

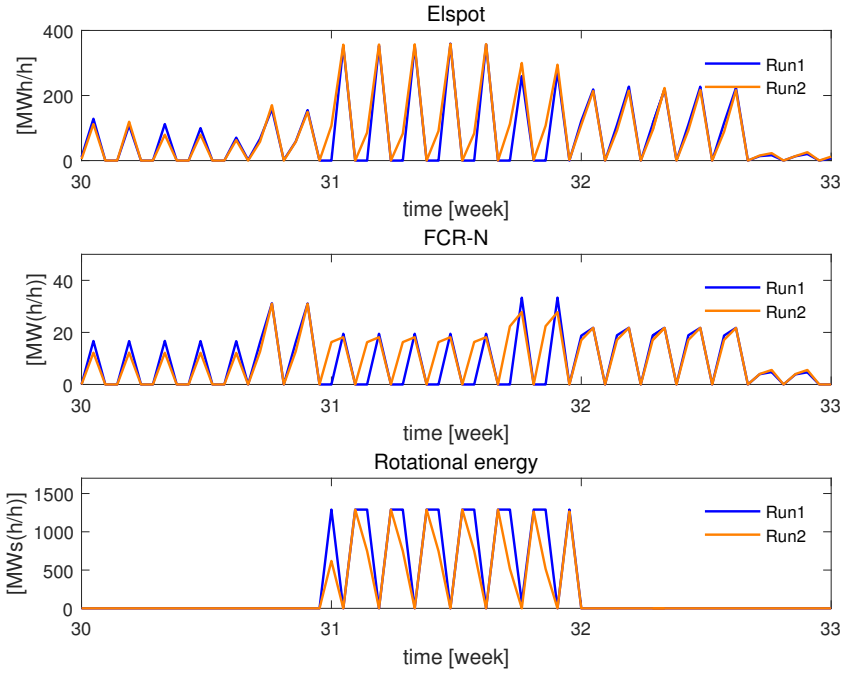

Figure 5.1: Expected Elspot (top), FCR-N (middle) and rotational energy (bottom) market participation in year 1 for model runs 1 and 2.

The difference in generation due to rotational energy market participation between the runs, compared to the total generation is small and has a negligible effect on the overall reservoir strategy. This is mainly due to the short time period the rotational energy market is open and that the rotational energy market is open during time blocks and stages with low Elspot prices. As previously discussed, only the first time block of each day during week 31 showed a significant change in the market participation strategy between the runs. For the given case study considering the year 2020, Rotational energy market participation has a small effect on medium term hydropower scheduling. It would therefore be interesting to study its effects in short-term models. It is viable that the demand for rotational energy will be higher further into the future, causing the rotational energy market to be open for a longer time period and have a larger impact on medium-term hydropower scheduling.

Table 5.3 shows yearly costs and income associated with SC operation. The values are averaged over the two years of the simulation period. In run 1, the income is higher than the required yearly income to cover the investment cost. This is an

expected result, as SC operation occurs in every time block the market is open. Because the price was set including start-up costs, which are higher than transition costs, transitioning from generation to SC operation causes a higher income than required. In run 2, the income is reduced by 17.7 %, due to the reduced market participation and the required yearly income to cover the investment cost is not met. The rotational energy prices would have to be increased by approximately 22 % to accumulate the necessary income to provide investment incentives.

Ideally, the rotational energy price would be at a level where it would not interfere with the optimal generation and capacity allocation strategy. This may be obtained by adjusting the income from sales of capacity and energy for the water value. It is found that a price of 1.02 and 0 NOK/MWs/h in the first and last time block of each day of week 31 respectively should mitigate interference in over 90 % of the time blocks and scenarios. A price of 0 NOK/MWs/h indicates that sales of energy and capacity is not profitable in that time block, and interference will not occur. Hence, rotational energy provision in the last time block will not be in conflict with the optimal Elspot and FCR-N market participation strategy. A price below 1.02 NOK/MWs/h in the first time block and a high price to accumulate the required income in the last time block would provide a strategy which does not cause interference, while covering the investment cost.

As mentioned in Section 3.1.7, the price of a rotational energy market governed by the supply and demand of hydropower producers and the TSO would likely be equal to the marginal cost of rotational energy provision. A higher price than the costs associated with SC operation would not lead to an increased amount of rotational energy provided. Instead it would cause hydropower producers to switch from generation to SC mode operation as the income from the rotational energy market surpasses that of the Elspot and FCR-N market, adjusted for the water value. To ensure investment in SC mode of operation of hydropower plants, the market must either have a fixed price (remuneration) which covers the investment cost, or investment support must be offered. Considering the short time period the rotational energy market is open and the needed rotational energy to meet the system requirement in the 2020 scenario, providing a remuneration rather than establish a market seems like the most practical solution.

Run	Income	Transition costs	Start-up costs	Profit
1	1 194.86	7.83	6.72	1 180.31
2	984.04	7.13	5.56	971.35

Table 5.3: Average yearly economic results from SC operation for the two runs (kNOK).

5.3 Additional Findings

This section will present additional results from the simulation, which are not included in the submitted paper.

5.3.1 Second year market participation

Figure 5.2 shows market participation from the second year of the simulation period, where the sampled Elspot prices are lower. Less participation in the Elspot and FCR-N market causes continuous SC operation to avoid start-up costs. This may not be a realistic result as the operational costs are neglected. As the optimal Elspot and FCR-N strategy in run 2 rarely coincides with an active rotational energy market, run 1 and run 2 experience similar SC operation strategies. Some deviation between the strategies is found towards the end of week 83. This is due to an increase in FCR-N prices causing several scenarios to generate at their minimum set point in order to participate in the capacity market. The sampled prices corresponding to figures 5.1 and 5.2 are shown in Figure 5.3.

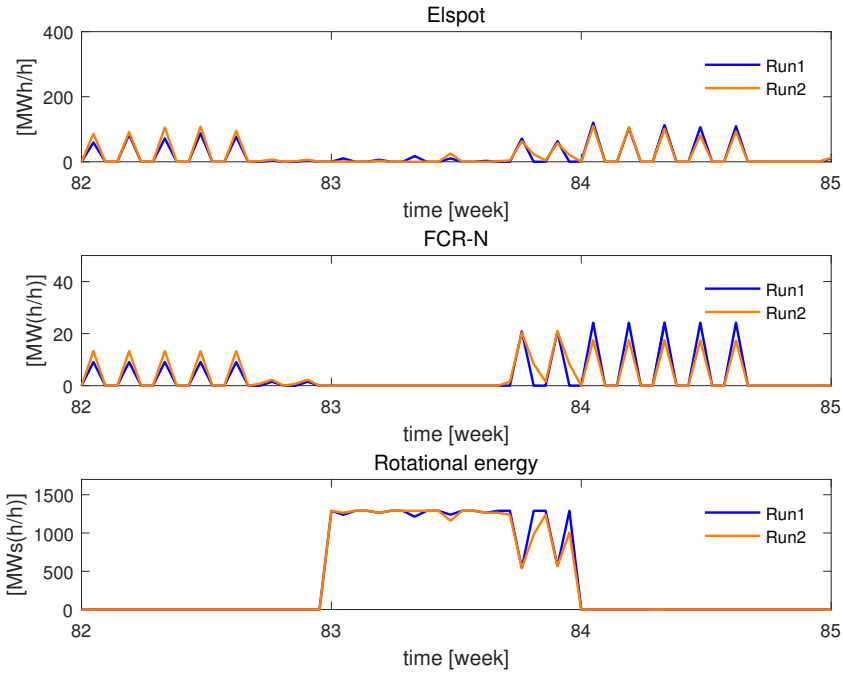

Figure 5.2: Expected Elspot (top), FCR-N (middle) and rotational energy (bottom) market participation in year 2.

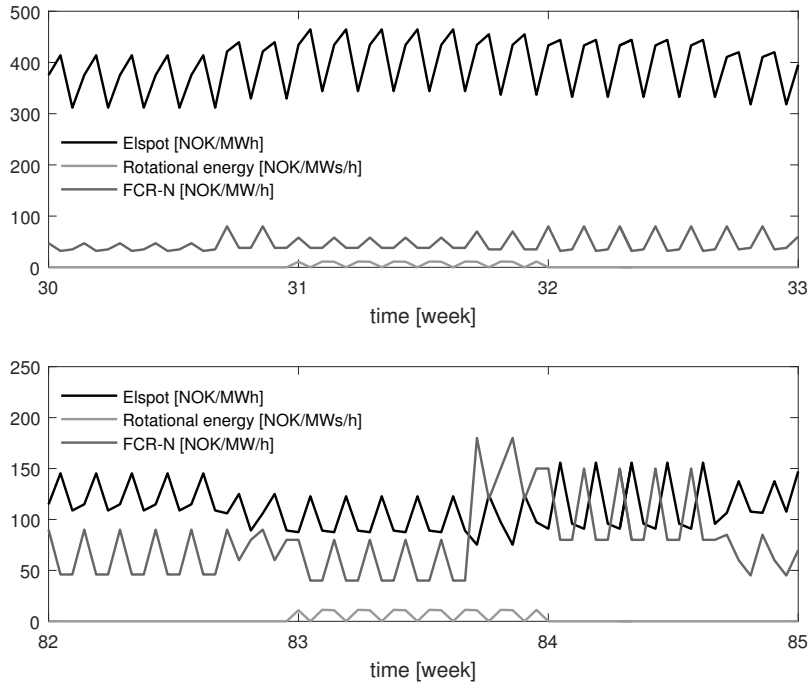

Figure 5.3: Expected Elspot, FCR-N and rotational energy market prices during weeks 30 to 32 (top) and 82 to 84 (bottom).

5.3.2 Rotational energy results

This section will present some additional results related to participation in the rotational energy market.

Socioeconomic cost

The required yearly income of 1 138.41 kNOK/year, from Table 4.5, results in a rotational energy price of 10.51 NOK/MWs/h (not adjusted for start-up costs). In [30], the median value of the strategy with the lowest socioeconomic cost, reducing the dimensioning fault, was 1247 EUR/GWs/h. This is equivalent to 11.59 NOK/MWs/h, using the exchange rate of June 2016[1]. Hence, SC mode of operation of hydropower plants is seen as a cost efficient strategy to ensure sufficient system inertia for the given case study. In [30] it is found that SC mode of operation results in a much higher rotational energy price. This is most likely due to the use of a system

[1] 100 EUR = 929.35 NOK

requirement of 90 GWs, which results in a shorter time period of critically low system inertia, leading to fewer operating hours in SC mode. As shown in Figure 3.3, the necessary rotational energy price to cover the investment in SC mode of operation of hydropower plants strongly depends on the number of SC mode operation hours.

Dual values of rotational energy

The dual values of rotational energy provision, i.e. of constraint (3.90), are equal to the rotational energy prices.

Non-interfering rotational energy price

The rotational energy price level, which does not cause interference with the optimal generation and capacity strategy mentioned in Section 5.2.2, is based on the optimal strategy in run 2. By subtracting the water value multiplied by the discharge from the income from sales of energy and capacity, an indication of the value of Elspot and FCR-N market participation in a given time block and scenario is obtained. Dividing it by the number of hours in the time block and E_m^R provides the rotational energy price level. A rotational energy price lower than this level should mitigate interference in the given time block and scenario. The calculated price levels of the first time block of each day are plotted in descending order in Figure 5.4, regardless of scenario and which day in week 31 they occur. Choosing a price just below 1.02 NOK/MWs/h should mitigate interference in 91.15 % of the cases. Evaluating each time block on its own could lead to higher rotational energy prices without causing interference. However, due to the uncertainty in future prices and the short time period, it is assumed that this would not reflect general trends, but rather characteristics specific to this simulation. The necessary prices to cover the required yearly income while avoiding interference are calculated assuming equal operation as that of run 2. Considering the rotational energy market participation in run 2, the price in the last time block of each day is adjusted for start-up costs, while the price in the first time block of a day is not. The prices are shown in Table 5.4.

Time stage	Time blocks	Rotational energy price
31	$[1, 4, ..., 19]$	1.02 NOK/MWs/h
31	$[2, 5, ..., 20]$	0.00 NOK/MWs/h
31	$[3, 6, ..., 21]$	30.25 NOK/MWs/h

Table 5.4: Modified rotational energy price parameters.

A model run was performed with the prices in Table 5.4, referred to as run 3. The first year market participation in run 3 is plotted against run 2 in Figure 5.5, and

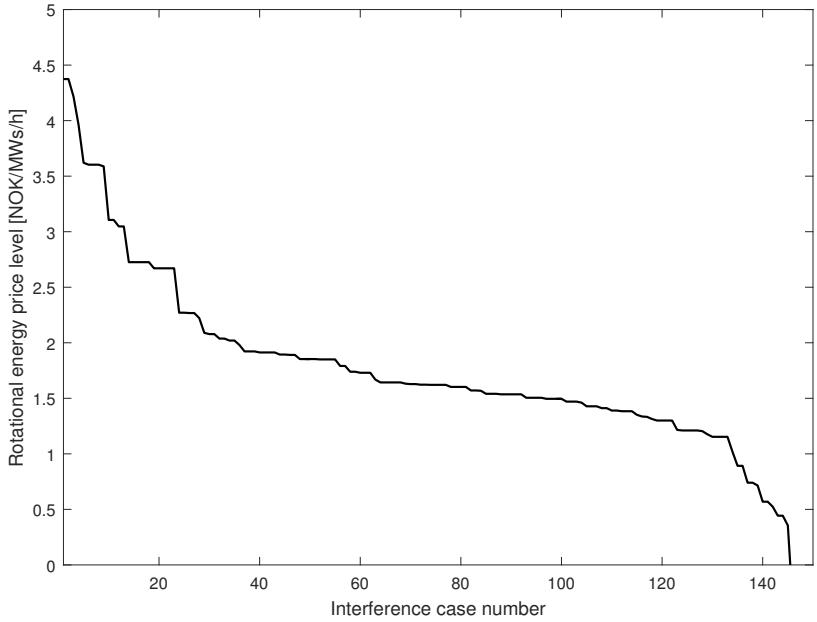

Figure 5.4: Rotational energy price levels for when interference with the optimal production and capacity strategy occurs.

Table 5.5 shows the yearly costs and income associated with SC operation of the runs, averaged over the two years of the simulation period. The results show very similar market participation strategies for the run 2 and 3, but different economic results. While run 2 fails to meet the required income to cover the investment cost, the accumulated income in run 3 is slightly higher than necessary. This is caused transitioning from generation to SC operation, as the rotational energy price in time blocks $[3, 6, ..., 21]$ is set including the start-up cost, which is higher than the transition cost. The results of run 3 will not be discussed further.

Run	Income	Transition costs	Start-up costs	Profit
2	984.04	7.13	5.56	971.35
3	1 152.95	7.5	4.84	1 140.61

Table 5.5: Average yearly economic results from SC operation for model runs 2 and 3 (kNOK).

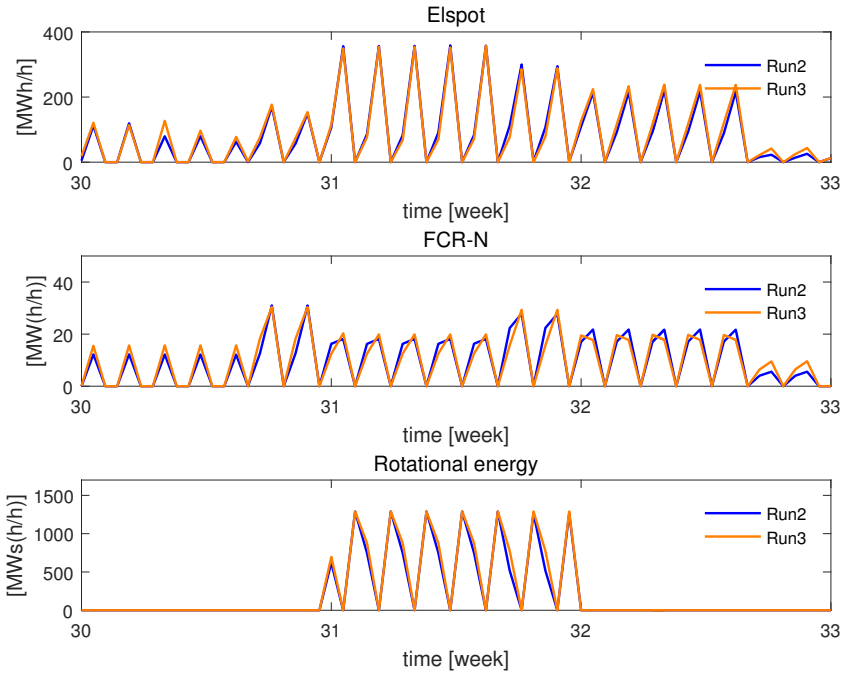

Figure 5.5: Expected Elspot (top), FCR-N (middle) and rotational energy (bottom) market participation for runs 2 and 3.

5.3.3 Reservoir strategy

In Figure 5.6 the expected reservoir levels throughout the simulation period is shown. The plots show a very similar reservoir strategy for the run 1 and 2, confirming that the rotational energy market has a negligible effect on medium-term hydropower scheduling, as previously discussed. Run 2 has a slightly lower reservoir level in Lyngsvatn after week 31, which may be caused by the reduced generation due to rotational energy market participation in run 1. However, the difference is so small that sample variations provide an equally probable explanation. The reservoir levels of Nilsebuvatn and Strandvatn vary frequently due to their low DORs, while the reservoir level of Lyngsvatn follows a yearly cycle.

Figures 5.7 and 5.8 show reservoir percentiles from run 1 and 2, respectively. The percentile curves of Lyngsvatn are spaced closely together, while Nilsebuvatn and Strandvatn have a large variation between the scenarios, especially during the autumn and winter. Due their low DORs and small size, sample variations between the

scenarios have a larger impact on the reservoir strategy.

Table 5.6 shows the expected end reservoir levels. Run 2 is seen to have slightly higher end reservoir levels in all reservoirs, causing the increased end water value seen in Table 5.2.

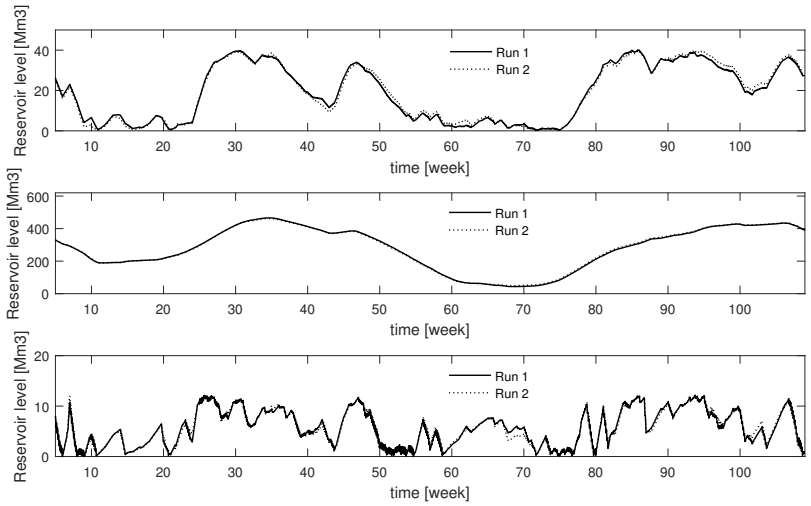

Figure 5.6: Expected reservoir levels for Nilsebuvatn (top), Lyngsvatn (middle), and Strandvatn (bottom) in the two model runs.

Module	Reservoir	Run 1	Run 2
1	Nilsebuvatn	27.44	28.46
2	Lyngsvatn	390.45	392.22
3	Strandvatn	0.70	0.77

Table 5.6: Expected end reservoir levels in [Mm^3].

The water values are plotted in Figure 5.9. The differences between the runs are small, showing that rotational energy market participation has little effect on the water values. The range of the water values clearly increases with decreasing DOR, in accordance with hydropower scheduling theory [33]. Towards the end of the simulation period, the water values converge towards the end cut value of each module. From the figure, it may seem that the end cut values are slightly too high, causing a rapid increase in the water values towards the end of the simulation period. The water values will be discussed further in the next section.

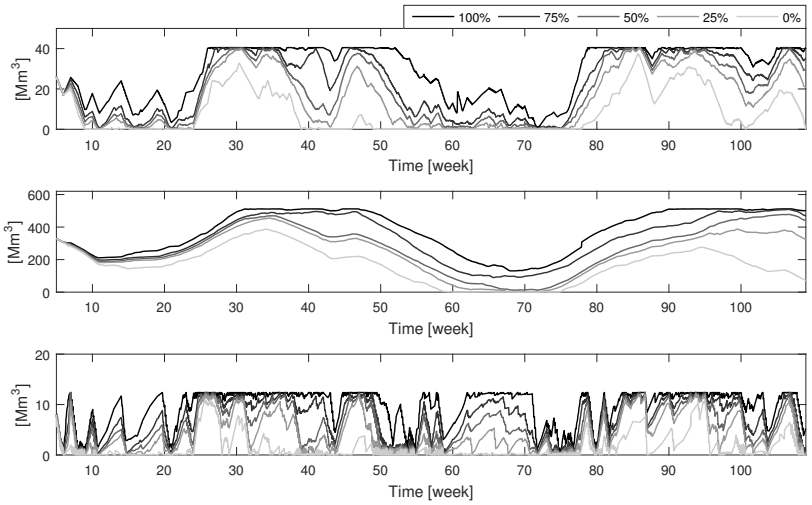

Figure 5.7: Reservoir percentiles for Nilsebuvatn (top), Lyngsvatn (middle), and Strandvatn (bottom) in run 1.

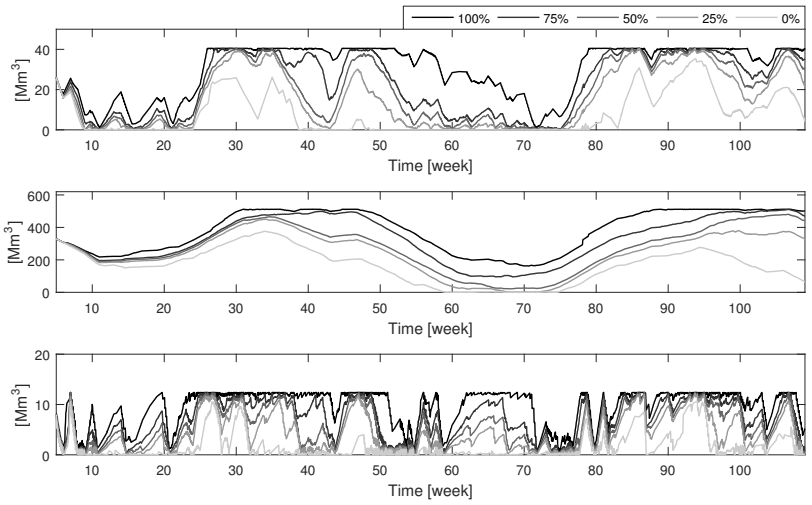

Figure 5.8: Reservoir percentiles for Nilsebuvatn (top), Lyngsvatn (middle), and Strandvatn (bottom) in run 2.

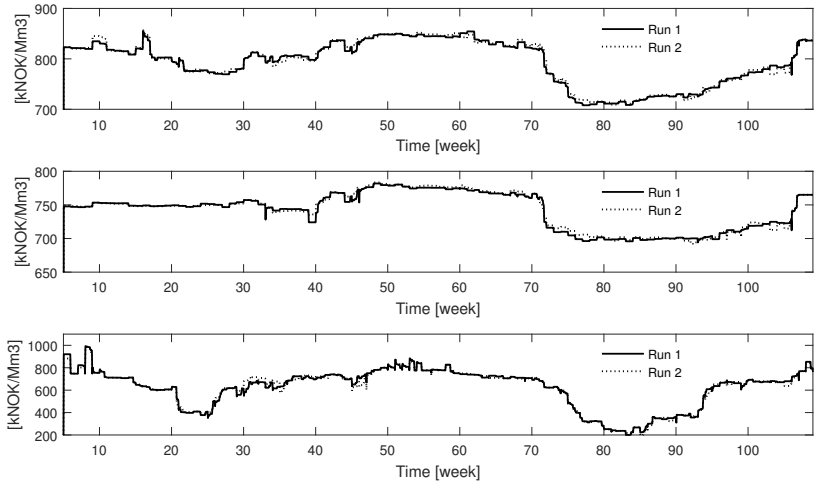

Figure 5.9: Expected water values for Nilsebuvatn (top), Lyngsvatn (middle), and Strandvatn (bottom) in the two model runs.

5.3.4 Generation and capacity strategy

Figures 5.10 and 5.11 show the generation and capacity strategies for the two model runs. The overall generation strategies of the two runs are quite similar, with exceptions when the rotational energy market is active, as previously shown.

The generation strategy of module 1 is greatly affected by the inflow. The maximum discharge of the power station in relation to the reservoir capacity is substantially lower than that of the other modules. Combined with a low DOR, this causes frequent generation. High generation is seen around weeks 20-30 and 75-85, time periods with high inflow and low prices. This is reflected in a lower water value around these periods. Capacity reservation occurs frequently, especially around the aforementioned periods as they experience high FCR-N prices. Sales of capacity is however not seen as a governing factor of the strategy. The generation strategy is also affected by the Elspot prices, as the reservoir is emptied during the high winter prices.

Module 2 has the highest maximum generation and its strategy is strongly affected by the Elspot prices. Although some sales of capacity are made, generation occurs almost exclusively at high Elspot prices. The high DOR is reflected in the small water value variation and accommodates a price based strategy with little impact from the inflow.

Module 3 is seen to generate at minimum generation and high sales of capacity during periods with low Elspot prices and high FCR-N prices. As Lysebotn-2 can generate from only one reservoir at a time, there is almost no generation when the Elspot prices are high and the power plant is generating from Lyngsvatn. Being refrained from generation causes high reservoir levels in Strandvatn as seen in figures 5.7 and 5.8, and is reflected in the very low water values around weeks 20-30 and 75 to 95. Low water values accommodate a strategy with generation at low Elspot prices and high FCR-N prices.

Module 4 generates less frequently than the power stations of the other modules, and the generation occurs at high Elspot prices with low capacity reservation. Figure 5.12 shows the bypass of run 1 and 2. The runs show similar results, and it is seen that bypass from module 2 to 3 occurs during the same periods as bypass from module 3 to 4. As the reservoir of module 4 is a dummy reservoir, water bypassed from Strandvatn must be generated in the same time block. Bypass from module 2 to 3 occurs almost exclusively at night, during the last time block of a day, when prices are low. The water is then bypassed from module 3 to 4 and generated in the two next time blocks, when the prices are higher. This is shown in Figure 5.13, which shows the bypass in the first three weeks of the simulation period. Note that this figure shows the total bypass during the time block, in [Mm^3]. Because some of the stored water in Strandvatn is used to generate and the second time block of a day is longer than the last, the bypass is higher from module 3 to 4 than from module 2 to 3.

As mentioned in Section 4.1.1, the PQ curve of module 4 makes the power station well suited for delivery of FCR-N. However, the strategy of module 4 is dominated by the Elspot market, while module 3 sells capacity when the FCR-N prices are high. Being connected to the same reservoir, these two modules cannot generate simultaneously. This is likely due to the low water values of Strandvatn, which decreases the impact of module 4's favourable PQ curve. Module 3 has a higher maximum power output than module 4. The maximum power available for capacity allocation is therefore higher for module 3, than for module 4. This causes the gain from sales of energy and capacity, adjusted for the water value, to be greater for module 4. Module 4 thus contributes by exploiting the inter-daily price variations by bypassing water at night, and generating during the day, simultaneously with module 2. This might change if other balancing markets are included when solving the hydropower scheduling problem.

Duration curves

The duration curves for the two years are shown in Figure 5.14. The small effect rotational energy market participation has on medium-term hydropower scheduling

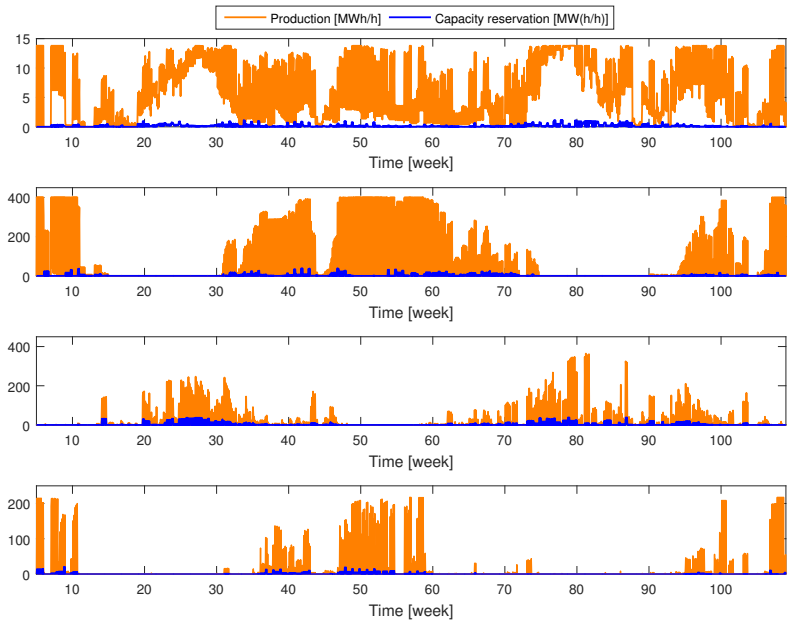

Figure 5.10: Generation and capacity strategy in run 1. From above: module 1 (Breiava power station), module 2 (Lysebotn-2, from Lyngsvatn), module 3 (Lysebotn-2, from Strandvatn) and module 4 (Lysebotn-1).

is reflected in the small difference between the runs. Module 1 has a high number of generating hours, due to the low maximum discharge, as discussed earlier. The generation from module 2 is mainly at maximum, as its strategy is governed by the prices in the Elspot market. Module 4 shows similar characteristics, but with a lower number of generating hours. Module 3 has a considerable amount of generation at minimum, as its strategy is greatly affected by the prices in the FCR-N market.

Dual values of generation

The marginal value of an increase in generation is equal to the Elspot price.

Dual values of capacity

The dual values of constraints (3.82) and (3.81) are shown in Figure 5.15. The dual value of (3.82), referred to as "Capacity up" in the figure, indicates the cost of capacity reservation combined with the associated delivery to the day-ahead market. The value is dependent on the power station's state. If it is not running, it indicates

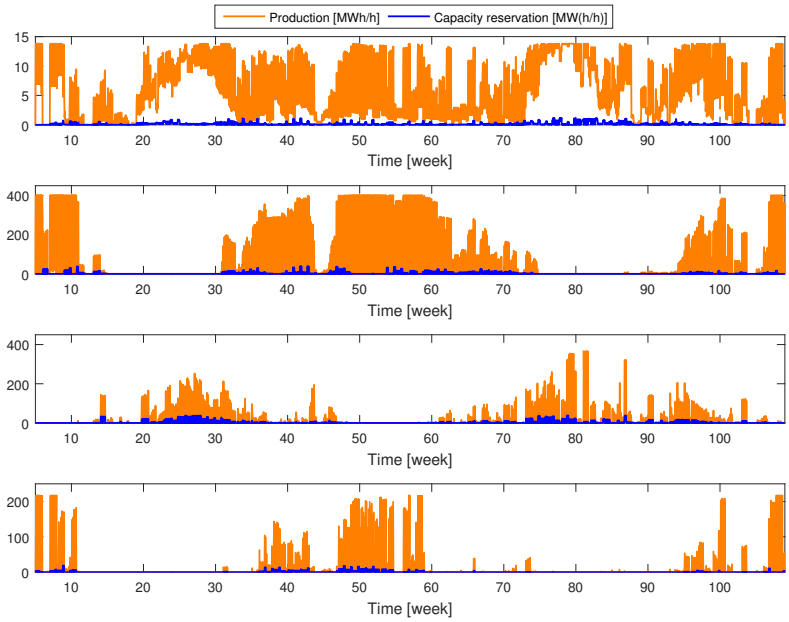

Figure 5.11: Generation and capacity strategy in run 2. From above: module 1 (Breiava power station), module 2 (Lysebotn-2, from Lyngsvatn), module 3 (Lysebotn-2, from Strandvatn) and module 4 (Lysebotn-1).

the cost of selling energy at an unfavorable time. If it is running, the dual value will be zero unless the constraint is binding. This occurs when the power station is producing at minimum, typically during high FCR-N prices and low Elspot prices, in order to sell capacity. The dual value will then be equal to the lost income from reduced sales of capacity or the cost of increased generation at a low price, whichever is smallest. The dual of (3.81), referred to as "Capacity down" in the figure, indicates the marginal income of selling more capacity or energy at times when Elspot prices are high, and the generation is at, or close to, maximum. The absolute values are referred to in the following discussion.

As seen in Figure 5.14, Module 1 has most of its generation at maximum. Additionally, the power station has a high number of generating hours. This causes high capacity down dual values, and small capacity up dual values. Module 2 also generates mainly at its maximum generation limit, but has a lower number of generating hours. The periods without generation experience large capacity up dual values, while the periods with maximum generation experience high capacity down dual values. In module 3, the generation is either at zero or minimum. This causes large capacity up dual

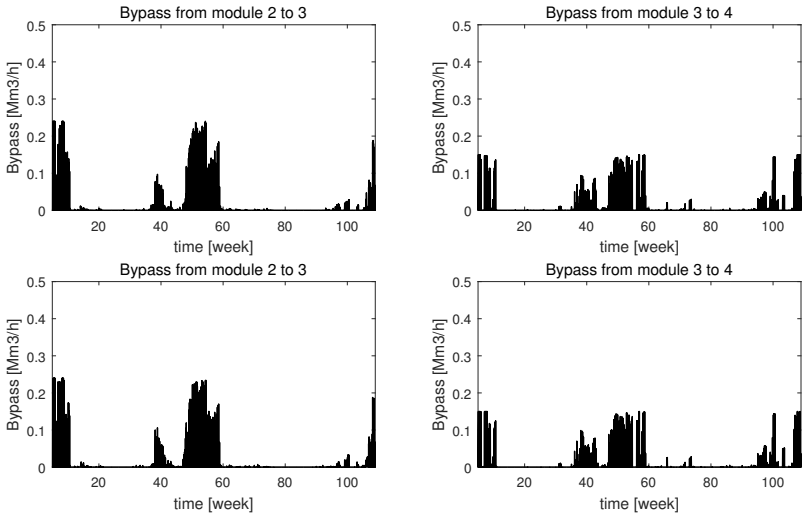

Figure 5.12: Bypass from module 2 to 3 (left) and module 3 to 4 (right) in run 1 (top) and run 2 (bottom).

values almost throughout the whole simulation period, with high capacity down dual values occurring in only a few time blocks. Module 4 has most generation at maximum, but a small number of generating hours. This causes large capacity up dual values most of the simulation period, and high capacity down dual values the short periods where generation occurs.

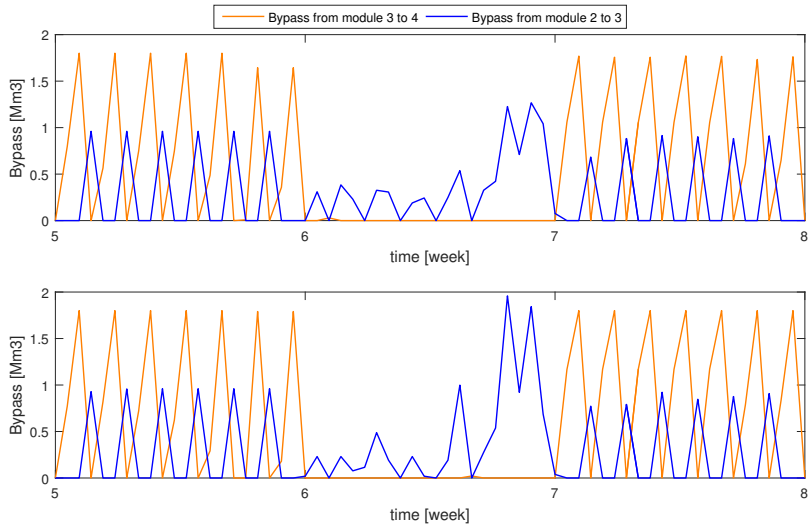

Figure 5.13: Bypass in the first three weeks of the simulation period in run 1 (top) and run 2 (bottom).

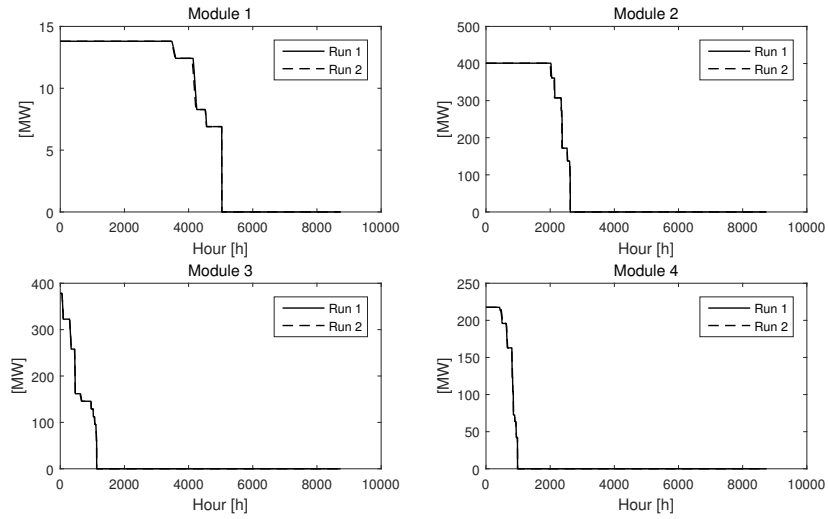

Figure 5.14: Duration curves for each module in the two years of the simulation period.

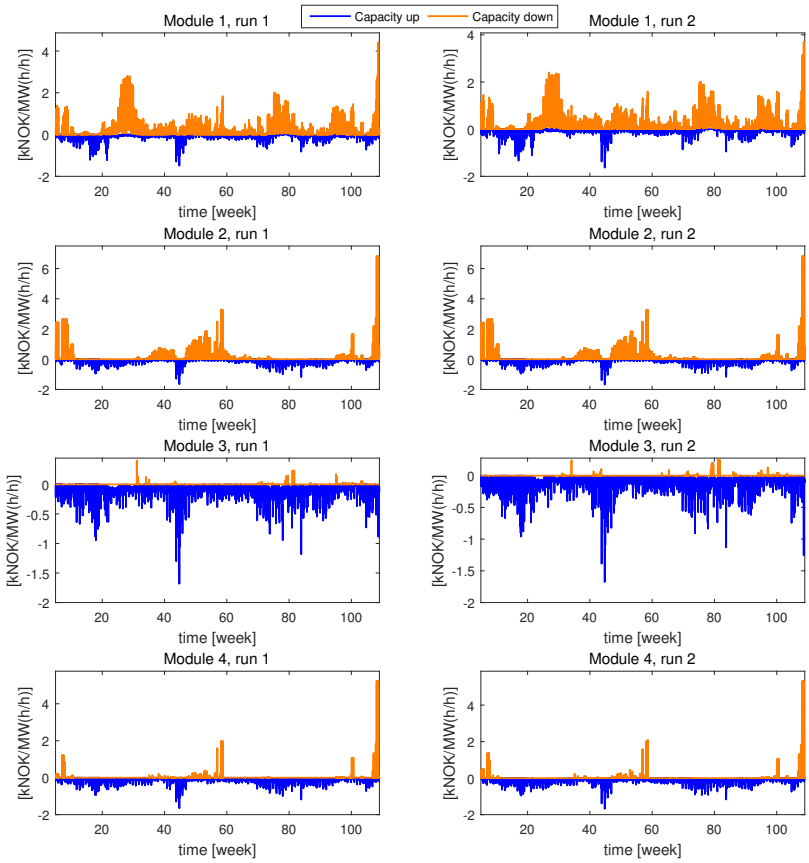

Figure 5.15: Dual values of up and down capacity for each module in run 1 (left) and run 2 (right).

5.3.5 Economic results

Income

Income from the Elspot, FCR-N and rotational energy market for each module is shown in Table 5.7 for run 1 and Table 5.8 for run 2.

Module	Elspot	FCR-N	Rotational energy	Total income
1	50.6	0.2	0.0	50.8
2	1 029.7	2.2	1.6	1 033.6
3	156.5	3.7	0.8	161.0
4	209.9	0.7	0.0	210.6
Sum	1 446.7	6.8	2.4	1 455.9

Table 5.7: Income in run 1 (MNOK).

Module	Elspot	FCR-N	Rotational energy	Total income
1	50.5	0.2	0.0	50.7
2	1 027.1	2.4	1.3	1 030.7
3	156.3	3.7	0.7	160.7
4	211.0	0.6	0.0	211.7
Sum	1 445.0	6.8	2.0	1 453.8

Table 5.8: Income in run 2 (MNOK).

Tables 5.9 and 5.10 show the income distribution between the markets for each module of run 1 and 2, respectively. The runs show fairly similar results, except for the rotational energy share being slightly higher in run 1. The Elspot market clearly makes up most of the income. As previously discussed, modules 1, 2 and 4 have very low shares of income from sales of capacity. Module 3 has an income share from sales of capacity over 6 times higher than module 1, which has the second highest share.

Tables 5.11 and 5.12 show the income distributions between the modules for each market in run 1 and 2, respectively. The two runs show similar results. Module 2 contributes with most of the income from the Elspot market. It also has a considerable share of the income from FCR-N market participation, which comes as a result of the high number of operating hours and capacity limit. The table clearly shows that module 3 has a FCR-N price based strategy, providing over 50 % of the income from the FCR-N market, while only contributing with approximately one tenth of the income from the Elspot market. Income from the rotational energy market is

Module	Elspot	FCR-N	Rotational energy
1	99.63 %	0.37 %	0.00 %
2	99.63 %	0.22 %	0.15 %
3	97.23 %	2.28 %	0.50 %
4	99.68 %	0.32 %	0.00 %

Table 5.9: Income distribution over each market in run 1.

Module	Elspot	FCR-N	Rotational energy
1	99.63 %	0.37 %	0.00 %
2	99.65 %	0.23 %	0.12 %
3	97.29 %	2.27 %	0.43 %
4	99.70 %	0.30 %	0.00 %

Table 5.10: Income distribution over each market in run 2.

only provided by modules 2 and 3. The distribution between them is likely due to transition costs from generation to SC operation being lower than the start-up cost of SC, so the model will prefer to provide rotational energy from a module that was generating in the previous time step.

Market	Module 1	Module 2	Module 3	Module 4
Elspot	3.50 %	71.18 %	10.82 %	14.51 %
FCR-N	2.80 %	33.17 %	54.20 %	9.83 %
Rotational energy	0.00 %	66.66 %	33.34 %	0.00 %

Table 5.11: Income distribution over each module in run 1.

Market	Module 1	Module 2	Module 3	Module 4
Elspot	3.50 %	71.08 %	10.82 %	14.60 %
FCR-N	2.74 %	34.46 %	53.48 %	9.33 %
Rotational energy	0.00 %	64.67 %	35.33 %	0.00 %

Table 5.12: Income distribution over each module in run 2.

Objective values

The upper and lower bounds of the objective functions for run 1 and 2 are shown in Table 5.13. As previously shown, the lower bounds are the average of the objective

values in each scenario, and the upper bounds are the average value of the sum of the first stage solution and the future income. The upper bounds give a more realistic result, while the lower bounds provide a better frame of reference for comparison between the runs being less affected by sample variations. The values include the end water values, which is the reason they are higher than the total income shown in tables 5.7 and 5.8. It is seen that the difference between the lower bounds is much smaller than the difference between the upper bounds.

Run	Upper bound	Lower bound
1	1 725.28	1 728.79
2	1 723.66	1 728.59

Table 5.13: Upper and lower bounds of the objective functions (MNOK).

Both runs have higher lower bounds than upper bounds. Occasional crossing of the bounds at early iterations of the Strategy Model when the problem is very relaxed may occur, but convergence towards a higher lower than upper bound is concerning. This is likely caused by using too few forward scenarios. Increasing the number of forward scenarios is believed to mitigate the result.

5.4 Computation Time

Table 5.14 shows the number of problems solved with associated variables and restrictions. Table 5.15 shows the computation time of each model run. Each run was performed on a Dell Latitude E6430s with 16 GB RAM and an Intel Core i7-3540M CPU with 3.00 GHz.

	Strategy Model	Simulator Model
Forward problems	5200	5200
Backward problems	327600	-
Restrictions	651	2625
Variables	1130	2737
Binary variables	-	924

Table 5.14: Model run characteristics.

	Strategy Model	Simulator Model
Run 1	26h 44m 19s	6h 28m 32s
Run 2	27h 1m 20s	6h 14m 15s

Table 5.15: Computation time for each run.

5.5 Validity of Results and Assumptions

The model runs provide a hydropower scheduling strategy and associated economic results from participation in the Elspot, weekly FCR-N and a hypothetical rotational energy market. The results are based on average values of scenarios with random samples of inflow and day-ahead price.

It is difficult to determine the length and frequency of the periods of critically low system inertia that occur during the night of week 31. It has been assumed that the system inertia is critically low during the first and last time step of each day. It is possible that only some nights will experience that the rotational energy limit is not met and that this lasts only a few hours. Should this be the case, the number of hours the rotational energy market is active in this thesis is too high, entailing that the corresponding rotational energy price which covers the investment cost is too low.

The rotational energy requirement is set to 100 GWs, a limit suggested by Statnett. There is some uncertainty associated with this estimate, as there is still ongoing work to map the amount of rotational energy in the system. Hence, there is a possibility

that the limit is set too high. With sufficient monitoring of the dimensioning fault, a dynamic limit can be obtained. Both a lower and a dynamic limit is likely to reduce the number of hours of critically low inertia. This would also entail that the number of hours the rotational energy market is active in this thesis is too high.

For computational tractability, each time stage is divided into 21 time blocks. The rotational energy market may have a completely different time resolution. Considering the TSO's wish to procure rotational energy provided by synchronous generation, an hourly resolution is likely, as it does not commit hydropower producers to several hours of SC operation. This may cause changes in the market participation strategy, and more frequently induced start-up costs would affect the income. The effects of a rotational energy market with an hourly resolution is however not suited for medium-term models, due to the high computation time it would induce.

The rotational energy price is set to cover the required income to cover the investment cost of the case study. Other hydropower producers may have different investment costs, specific to their hydropower stations. How this would affect the rotational energy price is not taken into account. It is however likely that all participants would recieve the same remuneration for the service.

The calculated rotational energy prices which mitigate interference with the optimal generation and capacity strategy are only valid for the given case study. These prices may be different for other hydropower systems, and are directly dependent on the Elspot and FCR-N price.

Reactive power injection and absorption is a service which is remunerated by the TSO, and can be provided when a power station is operating as a SC. The effects of this on the economic results have not been studied, but would lead to a lower required income from rotational energy provision.

The model assumes that the producer is a price taker. This is a fair assumption with regard to the day ahead market as the model is run for only one system participating in a large market. The FCR-N weekly market is considerably smaller. The assumption of being a price taker is therefore weak with regard to sales of capacity. The rotational energy market is potentially a very small market. As the estimated rotational energy in week 31 is 98.2 GWs and the rotational energy provided from SC operation of Lysebotn-2 is 1.29 GWs, only one more participant (equivalent to Lysebotn-2) is needed to meet the rotational energy limit of 100 GWs. However, the assumption does not affect the rotational energy market modelled in this thesis, with a a fixed price/remuneration to cover the investment cost.

The operational costs are assumed to be low, but neglecting them provides inaccurate marginal costs. Continuous SC operation is observed in the second year of the

simulation period. It is not known if this would occur if the operational costs are taken into account, and may therefore be an unrealistic SC operating strategy.

Equation (3.21) is not included in the cuts, despite being a time coupled constraint. Its dual value, i.e. its coefficient in the cuts, would be equal to the start-up costs. Comparing it to the water values, one of the cut coefficients of (3.1), assuming it to have a negligible effect on the cuts seems fair.

In Table 5.2, it is seen that the end water value is of a considerable size compared to the total income. As discussed in Section 3.1.8, using only one end cut value can give a poor estimate of the end water value. Running the model for a longer period of time would reduce the effects of the end cut. For example, running the model for three or four years and analysing only the first two could give more realistic results. Another solution would be to alter the model so that the end reservoir volume could be set equal to the initial reservoir volume.

The capacity prices are modelled by the historical price data of the past two years. They are therefore equal for every scenario. Whether the prices used are representative is unknown, they could be both higher and lower than what the actual prices will be the next two years. As previously mentioned, capacity prices seem to be correlated to the day-ahead market prices. Modelling this correlation, using a larger set of historical data and taking expected future trends into account would give more realistic results.

As the two runs are solved for the same price and inflow samples, potential sample variations were not observed. It is, however, believed that 50 scenarios might be too low, and a higher number of forward scenarios is favorable. This is indicated by the lower bound of the objective function being higher than the upper bound. Increasing the number of scenarios would cause an impractical computation time. A solution is to increase the number of scenarios in the last iteration of the Strategy Model. The Simulator Model would then be solved for the same scenarios. This would require some changes of the model with regard to memory allocation.

Finally, it should be mentioned that as the thesis is based on a prototype model which has been altered to fit the hydro system described in Section 4.1.1, the results may be subject to modelling errors. This is valid for both expected and unexpected results, although unexpected results imply a higher probability of modelling errors. Error checks have been performed, but there is no guarantee that something has not been overlooked.

6 Conclusion and Further Work

In this thesis the structure of the Nordic power markets, the inertial dependency of a power system and the SDDP optimization technique have been reviewed and used as a basis for the explanation of the combined SDP/SDDP hydropower scheduling model participating in several markets. By employing the model, the effects of participation in a hypothetical rotational energy market alongside the day-ahead and primary frequency reserve markets on medium-term hydropower scheduling have been studied.

6.1 Conclusion

The work of this thesis found that the provision of rotational energy has small effects on medium-term hydropower scheduling. This is valid for the given case study, considering an estimate of the rotational energy in the Nordic power system in the year 2020. It is believed that rotational energy provision will have a larger impact medium-term hydropower scheduling further into the future.

The results showed promising income potential from rotational energy provision compared to a day-ahead and capacity market. The yearly income did not cover the investment cost when speculation was removed. This indicates that the price should have been higher, to provide investment incentives. A higher price would however also provide stronger speculation incentives. It was found that a low rotational energy price in the first time step of a day, and a high price in the last time step provided an optimal operation strategy without interference between provision of rotational energy and sales of energy and capacity, while still covering the investment cost.

The economic results of rotational energy market participation were seen to have a high degree of uncertainty. This is associated with the number of hours the market is active, the rotational energy limit, the market's time resolution, remuneration for reactive power injection and absorption, and the investment cost of SC mode of operation of hydropower plants.

The performed simulations showed that continued operation of Lysebotn-1 did not provide substantial income from the FCR-N market. The main contribution of Lysebotn-1 was to exploit the inter-daily price variations by bypassing water from Lyngsvatn to Strandvatn at night, and generating during the day. Including other balancing markets in the scheduling process might affect this result.

6.2 Further Work

Further work should be put into analyzing the trade-off between speculation and investment incentives, from a socio-economic viewpoint. To achieve a better estimate of the cost of rotational energy provision, the income from reactive power injection and absorption should be analyzed. The operational costs should also be studied, to calculate the marginal cost of rotational energy provision. A short-term model should be applied to further study the effects of rotational energy provision on hydropower scheduling.

The ongoing work concerning the inertia in the Nordic power system should be followed closely, as better estimates of the future rotational energy would improve the accuracy of the results.

Better modelling of the FCR-N weekly prices would give a better insight into the income potential. Extending the model to include other reserve markets is also of interest, especially for evaluating continued operation of Lysebotn-1.

Finally, the model should be altered to accommodate an increase in forward scenarios in the last iteration of the Strategy Model, and subsequently the Simulator model.

References

[1] Statnett, "Systemdrifts- og markedsutviklingsplan," no. 20, 2014. In Norwegian. [Online]. Available: http://www.statnett.no/Drift-og-marked/Systemansvaret/Systemdrifts--og-markedsutviklingsplan/

[2] European Network of Transmission System Operators for Electricity (ENTSO-E), "NAG Future system inertia," 2015. [Online]. Available: https://www.entsoe.eu/Documents/Publications/SOC/Nordic/Nordic_report_Future_System_Inertia.pdf

[3] I. Wangensteen, *Power System Economics - The Nordic Electricity Market.* Trondheim: Tapir Academic Press, 2012.

[4] M. N. Hjelmeland, "Long-term scheduling of hydro power systems in multiple power markets," Master's thesis, Norwegian University of Science and Technology (NTNU) Trondheim, 2015.

[5] P. W. Christensen and G. C. Tarnowski, "Inertia for wind power plants–state of the art review–year 2011," in *proc. 10th International Workshop on largescale integration of wind power into power systems*, 2011.

[6] SINTEF Energy Research, "ProdRisk," 2015. [Online]. Available: http://sintef.no/en/sintef-energy/softwareenglish/allsoftware_english/prodrisk/

[7] Statnett, "Statnetts praktisering av systemansvaret," 2013. In Norwegian.

[8] Nord Pool Spot , "About us," 2016. [Online]. Available: http://nordpoolspot.com/About-us/

[9] Lovdata, "Forskrift om systemansvaret i kraftsystemet," 2016. In Norwegian. [Online]. Available: https://lovdata.no/dokument/SF/forskrift/2002-05-07-448

[10] Nord Pool Spot, "Day-ahead market Elspot," 2016. [Online]. Available: http://www.nordpoolspot.com/TAS/Day-ahead-market-Elspot/

[11] Nord Pool Spot , "Trading," 2016. [Online]. Available: http://www.nordpoolspot.com/TAS/

[12] Nord Pool Spot, "Price coupling of regions (PCR)," 2016. [Online]. Available: http://www.nordpoolspot.com/How-does-it-work/Integrated-Europe/Price-coupling-of-regions/

[13] EPEX Spot, "A major step towards market integration," 2016. [Online]. Available: http://www.epexspot.com/en/market-coupling

[14] Nord Pool Spot , "Intraday market," 2016. [Online]. Available: http://nordpoolspot.com/How-does-it-work/Intraday-market/

[15] Nord Pool Spot, "Nord Pool Spot intraday," 2016. [Online]. Available: http://www.nordpoolspot.com/TAS/nord-pool-spot-intraday/

[16] Statnett, "Vilkår for tilbud, aksept, rapportering og avregning i marked for primærreserver til Statnett," 2015. In Norwegian.

[17] European Network of Transmission System Operators for Electricity (ENTSO-E) , "System operation agreement," 2006. [Online]. Available: https://www.entsoe.eu/Documents/Publications/SOC/Nordic/System_Operation_Agreement_English_translation.pdf

[18] A. Helseth, M. Fodstad, and A. L. Henden, "Balancing markets and their impact on hydropower scheduling," 2015. Unpublished.

[19] Statnett, "Primary reserves," 2016. [Online]. Available: http://statnett.no/Drift-og-marked/Markedsinformasjon/Primarreserver/

[20] Statnett, "Secondary reserves," 2016. [Online]. Available: http://statnett.no/Drift-og-marked/Markedsinformasjon/sekundarreserver/

[21] Statnett, "Oppstart av nytt marked for automatiske sekundærreserver," 2016. In Norwegian. [Online]. Available: http://www.statnett.no/Media/Nyheter/Nyhetsarkiv-2012/Oppstart-av-nytt-marked-for-automatiske-sekundarreserver-/

[22] Statnett, "Tertiary reserves," 2016. [Online]. Available: http://statnett.no/Drift-og-marked/Markedsinformasjon/RKOM1/

[23] S. M. Hamre, "Inertia and FCR in the present and future Nordic power system," Master's thesis, Norwegian University of Science and Technology (NTNU) Trondheim, 2015.

[24] F. M. Gonzales-Longatt, "Effects of the synthetic inertia from wind power on the total system inertia: Simulation study," *2nd International Symposium on Environment-Friendly Energies and Applications (EFEA)*, pp. 389 – 395, 2012.

[25] Statnett, "KUBE2015: Markedsløsninger for neste generasjon kraftsystem," 2015. In Norwegian. [Online]. Available: http://www.statnett.no/Karriere/er-du-student/KUBE/Er-dagens-markedslosninger-tilstrekkelige-i-mote-med-Neste-generasjon-kraftsystem/

[26] P. Daly, D. Flynn, and N. Cunniffe, "Inertia considerations within unit commitment and economic dispatch for systems with high non-synchronous penetrations," *PowerTech, IEEE Eindhoven*, 2015.

[27] SEM Committee, "DS3 System services technical definitions decision paper," 2013. [Online]. Available: https://www.semcommittee.com/publication/sem-13-098-ds3-system-services-technical-definitions-decision-paper-final-0

[28] H. Lie, "Teknisk/økonomisk analyse av roterende fasekompensator," Master's thesis, Norwegian University of Science and Technology (NTNU) Trondheim, 2008. In Norwegian.

[29] Statnett, "Funksjonskrav i kraftsystemet," 2012. In Norwegian. [Online]. Available: http://www.statnett.no/Media/Nyheter/Nyhetsarkiv-2012/Funksjonskrav-i-kraftsystemet-FIKS-2012-publisert-/

[30] A. Karsrud, "Framtidig utvikling og sikring av rotasjonsenergi i det nordiske kraftsystemet," Master's thesis, Norwegian University of Science and Technology (NTNU) Trondheim, 2016. In Norwegian.

[31] M. V. F. Pereira and L. Pinto, "Multi-stage stochastic optimization applied to energy planning," *Mathematical Programming*, vol. 52, pp. 359–375, 1991.

[32] M. V. F. Pereira, "Optimal stochastic operations scheduling of large hydroelectric systems," *Electrical Power & Energy Systems*, vol. 11, no. 3, pp. 161–169, 1989.

[33] G. Doorman, *Hydro Power Scheduling.* Department of Electrical Power Engineering, NTNU, 2015.

[34] J. Lundgren, M. Rönnqvist, and P. Värbrand, *Optimization.* Lund: Studentlitteratur AB, 2012.

[35] J. R. Birge and F. Louveaux, *Introduction to Stochastic Programming.* Springer, 2011.

[36] A. Helseth, M. Fodstad, and B. Mo, "Optimal medium-term hydropower scheduling considering energy and reserve capacity markets," *IEEE Transactions on Sustainable Energy*, no. 99, pp. 1–9, 2016.

[37] A. Gjelsvik, M. M. Belsnes, and A. Haugstad, "An algorithm for stochastic medium-term hydrothermal scheduling under spot price uncertainty," *Power System Computation Conference (PSCC)*, vol. 13, pp. 1079–1085, June 28 - July 2nd, 1999.

[38] M. N. Hjelmeland, M. Korpås, and A. Helseth, "Combined SDDP and simulator model for hydropower scheduling with sales of capacity," 2016. In Review, accepted for presentation in EEM 2016.

[39] A. Gjelsvik, B. Mo, and A. Haugstad, "Long- and medium-term term operations planning and stochastic modelling in hydro-dominated power systems based on stochastic dual dynamic programming," *Handbook of Power Systems I*, pp. 33–35, 2012.

[40] O. Nilsson and D. Sjelvgren, "Hydro unit start-up costs and their impact on the short term scheduling strategies of Swedish power producers," *IEEE Transactions on Power Systems*, vol. 12, no. 1, pp. 38–44, 1997.

[41] M. Lei and Z. Feng, "A novel grey model to short-term electricity price forecasting for NordPool power market," *Proceedings of the 2009 IEEE International Conference on Systems, Man, and Cybernetics*, pp. 4347–4352, 2009.

[42] O. Wolfgang, A. Haugstad, B. Mo, A. Gjelsvik, I. Wangensteen, and G. Doorman, "Hydro reservoir handling in norway before and after deregulation," *Energy*, vol. 34, no. 10, pp. 1642 – 1651, 2009, 11th Conference on Process Integration, Modelling and Optimisation for Energy Saving and Pollution Reduction.

[43] Statistics Norway, "Producer price index for oil and gas, manufacturing, mining and electricity," 2016. [Online]. Available: https://www.ssb.no/en/priser-og-prisindekser/statistikker/ppi

[44] B. Jensen, "Diskonteringsrenten mv. i beregningsgrunnlaget for elendomsskatt på vannkraftverk," 2011. In Norwegian. [Online]. Available: https://www.regjeringen.no/contentassets/9a7910829ffe4e0bace71279f68784e1/62_landssamanslutninga_vedlegg.pdf

[45] Norges Bank, "Government bonds annual average," 2016. [Online]. Available: http://www.norges-bank.no/en/Statistics/Interest-rates/Government-bonds-annual/

[46] Norges Vassdrags- og Energidirektorat (NVE), "Samfunnsøkonomisk analyse av energiprosjekter," 2003. In Norwegian.

[47] Nord Pool Spot, "Historical market data," 2016. [Online]. Available: http://nordpoolspot.com/historical-market-data/

[48] Statnett, "Download centre," 2016. [Online]. Available: http://statnett.no/Drift-og-marked/Nedlastingssenter/Last-ned-grunndata/

A Conference Paper

This appendix includes the conference paper that the results of this thesis are based on.

Medium-term hydropower scheduling with provision of capacity reserves and inertia

Jacob Koren Brekke, Martin N. Hjelmeland, Magnus Korpås
Department of Electric Power Engineering
NTNU Norwegian University of Science and Technology
Trondheim, Norway
Email: jacobkorenbrekke@gmail.com

***Abstract*—In this article we study the effects of participation in a hypothetical rotational energy market alongside the day-ahead and primary frequency reserve markets on medium-term hydropower scheduling. Participants in the rotational energy market, where the hydropower unit operates in synchronous condenser mode, are remunerated for provision of rotational energy that does not alter production.**

Stochastic medium-term hydropower scheduling models are usually based on optimization techniques which require Linear Programming (LP) problems to ensure computational tractability. This imposes simplifications on the problem formulation, such as operating states which typically have a binary nature. Utilizing a strategy obtained by Stochastic Dual Dynamic Programming (SDDP) in a simulator model based on Mixed Integer Programming (MIP), yields a detailed system description and practical computation time.

For the given case study, it was found that rotational energy provision has a small effect on medium-term hydropower scheduling, due to the short time period of critically low inertia. If was also found that the necessary price to cover the investment cost, associated with rotational energy provision, was at a level that caused interference with the optimal production strategy. However, increasing the price in certain time steps and decreasing it in others is likely to mitigate this problem.

NOMENCLATURE

Sets and indices

$i \in \mathcal{U}$	Set of hydro power units.
$k \in \mathcal{K}$	Set of time steps.
$t \in \mathcal{T}$	Set of time stages.

Parameters

E_i^R	Rotational kinetic energy of power station. [MWs]

Variables

α_t	Future income function. [kNOK]
δ_{tki}	Binary start-up variable.
θ_{tki}	Binary transition variable.
e_{tk}^R	Rotational kinetic energy provided. [MWs]
o_{tki}	Binary state of rotational energy provision.
u_{tki}	Binary state of power station.

I. INTRODUCTION

In the EU there are ambitious targets for increasing the renewable electricity generation, especially wind and solar power. In order to facilitate this large scale integration of renewable energies, a set of mechanisms has to be established. By improving the transmission capacity in the power system, by coupling of regions through HVDC cables, synergies can be exploited, reducing the need for dispatchable thermal generation in the regions, and subsequently the CO_2-emissions. A challenge is however that the renewable power generation varies a lot depending on weather conditions and do not easily provide the grid with inertia [1], compromising the stability of the grid. It is therefore crucial to ensure sufficient capacity and energy reserves, and system inertia to secure stability in the power grid.

Especially during summer months, it is expected that low dispatchable generation and a significant import of cheap renewable energy from the continent will reduce the system inertia in the Nordic region. This provides an incentive for the Transmisstion System Operator (TSO) to either invest in equipment, such as flywheels, or remunerate power producers, for the provision of inertia to the power system. This provision of inertia would, however, impose a cost on the hydropower producer which should be analyzed.

A market for inertia is already under development in Ireland, where Synchronous Inertial Response (SIR) has been approved as a new service [2]. The service is only approved in principle and not yet implemented, but it still emphasizes the importance of a sufficient amount of inertia in a power system.

The main objective of this work is to study the effects of participation in several markets, including a rotational energy market, on hydropower scheduling using a combined SDDP and simulator approach. The SDDP Model will incorporate provision of inertia and balancing reserves to the system and generate a strategy, represented by the expected future profit function, that is used in the detailed Simulator Model. A case study on a Norwegian hydropower system will be conducted with focus on evaluating the cost of providing ancillary services. The novel contribution of the work will henceforth be to present a method for evaluating the cost of providing inertia, which could provide decision support, especially in a future market with large amounts of variable renewable generation and HVDC interconnectors.

A. Inertia in the power system

System inertia is defined as the ability of a power system to oppose changes in the system frequency due to resistance provided by rotating masses [3]. Following a power imbalance, the system inertia determines the initial rate of change in the frequency. Hence, system inertia is important to the stability

of the grid. Traditionally, a large share of the demand in the Nordic power system has been covered by large rotating machines supplying a base load. Wind power and imported power through HVDC cables do not contribute to the system inertia with current technology. As the share of unpredictable renewable power sources and use of HVDC cables increases, there is a rising concern that the system inertia will become inadequate [4].

There is currently no system requirement for the amount of rotational energy in the Nordic power system. Such a system requirement may be derived from keeping the frequency within its transient limit should a dimensioning fault occur. In [5] a limit of 90 GWs was suggested while the current limit recommended by the Norwegian TSO, Statnett, is 100 GWs.

B. Methods for ensuring sufficient system inertia

In consideration to the future stability of the power grid, there are different ways to procure a sufficient amount of rotational energy [5]. This section will discuss strategies that ensure the rotational energy to be above a system requirement.

1) Reducing the dimensioning fault: In [3], it was found that the maximum frequency deviation has a linear relation to the power imbalance and rotational energy of the system. By reducing the potential power imbalance, i.e. the dimensioning fault, at times with low system inertia, the required rotational energy of the system would be reduced. In practice, this entails replacing the largest active power infeed/outfeed with smaller units.

2) Existing market solutions: The rotational energy requirement can be met by employing existing market solutions to increase the amount of synchronous generators in the system.

As of today only rotating machines participate in the primary reserve market [5]. Hence, the primary reserves system requirement will ensure a certain amount of rotational energy in the system. Increasing the primary reserve requirement will increase the number of rotating synchronous generators and the amount of rotational energy. The system inertia can also be increased by introducing a criteria for the number of activated bids, when clearing the primary reserves market. This allows the TSO to ensure that a certain amount of synchronous generators will be connected to the grid.

By participation in the market for Tertiary Control Reserve (TCR), power stations which contribute with little or no rotational energy may be regulated down and be replaced by upward regulation of power stations with a more substantial contribution of rotational energy.

In [5], it is concluded that considering costs and difficulty of implementation, the market for TCR is the best way of ensuring sufficient amounts of rotational energy using existing market solutions.

3) New market designs: A new market design will provide producers with incentives to provide rotational energy in a cost efficient manner through investments and technological improvements. A challenge is however that such a market may affect the existing power markets and provide a competitive advantage based on the production type and technology of certain power producers.

In [5] several different rotational market designs are discussed. This paper will focus on a market design cleared after the day-ahead market, which is only active at times with critically low system inertia. The clearing of the day-ahead market can be used by the TSO to estimate the rotational energy in the system. Should the estimate fall below the system requirement, the TSO can activate the rotational energy market. It is stressed that, as the TSO will have an almost perfectly inelastic demand for this service, participants will have strong incentives to exploit potential market power. To avoid this, a sufficient number of market participants or close monitoring of the market will be necessary.

A key discussion is whether all providers of rotational energy should be remunerated. This depends on the volume of rotational energy needed and the number of power producers able to provide inertia without altering their production. Remunerating all parties supplying the grid with inertia reduces the risk of rotating power plants shutting down, should low prices in the intraday market, due to unexpected renewable power, occur. This will however result in an energy ineffective production mix, using storable water instead of instantaneous wind or solar power. Additionally, the total cost for the TSO will be high as synchronous generators already cleared in the day-ahead market are unnecessarily remunerated.

An alternative is to only remunerate the providers of the rotational energy needed to meet the system requirement, excluding rotational energy provision from synchronous generation. This market design requires participants to be able to provide rotational energy without altering their production. The design is considerably more cost efficient as it remunerates fewer participants. However, a high remuneration provides incentives for power producers to speculate in refraining from day-ahead market participation at times they believe that the rotational energy market will be activated. Should a producer follow this strategy with several hydropower plants, the system inertia may drop below the system requirement as a direct result of the speculation. This shows one of the potential flaws of this market design, with exploitation of market power. Hydropower producers may also downward regulate plants in the intraday market, in order to participate in the rotational energy market. It is however assumed that the income from the day-ahead market will be dominating, marginalizing this problem.

C. Synchronous Condenser (SC) mode of operation

A rotating SC is a synchronous machine that operates without any load or prime mover. SCs can inject or absorb reactive power, and have traditionally been used to improve voltage conditions. From the 1980s, power electronics were preferred due to lower investment and maintenance costs. In recent years, attention has been brought to two other attributes of rotating SCs; they provide inertia and counteract faults related to the commutating of rectifiers when placed near HVDC cable connections [6]. This substantially increases their utility in the power system. In 2008 a rotating SC was

installed in Feda, a substation south in Norway. In relation to system inertia, the investment costs are estimated to 40100 kNOK/MWs/year [7].

By equipping a hydropower plant with a compressor, water may be pumped out of the turbine chamber. This would allow the turbine to idle, acting as a SC. Several costs are associated with SC mode of operation. These include, but are not limited to, higher maintenance costs due to an increased number of operational hours and technical components, operation of compressors and cooling system and power consumption due to friction. If the cooling system uses water that could potentially be used for production, there is a cost associated with the resulting lost income as well. In [7], the investment cost was estimated to 10-20 kNOK/MWs.

Considering investment in SC mode of operation of hydropower plants the hydropower producer would require a remuneration for supplying the service. In the presented work we study the impacts of SC mode of operation on hydropower scheduling and evaluate what the required remuneration should be.

II. Methodology

In this chapter, the combined SDDP and Simulator Model will be described. A similar model was described in detail in [8]. The SDDP Model used is also well documented in [9].

The model's objective is to maximize income by selling energy in the day-ahead market, capacity in the weekly primary reserves market and rotational energy to a hypothetical rotational energy market.

A. SDDP Model

The SDDP Model is based on an extended version of the combined SDP/SDDP algorithm presented in [10], solving a hydropower scheduling problem for each time stage of the model period. The following is a general formulation of the one-stage problem:

$$\alpha_t(\mathbf{x}_{t-1}, \omega_t) = \max\left\{L_t(\mathbf{x}_t, \mathbf{u}_t) + \alpha_{t+1}(\mathbf{x}_t, \omega_{t+1})\right\} \quad (1)$$

subject to

$$\mathbf{A}\mathbf{x}_t + \mathbf{B}\mathbf{u}_t = \mathbf{C}\mathbf{x}_{t-1} + \mathbf{D}\mathbf{a}_t(\omega_t) \quad (2)$$

$$\mathbf{E}\mathbf{u}_t + \mathbf{F}\mathbf{x}_t = \mathbf{d}_t \quad (3)$$

$$\mathbf{H}\mathbf{x}_t + \mathbf{I}\mathbf{x}_{t-1} \leq \mathbf{c}_t \quad (4)$$

$$\mathbf{u}^{\mathrm{lb}} \leq \mathbf{u}_t \leq \mathbf{u}^{\mathrm{ub}} \quad (5)$$

$$\mathbf{x}^{\mathrm{lb}} \leq \mathbf{x}_t \leq \mathbf{x}^{\mathrm{ub}} \quad (6)$$

$$\alpha_{t+1} + \pi_{t+1}\mathbf{x}_t \leq \mathbf{b}_t \quad (7)$$

The problem maximizes current and future income, subject to the state and decision variables x_t and u_t, as well as realizations of the stochastic parameter ω_t. State variables include reservoir level, turbine states, normalized inflow and inertia provision, while decision variables are generation and provision of capacity and rotating reserves.

The current income is given by L_t, a function consisting of income from market participation and costs and penalties. The reservoir balance is included in (2), along with a linearized model of the start-up of power stations, described in [11]. Matrices $\mathbf{A}$, $\mathbf{B}$, $\mathbf{C}$ and $\mathbf{D}$ describe the hydrological connections of the system. (3) includes the energy balance, capacity balance and rotational energy balance. Matrices $\mathbf{E}$ and $\mathbf{F}$ are comprised of factors coupling discharge to energy and SC operation to rotational energy. Variations in head will affect the energy-discharge relation. However, as it may lead to non-convex problems and greatly increases model complexity, this characteristic is not included in the model. (4) models limits on operational states such as start/stop and rotational energy provision. $\mathbf{H}$ and $\mathbf{I}$ describe the coupling between current and previous states and $\mathbf{c}_t$ includes the limit values. (7) consists of cuts which describe the expected future income function.

Capacity allocation is in the form of symmetrical spinning capacity. Hence, a power station must be generating to sell capacity and the amount of capacity sold must be available for both upward and downward regulation. The maximum capacity allocation possible is given by the droop setting in the turbine governor. Capacity sold must be available for certain time steps of the capacity delivery period, specific to the capacity market.

Hydropower units can be modelled with the ability to provide rotational energy without generating power. As mentioned, (4) models this feature as well as costs associated with the start-up of, and transitions between, generation and rotational energy provision.

The inflow is modelled by historical inflow data and a linear stochastic model of normalized inflows, obtained with a first stage auto-regressive model. A detailed derivation can be found in [12].

To ensure problem convexity the spot price is modelled as discrete values represented by a set of price points with transition probabilities between time-stages, generated from a Markov process. A more detailed explanation is given in [10].

Both the capacity reserve and rotational energy markets are modelled as deterministic price series.

The various market prices for a time stage is known at the beginning of that time stage, clearing all markets simultaneously. This provides the optimization process in a given time stage with more information than what is actually available and provides the hydropower producer with the opportunity to perfectly speculate when the rotational energy market will be open. Altering the one-stage problem to allow simultaneous rotational energy provision and generation provides a strategy which refrains the hydropower producer from speculation. This requires some modification of the results, to remove impossible operational states.

B. Simulator Model

The Simulator Model utilizes the strategy obtained from the SDDP Model and applies a more detailed description of the system when solving the problem, adding cuts from the SDDP Model at the end of each time stage. It is modelled as a Mixed Integer Programming (MIP) problem, accommodating integer and binary variables. This allows it to capture the binary nature of a power station's state, which is vital for

a realistic rotational energy strategy. The one-stage problem formulation of the Simulator Model is similar to that of the SDDP Model, with some changes due to the enhanced system description.

1) Hydropower unit: As the Simulator Model is no longer bound by the convex requirement as in SDDP, the Simulator Model includes a detailed modelling of the non-convex power-discharge function. This also enables a minimum generation level constraint for the hydropower units. Previous studies have shown that this has a large impact when dealing with capacity markets [8].

2) State transitions: There are costs associated with the transitioning between standstill, generation and rotational energy provision. The cost of shutting down either generation or rotational energy provision is included in the start-up costs. The transitions are modelled by the following equations:

$$u_{tki} - u_{t(k-1)i} - \delta_{tki} \leq 0, \qquad \forall i, \forall k \qquad (8)$$

$$o_{tki} - u_{t(k-1)i} - o_{t(k-1)i} - \delta_{tki} \leq 0 \qquad \forall i, \forall k \qquad (9)$$

$$o_{tki} - u_{tki} + u_{t(k-1)i} - \theta_{tki} \leq 1 \qquad \forall i, \forall k \qquad (10)$$

$k = 0$ refers to the last time step for the previous time stage, i.e. $t - 1$. (8) models the transition from standstill to generation, (9) the transitions from standstill and generation to rotational energy provision and (10) the transition from providing rotational energy to generation. The equations are formulated so that they induce the correct costs, should the model be run with simultaneous generation and rotational energy provision. Both δ_t and θ_{tki} are included with their associated cost in the objective function.

3) Provision of rotational energy: The provision of rotational energy is modelled by the following constraints:

$$u_{tki} + o_{tki} \leq 1 \qquad \forall i, \forall k \qquad (11)$$

$$\sum_{i \in \mathcal{U}} E_i^R o_{tki} - e_{tk}^R = 0 \qquad \forall k \qquad (12)$$

Eq. (11) limits simultaneous generation and rotational energy provision and is removed if it is allowed. Eq. (12) couples the power station's operating states to the delivery to the rotational energy market.

4) System constraints: System constraints limiting simultaneous bypass and generation of power stations with bypass connectivity, and the operation of power stations connected to more than one reservoir are also included in the model.

III. Case Study

A. Case Study

1) Hydro system: The hydro system used in the model is shown in Fig. 1. The dashed lines in the physical model representation show the planned hydrological connections of power station 2, which is currently under construction.

2) SC operation: A decision has been made to invest in SC mode of operation of the power station shared by units 2 and 3, making them capable of supplying rotational energy without generating. Associated parameters to the operation are shown in Table I.

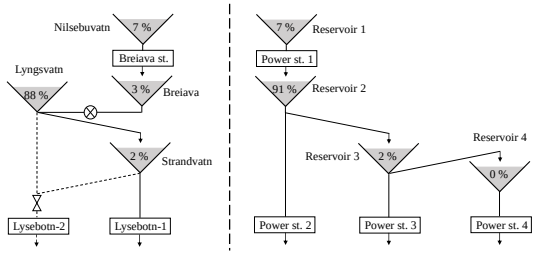

Fig. 1. Physical (left) and modelled (right) hydro system representation. Reservoirs are shown with their storage capacity in percent of the total system. In the modelled system representation, reservoirs and power stations are shown with its associated unit number. Units 2 and 3 share the same power station.

TABLE I
SC mode parameters for Lysebotn-2.

Inertia constant	Rated power	Rotational energy
3.0 s	2×215 MVA	1290 MWs

Investment analysis parameters are shown in Table II. The required yearly income is calculated using the net present value method and setting the NPV to zero, with an analysis period of 40 years and a discount rate of 3.76%, calculated as the sum of the current risk-free real interest rate, set equal to Norwegian 3-year government bonds, and a risk premium, set by the Norwegian Ministry of Finance.

TABLE II
Investment analysis parameters and results.

Investment cost	Required yearly income
23.36 MNOK	1 138.41 kNOK/year

3) Markets and market prices: The day-ahead market used is the Nord Pool Spot Elspot market. The price series used are obtained from the fundamental market model, EMPS [13]. A price profile, from historical Elspot prices from week 5 in 2014 to week 4 in 2016, is used to resemble price differentiations within weeks. Sales of capacity are to the weekly Frequency Containment Reserves - Normal (FCR-N) market, operated by Statnett.

The rotational energy market is assumed to be open only in time periods where the rotational energy in the system falls below a system requirement. With a system requirement for rotational energy of 100 GWs the future system inertia is expected to be too low during the night of week 31, based on an estimate of the 2020 generation mix provided by Statnett. Only provision of rotational energy without generation is remunerated, and the market is assumed to be cleared after the Elspot market.

The rotational energy price is set so that it provides the required yearly income to cover the investment cost. It is calculated under the assumption that the power station operates as a SC in every time period the rotational energy market is

open and provides the same income in every time step and time stage it is open. Operational costs are neglected. The necessary rotational energy price to cover the income in Table II is shown in Table III, along with other market parameters. Start-up costs are included in the price, assuming start-up of SC operation in every period. Fig. 2 shows the rotational energy prices plotted against expected Elspot and FCR-N prices.

TABLE III
ROTATIONAL ENERGY PRICE PARAMETERS.

Time stage	Time step	No. of hours	Rotational energy price
31	00:00 - 08:00	56	10.90 NOK/MWs/h
31	08:00 - 20:00	84	0.00 NOK/MWs/h
31	20:00 - 00:00	28	11.29 NOK/MWs/h

4) Model parameters: Table IV includes some selected model parameters.

TABLE IV
HYDROPOWER UNIT PARAMETERS.

Parameter	Unit	unit 1	unit 2	unit 3	unit 4
Maximum production	[MW]	14	400	380	220
Minimum production	[MW]	7	62	58	42
Reservoir capacity	[Mm^3]	40	510	12	0
Rotational energy	[MWs]	-	1290	1290	-

IV. RESULTS

The model was run once with perfect rotational energy speculation (run 1) and once without speculation (run 2). Every model run was executed with 50 forward sampled scenarios, 9 backward inflow samples and 15 iterations.

Table V shows the average income from the various markets. Run 1 has a slightly higher income from sales of energy, but also has less stored water in the reservoirs at the end of the simulation period. Due to perfect speculation, run 1 has a higher income from the rotational energy market. The contribution from rotational energy provision is substantial, considering the number of hours the rotational energy market is open. Run 2 has a higher income from sales of capacity, mainly caused by participation in the FCR-N market in the time steps where run 1 participates in the rotational energy market.

TABLE V
EXPECTED INCOME, IN MNOK.

Run	Elspot	FCR-N	Rotational energy	End water value
1	1 446.70	6.77	2.39	322.24
2	1 444.99	6.83	1.97	324.51

Fig. 3 shows the average values of Elspot, FCR-N and rotational energy market participation during weeks 30 to 32. As sales of both capacity and rotational energy tend to either be at their maximum value or zero, the values provide information about the frequency of scenarios where market participation occurs. In run 1, SC mode of operation occurs in every time step the rotational energy market is open. The gain from participating in the rotational energy market is higher than that of combined Elspot and FCR-N market participation. In run 2, the optimal strategy for Elspot and FCR-N market participation is followed. The figure shows that the Elspot and FCR-N markets are frequently participated in during the first time step of a day. These time steps have high FCR-N prices and lower Elspot prices, so the generation is at minimum in most scenarios to allow sales of capacity. There are no sales of energy or capacity in the last time step due to low Elspot prices, allowing participation in the rotational energy market.

The difference in production due to rotational energy market participation between the runs is small compared to the total production and has a negligible effect on the overall reservoir strategy. This is mainly due to the short time period the rotational energy market is open and that the rotational energy market is open during time steps and stages with low Elspot prices. For the given case study considering the year 2020,

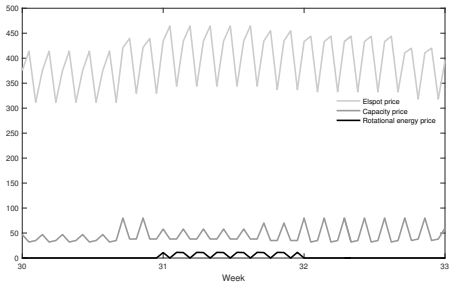

Fig. 2. Expected Elspot [NOK/MWh], FCR-N [NOK/MW/h], and rotational energy [NOK/MWs/h] prices from week 30 to 33.

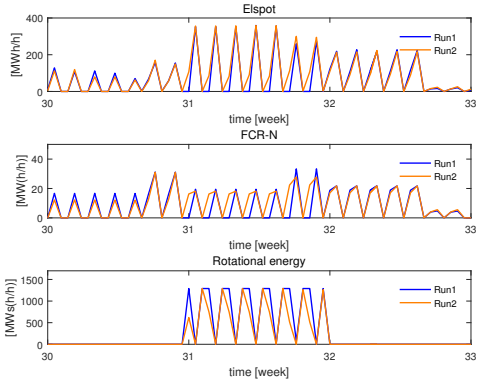

Fig. 3. Expected Elspot (top), FCR-N (middle) and rotational energy (bottom) market participation of units 2 and 3 in year 1.

rotational energy market participation has a small effect on medium term hydropower scheduling and it would therefore be interesting to study in short-term models.

Table VI shows costs and income associated with SC operation. The values are averaged from the two years of the simulation period. In run 1, the profit is higher than the required yearly income to cover the investment cost. This is an expected result, as SC operation occurs in every time step the market is open. Because the price was set including start-up costs, transitioning from production to SC operation causes a higher income than required. In run 2, the profit is reduced by 17.7 %, due to the reduced market participation and the required yearly income to cover the investment cost is not met. An increase of the rotational energy prices by approximately 22 % is needed to provide investment incentives.

Ideally, the rotational energy price would be at a level where it would not interfere with the optimal generation and capacity allocation strategy. This may be obtained by adjusting the income from sales of capacity and energy for the water value and it is found that a price of 1.02 and 0 NOK/MWs/h in the first and last time step of each day of week 31 respectively should mitigate interference in over 90 % of the time steps and scenarios. A price of 0 NOK/MWs/h indicates that sales of energy and capacity isn't profitable in that time step, and interference won't occur. A price below 1.02 NOK/MWs/h in the first time step and a high price in the last time step would provide a strategy which causes little interference, while covering the investment cost.

Should the rotational energy market be governed by the supply and demand of hydropower producers and the TSO, the price would likely be close to the marginal cost of rotational energy provision. A higher price would not lead to an increased amount of rotational energy, but rather cause hydropower producers to switch from generation to SC mode operation. To ensure investment in SC mode of operation of hydropower plants, the market should either have a fixed premium which covers the investment cost, or investment support should be offered.

TABLE VI
AVERAGE YEARLY ECONOMIC RESULTS FROM SC OPERATION, IN KNOK.

Run	Income	Transition costs	Start-up costs	Profit
1	1 194.86	7.83	6.72	1 180.31
2	984.04	7.13	5.56	971.35

V. CONCLUSION

Medium-term hydropower scheduling considering participation in a hypothetical rotational energy market has been studied. The results showed promising income potential from rotational energy provision compared to a day-ahead and capacity market. It was found that the provision of rotational energy had small effects on medium-term hydropower scheduling. The yearly income did not cover the investment cost when speculation was removed. This indicates that the price should have been higher, to provide investment incentives. A higher price would however also provide stronger speculation incentives. It was found that a low rotational energy price in the first time step of a day, and a high price in the last time step is likely to provide an optimal operation strategy without rotational energy and generation interference, which will cover the investment cost.

Further work should be put into analyzing the trade-off between speculation and investment incentives, from a socio-economic viewpoint. The operational costs should also be studied, to calculate the marginal cost of rotational energy provision. A short-term model should be applied to further study the effects of rotational energy provision on hydropower scheduling.

ACKNOWLEDGMENT

The authors would like to thank Magnus Landstad and his colleagues at Lyse Produksjon AS for valuable discussions and the provision of data for the case study.

REFERENCES

[1] P. Christensen and G. Tarnowski, "Inertia for wind power plants–state of the art review–year 2011," in *proc. 10th International Workshop on largescale integration of wind power into power systems*, 2011.

[2] SEM Committee, "DS3 System services technical definitions decision paper," 2013. [Online]. Available: https://www.semcommittee.com/publication/sem-13-098-ds3-system-services-technical-definitions-decision-paper-final-0

[3] European Network of Transmission System Operators for Electricity (ENTSO-E), "NAG Future system inertia," 2015.

[4] Statnett, "Systemdrifts- og markedsutviklingsplan," no. 20, 2014. In Norwegian. [Online]. Available: http://www.statnett.no/Drift-og-marked/Systemansvaret/Systemdrifts–og-markedsutviklingsplan/

[5] Statnett, "KUBE2015: Markedslsninger for neste generasjon kraftsystem," 2015. In Norwegian. [Online]. Available: http://www.statnett.no/Karriere/er-du-student/KUBE/Er-dagens-markedslosninger-tilstrekkelige-i-mote-med-Neste-generasjon-kraftsystem/

[6] Statnett, "Funksjonskrav i kraftsystemet," 2012. In Norwegian. [Online]. Available: http://www.statnett.no/Media/Nyheter/Nyhetsarkiv-2012/Funksjonskrav-i-kraftsystemet-FIKS-2012-publisert-/

[7] A. Karsrud, "Framtidig utvikling og sikring av rotasjonsenergi i det nordiske kraftsystemet," Master's thesis, Norwegian University of Science and Technology (NTNU) Trondheim, 2016. In Norwegian.

[8] M. N. Hjelmeland, M. Korpås, and A. Helseth, "Combined SDDP and simulator model for hydropower scheduling with sales of capacity," 2016. In Review, accepted for presentation in EEM 2016.

[9] A. Helseth, B. Mo, M. Fodstad, and M. N. Hjelmeland, "Co-optimizing sales of energy and capacity in a hydropower scheduling model," in *PowerTech, 2015 IEEE Eindhoven*, June 2015, pp. 1–6.

[10] A. Gjelsvik, M. M. Belsnes, and A. Haugstad, "An algorithm for stochastic medium-term hydrothermal scheduling under spot price uncertainty," *Power System Computation Conference (PSCC)*, vol. 13, pp. 1079–1085, June 28 - July 2nd, 1999.

[11] A. Gjelsvik, U. Linnet, , A. Gjelsvik, and B. Mo, "A model for optimal scheduling of hydro thermal systems including pumped-storage and wind power," *IET Generation, Transmission & Distribution*, vol. 7, no. 12, pp. 1426–1434, 2013.

[12] A. Gjelsvik, B. Mo, and A. Haugstad, "Long- and medium-term term operations planning and stochastic modelling in hydro-dominated power systems based on stochastic dual dynamic programming," *Handbook of Power Systems I*, pp. 33–35, 2012.

[13] O. Wolfgang, A. Haugstad, B. Mo, A. Gjelsvik, I. Wangensteen, and G. Doorman, "Hydro reservoir handling in norway before and after deregulation," *Energy*, vol. 34, no. 10, pp. 1642 – 1651, 2009, 11th Conference on Process Integration, Modelling and Optimisation for Energy Saving and Pollution Reduction.

B Solution Algorithms

B.1 Strategy Model

The solution is obtained by solving the problem with SDDP, in a similar manner as described in Section 2.4.2.

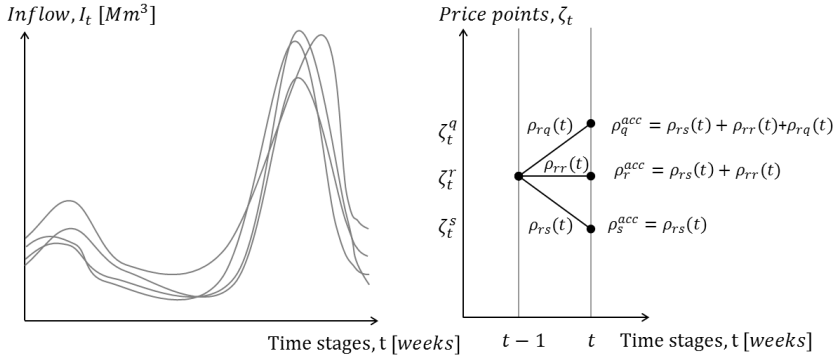

Figure B.1: Illustration of inflow scenarios (left) and price point sampling for time stage t (right).

The forward iteration starts by sampling a number of inflow scenarios, $|\mathcal{N}|$. The inflow in each time stage for every scenario is sampled as described in Section 3.1.2. After the inflow scenarios are sampled, a price point is sampled for each scenario in each time stage. The price point is set to the point that has a higher accumulated transition probability from the previous price point, than a random generated number between zero and one. Figure B.1 shows an illustration of inflow scenarios and a representation of the price point sampling. Note that in the figure there is only one price point in time stage $t-1$, as this has already been sampled. $\rho_r^{acc}(t)$ is the accumulated transition probability. The one stage problem is solved iteratively for the scenarios in each price stage, so that the previous time stage variables $v_{t,w-1,m}$, $z_{t-1,m}$, and $u_{t,w-1,m}$ have been found when solving for time stage t. After iterating through all time stages and scenarios, the upper and lower bounds are calculated.

These are given in the following equations

$$\overline{z} = \frac{1}{|\mathcal{N}|}\Sigma_{n\in\mathcal{N}}\ \alpha_1 \tag{B.1}$$

$$\underline{z} = \frac{1}{|\mathcal{N}|}\left(\Sigma_{n\in\mathcal{N}}\Sigma_{t\in\mathcal{T}}\ [\alpha_t - \alpha_{t+1}] + \alpha_{|\mathcal{T}|+1}\right) \tag{B.2}$$

In the last forward iteration, pre-sampled inflow scenarios and price points may be used to facilitate comparison between different model runs.

In the backward simulation, an additional set of inflow samples $\mathcal{D}$ is used to generate cuts in each scenario. These inflow samples are called backward openings. Because the iteration is backwards, all price points are a possibility for the price point in the previous stage. A cut is therefore generated for all backward openings for each price point. The one stage problem is solved for the current time stage. Dual values $\pi^j_{t,m}$ and $\phi^j_{t,m}$ for the first time block, and $\mu^j_{t,m}$ accumulated over all time blocks, of time stage t are calculated to be used in the previous time stage:

$$\alpha^*_t = \hat{\alpha}_t + \Sigma_{m\in\mathcal{M}}\ \pi^j_{t,m}v_{t-1,m} + \Sigma_{m\in\mathcal{M}}\ \mu^j_{t,m}z_{t-1,m} + \Sigma_{m\in\mathcal{M}}\ \phi^j_{t,m}u^L_{t-1,m}$$

The cuts are weighted according to transition probability between their associated price point and the price point in the previous stage.

For further explanation, the forward and backward iteration algorithms from [4] are reproduced below, with some minor changes for better compatibility with this thesis.

Algorithm B.1: Strategy model forward iteration [4]

Sample inflow scenarios
- Initialize the normalized inflow for stage 0 as $z_{0,m}\ \forall m \in \mathcal{M}$
- **for** $n = 1...|\mathcal{N}|$ **do**
  - **for** $t = 1...|\mathcal{T}|$ **do**
    - **for** $m = 1...|\mathcal{M}|$ **do**
      - Calculate $z_{t,m} = z_{t-1,m} + \epsilon_{t,m}$ where $\epsilon_{t,m}$ is drawn from a random distribution of the mean sample noise.
      - Calculate $I_{t,m} = \sigma_{t,m} z_{t,m} + \overline{I}_{t,m}$
    - **end**
  - **end**
- **end**

Sample price points
- Initialize starting price point at $t = 1$
- Load price point scenarios and transition probabilities
- **for** $t = 2...|\mathcal{T}|$ **do**
  - **for** $n = 1...|\mathcal{N}|$ **do**
    - From the transition probability of price point scenarios, sample the next price point that has a higher accumulated probability than a generated random variable between 0 and 1.
  - **end**
- **end**

end

for $n = 1...|\mathcal{N}|$ **do**
- **for** $t = 1...|\mathcal{T}|$ **do**
  - Collect the right hand side coefficients; inflow, reservoir, and the start-up associated variable.
  - Collect the spot price, capacity sales price and rotational energy prices.
  - Solve the one stage LP problem and store the results.
- **end**

end

Calculate upper and lower bounds.

Check convergence.

Algorithm B.2: Strategy model backward iteration [4]

for $t = |\mathcal{T}|..2$ **do**
  for $r = 1...|\mathcal{R}|$ **do**
    for $n = 1...|\mathcal{N}|$ **do**
      for $d = 1...|\mathcal{D}|$ **do**
        Update right hand side coefficients with the start-up associated variable and end reservoir level from stage $t-1$, and inflow from backwards opening d.
        Solve the one stage LP problem.
        Store α_{t+1}
        Store dual values $\pi^j_{t,m}$ and $\phi^j_{t,m}$ for the constraints in the first time block, for each module m.
        Accumulate and store dual values $\mu^j_{t,m}$ over the time blocks w, for each module m.
        Calculate a cut for the state:

        $\alpha^*_t = \hat{\alpha}_t + \Sigma_{m\in\mathcal{M}}\ \pi^j_{t,m} v_{t-1,m} + \Sigma_{m\in\mathcal{M}}\ \mu^j_{t,m} z_{t-1,m} + \Sigma_{m\in\mathcal{M}}\ \phi^j_{t,m} u^L_{t-1,m}$
        $\pi^j_t = \Sigma_{m\in\mathcal{M}}\ \pi^j_{t,m}$ and $\phi^j_t = \Sigma_{m\in\mathcal{M}}\ \phi^j_{t,m}$ and $\mu^j_t = \Sigma_{m\in\mathcal{M}}\ \mu^j_{t,m}$

      end
    end
  end
  for $r_{from} = 1...|\mathcal{R}|$ **do**
    for $n = 1...|\mathcal{N}|$ **do**
      for $t_{to} = 1...|\mathcal{R}|$ **do**
        for $m = 1...|\mathcal{M}|$ **do**
          Weigh, by transition probability, cuts from price points r_{to} in time stage t to cuts for price point r_{from} in stage $t-1$.
        end
      end
    end
  end
end

B.2 Simulator Model

As previously mentioned, the Simulator Model is solved for the same scenarios as the last forward iteration of the Strategy Model. For a time stage in a scenario, the branch and bound method[1] is used to solve the one stage MIP problem without constraint (3.103), which represents the cuts. Then the most violated cut is found and added to the problem, and the problem is solved using branch and bound again. This process of adding the most violated cut is repeated until the most violated cut is below a tolerance limit.

As MIP problems are non-convex [34], the dual scenario is not as easily obtained as in the Strategy Model. A fixed problem is made by keeping the binary variables constant. This provides an LP problem which may be solved by the simplex method to achieve the dual values.

The whole process is then repeated for the next time stage, and when the last time stage is reached the process is repeated for the next scenario. The solution algorithm of the Simulator Model is given below. In Figure B.2, a simplified flowchart of the Strategy and Simulator Model is shown, illustrating their interaction.

Algorithm B.3: Simulator model [4]

```
for n = 1...|𝒩| do
    for t = 1...|𝒯| do
        Collect the right hand side coefficients; inflow, reservoir, and the start-up
        associated variable.
        Collect the spot price, capacity sales price and the rotational energy price.
        Solve the one stage MIP problem without cuts.
        while Cut violation do
            for j = 1...|ℋ| do
                Find the most violated cut.
            end
            Add the most violated cut to the one stage MIP problem.
            Solve the one stage MIP problem.
        end
        Create and solve the fixed problem to obtain dual values.
        Store the results.
    end
end
```

[1] An optimization technique for MIP problems which uses a combination of enumeration of solutions and optimistic estimates of the optimal objective function value [34].

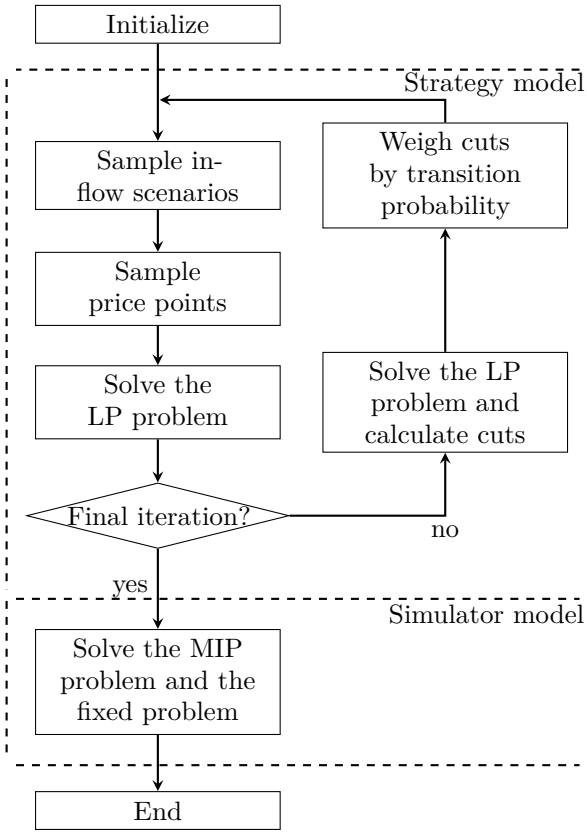

Figure B.2: Simplified flowchart of the Strategy and Simulator Model.